TIME AND LENGTH SCALES OF CRUST-MAGMA INTERACTION IN RIFT SETTINGS

A Dissertation
Presented to
The Academic Faculty

by

Ozge Karakas

In Partial Fulfillment
of the Requirements for the Degree
Doctor of Philosophy in the
School of Earth and Atmospheric Sciences

Georgia Institute of Technology
August 2015

TIME AND LENGTH SCALES OF CRUST-MAGMA INTERACTION IN RIFT SETTINGS

Approved by:

Dr. Josef Dufek, Advisor
School of Earth and Atmospheric Sciences
Georgia Institute of Technology

Dr. Andrew Newman
School of Earth and Atmospheric Sciences
Georgia Institute of Technology

Dr. Christian Huber
School of Earth and Atmospheric Sciences
Georgia Institute of Technology

Dr. Zhigang Peng
School of Earth and Atmospheric Sciences
Georgia Institute of Technology

Dr. Margaret Mangan
California Volcano Observatory
U.S. Geological Survey

Date Approved: May 08, 2015

This work is dedicated to the memory of my grandmother,
Ayşe Karakaş.

ACKNOWLEDGEMENTS

My research experience and life as a graduate student has been a delightful journey thanks to the contributions of many people around me. I would like to start by thanking my advisor Josef Dufek, for giving me the opportunity to work as a part of his research team. His patience, scientific guidance, and support have been very helpful during my research life. I also would like to thank Christian Huber for his tremendous support during difficult times, suggestions, and scientific discussions that we had. My thankfulness also goes to Andrew Newman, who has always supported me and taught me a lot during our meetings and field trips. I would like to express my gratefulness to Margaret Mangan for her trust, patience, and scientific discussions that we have had. I had a great experience thanks to the opportunities that she gave me. I also thank Zhigang Peng for accepting to join my comprehensive exam and dissertation committees and also for valuable discussions particularly on Turkey and Salton Sea seismicity. I am also thankful to Carol Paty for her suggestions about research and career.

My gratefulness also goes to Dufek research group: Mary Benage, Wim Degruyter, Joshua Mendez, Ryan Cahalan, Leah Courtland, Gabriel Eggers, Taryn Black, Le Qiao, Julian McAdams, Jennifer Telling, Joseph Estep, and Cindy Young, for their friendships, and being very patient about going over my drafts and giving me feedbacks that greatly improved my research. I especially like to thank Mary Benage, for her unlimited support, being a great friend, and being there in good and bad times. I appreciate her encouragement and help. I also thank Wim Degruyter who always helped my research, gave suggestions about my career, and also supported me during difficult

times. I want to thank Jaime Convers for checking me every day during my thesis time. I appreciate his motivational speeches and the funny videos that he sent that made me laugh when I was having a bad day. I also want to thank greater EAS family for their friendship and making me feel welcomed since the first day I started graduate school.

Of course, this work would never complete without the support and endless love of my family (Osman, Firdevs, Ozgur, Ozge, Uzay Karakas) and my friends in Turkey (Ebru Erol, Handan Apaydin, Yaprak Senturk, Incila Gurol). Thanks for being there whenever I need. Lastly, I like to thank Benek, who has been my funny roommate for the last two years and made me laugh all the time.

TABLE OF CONTENTS

LIST OF TABLES

LIST OF FIGURES

NOMENCLATURE

c_p	specific heat
E	efficiency
E_T	energy budget
f	melt fraction
H_0	radiogenic heat
k	thermal conductivity
l	radiogenic lengthscale
L	latent heat
v_i	velocity
V	volume
ρ	density
T	temperature
t	time
q_s	surface heat flux
q_m	heat flux at the mantle-crust boundary

SUMMARY

A novel thermal-petrographic numerical model was developed to quantify the time and length scales involved in the thermal and compositional evolution of crustal magmas in rift settings. General trends of magma evolution were characterized in various rift systems as a function of magma flux, tectonic extension, and magmatic water content. Results indicated that magma flux has a primary control on the generation and the formation of crustal magmatic systems. Once magma reservoirs are formed in the crust, tectonic extension and magmatic water content impose important controls on the volume and compositions of these reservoirs. It is suggested that the composition of magma bodies in rift settings is mainly derived from fractionation of basalt with minor contribution from crustal melting. The numerical model was applied to Salton Sea Geothermal Field (SSGF) as a natural setting. The results suggested that the SSGF magmatic system has a long-lived highly crystalline magma reservoir in the lower crust that supplies heat to the hydrothermal system. Outcomes of this work deliver detailed insights to the interaction of basalt and crust in extensional tectonic settings and address questions regarding volume and longevity of the crustal magma bodies. Implications and future directions are discussed in the light of compositional diversity observed in different magmatic systems.

CHAPTER 1

INTRODUCTION

1.1. Background and motivation

Magmatic processes in the Earth's crust operate at various time and length scales. Time scales ranging from minutes to millions of years and length scales ranging from micro to macro scales have been detected by indirect (seismic, geodetic) and direct observations (petrologic, field). Seismic signals, for example, can detect increased volcanic activity within seconds (e.g., Chouet, 1996). In 1991, the eruption of Mount Pinatubo was predicted by an increase in seismicity to 50-150 volcano-tectonic events per day (Harlow et al., 1996). An eruption can last for hours (e.g., May 18, 1980 eruption of Mount St Helens, e.g., Papale and Dobran, 1994), for weeks (e.g., Oruanui ignimbrite, Wilson, 2001), even for years (e.g., Huckleberry Ridge Tuff, Wilson, 2008). Geodetic studies detect the rate of ground deformation in response to volume change in the crustal magma body, which typically give information about the state of the magma chamber within months to years (e.g., Santorini Caldera, Newman et al., 2012). Geochronologic studies provide a more general picture of magma evolution in its crustal reservoir. For example, the isotopic evidence preserved in zircon crystals suggest lifetimes of ~100 ka to >1 Ma (e.g., Bacon and Lowenstern, 2005; Reid et al., 1997), while these individual magmatic storage systems are suggested to have remobilized over short timescales (months to years, e.g., Druitt et al., 2012).

Similarly, various lengthscales ranging from micro scale processes in individual crystals to macro scale dimensions in eruptive products are reported in several studies within the past century. Orders of magnitudes of difference in erupted volumes is also recorded at various volcanic centers, that can be exemplified by ~5000 km^3 for Fish Canyon Tuff (Bachmann et al., 2002) compared to ~1 km^3 for the Mount St Helens eruptive deposits (Carey et al., 1990). A consequence of these different time and length scales is the petrologic diversity observed in the volcanic products and plutonic rocks, ranging from high-silica rhyolites (Taupo Volcanic Zone, e.g. Deering et al., 2008) to mafic volcanic products (e.g., Zimbabwe, Shimizu et al., 2005). These observations open up questions regarding the conditions that result in various volumes, compositions, and timescales of magmatic products in different volcanic centers. A key question is how does the magma generate and evolve in the crust?

Much of the melt in the crust is fundamentally generated in the deep mantle by an increase in temperature, decrease in pressure (decompression melting, e.g., Kushiro, 2001), or introduction of fluids and volatiles in the mantle (e.g., Ulmer, 2001). An increase in temperature is usually attributed to hot-spot volcanism, or when the rise of the mantle plume advects heat to initiate partial melting processes. Decrease in pressure is typically observed in rifting environments, where 'decompression melting' takes place. Finally, fluid and volatile flux typically occurs in arc environments, where the subducting slab undergoes geochemical reactions, release volatiles to the mantle wedge, and induces melting of the mantle material. The generated melt in the mantle usually ponds in the upper mantle and emplaces in the crust, where they usually trap at different levels and evolve.

Large accumulations of mafic magma in the crust of various volcanic settings have been documented in several seismic, petrologic, and field observations. Some examples include: the Salton Sea Trough (12-18 km depth, Fuis et al., 1984), the Ivrea-

Verbona Zone (10 km thick mafic complex, Sinigoi et al., 1994), Kohistan (10 km thick mafic complex, Jagoutz et al., 2009), the Taupo Volcanic Zone (15 km thick mafic intrusion, Deering et al., 2008; Harrison and White, 2004). If the voluminous mafic magma in the crust is transported from the mantle, it must bring considerable mass and enthalpy from the mantle into the crust.

The presence of voluminous magma in the crust has been a topic of debate within the past century that questions how the space is created in the crust to accommodate large volumes of magma input (crustal room problem, e.g., O'Hara, 1998). Several mechanisms have been suggested to address this question (Fig. 1): 1) deformation and doming of the upper layers in response to magma emplacement, 2) partial melting and assimilation of the crustal material, 3) magma stoping, 4) wall rock deformation and return flow, 5) lateral wall rock displacement by faulting and folding, and 6) tectonic extension. It is likely that all these processes operate to different degrees in response to magma accumulation in the crust (e.g., Gill, 1981; Grove et al., 2002; Hildreth and Moorbath, 1988).

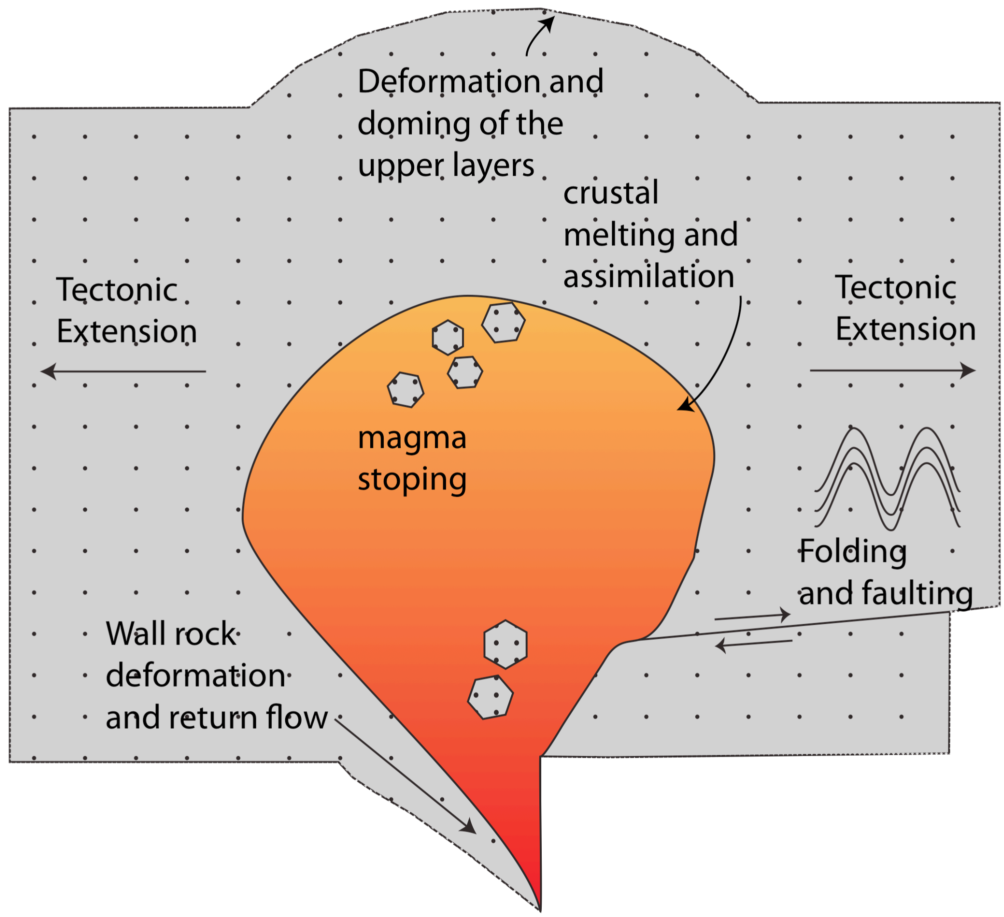

Fig. 1. Schematic representation of the magma emplacement in the crust, after Winter (2001) and Patterson et al. (1991). This thesis work is particularly focused on the tectonic extension, partial melting, and fractionation processes. Sketch is not to scale.

Among these processes, the interaction of tectonic extension and magma evolution in the *crustal level* has received little attention although its influence on the magma generation and transport in the mantle is well studied over the past decades (e.g., Buck, 2004; McKenzie and Bickle, 1988). Early calculations quantified melt generation in the mantle in response to continental extension, extraction of this melt from its mantle residue, and transport into the crust through a melting column (e.g., McKenzie, 1985). A series of processes operate at the mantle level during melt generation, extraction, and transport. At the most fundamental level, melt generation in the mantle is a function of mantle potential temperature, thickness of the mechanical boundary layer, and the amount of decompression (McKenzie and Bickle, 1988). In addition, pressure, rift duration, extension velocity, presence of volatiles, and strain rate have strong influence on melt generation in the mantle (e.g., Foucher et al., 1982; Pedersen and Ro, 1992; White et al., 1987). Once the melt is generated in the mantle, extraction of the melt from its mantle residue depends on several processes such as porosity, compaction length and timescale, and separation velocity (McKenzie, 1985). Transport and emplacement of the extracted melt into the crust also depends on different parameters such as subsidence rate in response to stretching, uplift by addition of new material in the crust, lithospheric rheology, rupture, and dike opening (e.g., Bialas et al., 2010; Ruppel, 1995; White et al., 1987; Ziegler and Cloetingh, 2004). As a consequence of these processes, a considerable variety on the timing and volume of the volcanic processes has been observed in several rifted regions.

While some rifts or segments of rifts have been characterized by intense volcanic activity, others showed minor magmatic contribution (e.g., Ziegler and Cloetingh, 2004). For example, Ruppel (1995) observed minor magmatism in the western branch of the East African Rift (EAR) and effusive magmatism in Kenya and Ethiopian rifts in EAR. In North Atlantic, White et al. (1987) argued that elevated mantle potential temperatures by advection (~100-150˚C) in Hatton Margin created the extensive magmatism (~20 km thick) while Biscay margin only showed minor magmatism (a few km thick). In the Main Ethiopian Rift (MER), Kendall et al. (2005) argued that 80% of the strain is accommodated by heavy intrusions, therefore in this region there is relatively little stretched crust coupled to high magmatic input.

Due to a number of non-linear processes that control the tectonic extension, magma production and transport from mantle into the crust, the time and length scales of the magma evolution *in the crust* remain poorly constrained. Geophysical studies can locate high-temperature regions in volcanic settings and constrain the tectonic evolution, however, they do not give detailed temporal and compositional evolution during magma emplacement in the crust, which can occur in 10^5-10^6 years. Similarly, petrologic studies provide information about exposed plutonic rocks and erupted volcanic products, which provide information about the mid-upper crustal magma accumulations. Recently, application of thermal models constrained by seismic, petrologic, and geodetic studies have started revealing the temporal evolution of magma and the interaction of magma input with the static (not deforming) crust (e.g., Annen and Sparks, 2002; Dufek and Bergantz, 2005; Petford and Gallagher, 2001). This thesis work focuses on the influence of extensional tectonics on the crustal magma evolution and addresses several debated topics in volcanology on magma composition, size, and longevity in rifted settings. In particular, this work focuses on addressing the following questions:

- What are the conditions that permit extensive volumes of magma to emplace and reside in the crust in rift settings?
- Do silica-rich magmas mainly derive from fractional crystallization of a basaltic parent, or from partial melting of the crust?
- How long and at what melt fraction do partially molten regions exist?

- Are plutons and extrusive volcanic products related to each other? (Future work)

The following discussion and chapters will give insight to the time and length scales of magma evolution in the crust by addressing these questions with respect to rifted environments.

1.2. Magma emplacement and partially molten regions in the crust

Since the pioneering work of Harker (1909), Bowen (1928), and Daly (1914), the classical view stating that magma stays in a large 'tank' in the crust has changed. Instead, magma in the crust is suggested to stay in a sponge-like zone (Daly, 1914; Harker, 1909) that is a combination of dikes and melt pods forming the partially molten region (Hildreth, 2004). The crystals in the partially molten region can vary between 0-100% by volume. The magma at its liquidus has 0 vol. % crystals, and as it cools down, the crystal fraction increases and finally reaches 100 vol.% at its solidus. When the crystal fraction is between 0-50 vol.%, the crystals are suggested to move freely within the magma body. In contrast, when the crystal fraction reaches >50 vol.%, the crystals are suggested to form a 'rigid skeleton', where they touch each other and cannot freely move within the magma body (e.g., Marsh, 1981). This highly crystalline partially molten zone is referred to as the 'mush' region (e.g., Hildreth, 2004). The mush zones in the crust are constructed by distributed diking of mantle-derived basalt over millions of years of intrusion events, typically by locally concentrated and intense intrusions (Hildreth, 1981; Hildreth and Moorbath, 1988), and experience re-melting and cooling between successive intrusions. In the lower crust, the mush regions typically experience fractionation, melt segregation, and ascent and constitute the main source for upper-crustal magma bodies (Hildreth, 2004).

A key topic is the temporal evolution of the size and melt fraction of these mush regions at different levels in the crust. Recently, seismic imaging techniques successfully located melt regions and gave constraints to the lower and upper crustal melt accumulations (e.g., Lees and Crosson, 1990). A recent study by Huang et al. (2015) constrained the size and melt fraction of the mantle plume and upper crustal magma body in the Yellowstone System. These studies, while useful, provide a snapshot of the magma accumulations in the crust. However, understanding the long-term thermal and compositional evolution of the crustal magma bodies is necessary to address the questions regarding the chemical and thermal evolution of magmas. In this context, I introduce a thermal model in chapters 2 and 3, a study that I conducted with Josef Dufek (Karakas and Dufek, 2015) that constrains the time and lengthscales of the magmas that reside in the crust of rift settings. This study focuses on rift settings in order to quantify the control of extensional tectonics on the magma-crust interaction. In chapter 4, I present a case study that is applied to the Salton Sea Geothermal Field (Karakas et al., in prep.), and discuss the size and melt fraction constraints of the lower crustal magma accumulation in this region. These constraints give important information about the compositional state of the magma bodies at particular depth and melt fraction.

1.3. The origin of evolved magmas

The compositional evolution of magma in the crustal mush zones is a topic of debate in volcanology as it provides a link between mafic magma emplacement in the lower crust and large-scale silicic eruptions at the surface. In many explosive systems, intermediate to highly evolved magmas are observed (Taupo Volcanic Zone, e.g., Deering et al., 2008), however, less-evolved magmas are also recognized in numerous other settings (e.g., Cerro Prieto and Roca Consag, Schmitt et al., 2013). The variety in magmas is not only observed compositionally, but also observed in their crystallinity. An important question is: how do evolved magmas form from a common mafic source? In many magmatic systems, the primary magmas emplaced in the crust often have similar compositions, and therefore some process(es) must take place during magma residence in the crust in order to produce the observed compositional diversity in volcanic and plutonic products.

Among the several mechanisms that have been suggested to generate the chemical diversity of the magmas, two main processes are believed to be the main drivers: 1) fractional crystallization of the emplaced melt (mantle-derived) and 2) partial melting of the crustal material as a result of conduction of heat from the emplaced magma to the surrounding crust. It is likely that these two processes both operate to some degree (AFC processes, e.g., Allegre and Minster, 1978; DePaolo, 1981b; Taylor, 1980), however, their relative contribution to crustal magmas remains controversial since both fractionation and assimilation processes can result in evolved, silicic magmas.

1.3.1. Fractional crystallization of primitive mantle-derived magma

Since Bowen (1928), fractionation of mantle-derived melt to form evolved magmas has been supported by several studies (e.g., Bacon and Druitt, 1988; Mahood, 1981). During fractional crystallization processes, physical separation of crystals and melt takes place in the magma body as the temperature and pressure conditions of the magma changes (Harker, 1894). Redistribution of the chemical components in the magma into new phases creates various compositions as the magma evolves, and finally produces highly evolved silicic magmas (e.g., Bachmann and Bergantz, 2008). This process is suggested to be the main mechanism for formation of highly-evolved magmas in many settings, exemplified by Kos Plateau Tuff (e.g., Bachmann et al., 2007a), Taupo Volcanic Zone (e.g., Deering et al., 2008), Kohistan (e.g., Jagoutz et al., 2009), and Basin and Range (e.g., DePaolo, 1981a).

However, fractional crystallization being the main contributor to the crustal magmas is challenged by two observations: 1) if the evolved magmas are formed mainly by fractional crystallization of magma, there must be dense and mafic residues left behind in the crust. However, these 'cumulates' are rare and have not been detected in various locations by geophysical and petrologic studies. Additionally, in the upper crust, the formation of the rhyolitic melt necessitates presence of residual (and more mafic) crystalline bodies in the upper crust, which is not observed in many locations. 2) Fractional crystallization of the magma should produce a continuum in the composition, ranging from mafic to intermediate to felsic as the magma evolves (e.g., Chayes, 1963). Therefore, the 'Daly-gap' (lack of intermediate compositions) observed in many eruptions cannot be explained only by the fractionation processes. These two main discussions have led some authors to rule out fractional crystallization as the main process that generates evolved magmas. However, some thermal and petrologic studies have suggested possible mechanisms that can explain the absence of cumulates and possibility of Daly-gap by fractionation processes (e.g., Dufek and Bachmann, 2010; Gelman et al., 2014).

One of the explanations suggests density stratification due to crystallization of magma in deep crustal portions. In the lower crust, it is suggested that fractional crystallization results in an evolved silicic magma and formation of mafic cumulates. These mafic cumulates include heavy minerals like garnet, which can be denser than the lower crust and form density instabilities that allow the cumulate to recycle back to the underlying mantle (e.g., Jagoutz and Schmidt, 2013; Jull and Kelemen, 2001; Kay and Kay, 1993). This process, known as crustal foundering/delamination, is suggested as a mechanism where the mafic and ultramafic cumulates are not observed in the lower crust (e.g., Ducea, 2002; Dufek and Bergantz, 2005). In the upper crust, evolved melt likely resides in the upper portion of the mush, known as the ‘rhyolite cap’. In this case, the crystalline residue can also be silicic and can show dimmed fractionation signatures (e.g., Bachmann et al., 2007b; Gelman et al., 2014; Lee and Bachmann, 2014). In this context, presence of granitoid rocks in the upper crust, which is widespread in the upper continental crust (Taylor and McLennan, 1985), can explain the cumulates that are left behind after extraction of evolved magmas (Gelman et al., 2014).

Another argument, which is the development of Daly-gap in volcanic products, is explained by the thermodynamic study of Dufek and Bachmann (2010). According to this thermodynamic model, at high crystallinity (>70%), the rigid skeleton formed by high crystal fraction cannot deform easily by compaction, and melt withdrawal from this body is limited (e.g., McKenzie, 1985). At low crystallinity (<50%), the crystals are coupled to convective motions in the magma body (St~1), prohibiting the melt and crystal separation. Therefore, separation of crystals from the melt is most efficient between 50-70 vol.% crystals, allowing for the fractionation processes to generate the compositional gap that is observed in various settings. In other words, the likelihood of melt extraction from the crystalline mush varies as the magma evolves, disrupting the expected compositional continuum in the evolving magma during fractional crystallization.

1.3.2. Partial melting of crustal lithologies

In opposition to the arguments that support fractional crystallization of magma, a vast number of petrologic and thermal models argue that melting and assimilation of crustal material has a significant contribution to the formation of evolved products (e.g., Bergantz, 1989; Clemens and Vielzeuf, 1987). For example, in the Andes, petrologic study of Hildreth and Moorbath (1988) showed that crustal contribution to the evolved magma products is significant. The thermal model of Bindeman and Simakin (2014) suggested that once the rhyolitic bodies are formed in the upper crust, re-melting and recycling of this material is energetically efficient, and allows for significant crustal contribution for silicic eruptions that we commonly observe. Many of these studies have argued that the crustal room problem and formation of bimodal magma (and Daly-gap) can easily be explained by crustal melting alone because crustal lithologies are silicic in composition whereas intruded magma is mafic (as observed in xenoliths). However, thermal models that disagree with this argument suggest that the energy needed for melting of the crustal material must be exceptionally high for most of the conditions (particularly in the upper crust where large eruptions can occur), ruling out the crustal melting being the dominant process for formation of the evolved magmas (e.g., Dufek and Bergantz, 2005).

The discussion on the origin of magma has been an important topic as it has important implications on the mass and heat balance in the crust. If the crustal melting is an efficient process, then the energy needed to melt the crust is not excessive; therefore smaller amounts of mantle-magma magma input would be enough for extensive magma bodies in the crust. In this case, crustal growth is insignificant because the material being melted is eventually recycled back in the crust. Similarly, if most of the melt in the crust is originated from melting of the crustal lithologies, the crustal room problem is explained easily. On the other hand, if the crustal melting is minor (fractional crystallization dominates), this necessitates voluminous amounts of mantle-derived magma entrance in the crust, allowing for significant crustal growth.

Thermodynamically, these two processes (fractionation versus crustal melting) dominate in different conditions as a function of magma input, ambient temperature, and volatile content (e.g., Bachmann et al., 2007b; Dufek and Bergantz, 2005). Recent thermal models have shown that crustal melting is thermally inefficient process, especially in thin, cold, dry crusts (e.g., Annen et al., 2006; Dufek and Bergantz, 2005). On the other hand, in thick crusts, the ambient lower crustal temperatures will be closer to melting temperatures of the lithologies, and hence, will induce greater crustal melting signature as observed in the Andes (Hildreth and Moorbath, 1988). In chapters 2 and 3, the relative contribution of the crustal melting versus fractional crystallization is quantified in rift settings by the thermodynamic model. I discuss the energy input in the crust and composition of the magma as it evolves in rift settings. In chapter 4, the contribution of the crustal material versus mantle-material in crustal magmas is discussed in the case study of Salton Sea Geothermal Field. Discussions on the origin of bimodal magmatism have remained controversial in this region.

1.4. Longevity of crustal magma bodies: short-lived or long-lived?

A related and highly debated topic is the longevity of the crustal magmatic systems. A key question is: how long does a magma bodies stay at a partially molten state in the crust? To give insight to this topic, I first discuss the plutonic and volcanic rocks that are the two end-member products of Earth's magmatism. Volcanic rocks usually provide information about the state of the magma chamber at the time of eruption, or at the time of peak magmatic activity. Plutonic rocks often include information about the state of the magma body as it evolves temporally, however they require careful interpretation because magma spends time both below and above solidus and the evolution of magmatic state can be over printed by rejuvenation processes. Therefore, quantification of long-term evolution of crustal magmatic systems is essential.

Arguments on the longevity of crustal magma bodies mainly fall into two categories, suggesting either short or long lifetimes. Recently, a number of studies have argued that the magma chambers that feed large volcanic eruptions must be rare and short-lived (e.g., Annen, 2009; Glazner et al., 2004; Tappa et al., 2011). These studies claim that if the magma does not erupt on short timescales, then it must completely solidify to form plutons. This necessitates that the magma must evolve to its final state (composition) in the lower crust and transport to the upper crust shortly before the eruption. In this case, only textural changes can be observed in the upper crustal magma bodies without any significant compositional evolution (e.g., Annen et al., 2006). These studies suggest that, if the volume flux of magma in the upper crust is high (>10-2 km3/yr, Annen, 2009), then the magma erupts after short residence in the upper crust (years to thousand years, e.g., Menand et al., 2015). Correspondingly, if the volume flux of magma is lower than 10^{-3} km^3/yr, each magma pulse solidifies before the next injection, and incremental assembly of magma pulses eventually form plutonic rocks (e.g., Annen, 2009; Glazner et al., 2004). These studies also argue that, depending on the magma influx, the magma either erupts at the surface or solidifies in the crust, and the erupted volcanic products and solidified plutonic rocks are not genetically related. Discussion of this topic (volcanic-plutonic connection) is included in more detail in section 1.3.

In contrast to short-timescale arguments, a number of studies argue that the magma can stay in the crust for long time periods providing that the magma stays at high crystallinity (10^5 to10^6 years, Bachmann and Bergantz, 2008; Huber et al., 2009). This is best explained by the mush model, where the magma can stay in the cap formed in the upper portion of the mush, where the latent heat buffering of the mush region allows for long timescales of magma residence given its high crystallinity (Bachmann et al., 2007b; Hildreth, 2004). Long timescales of the crustal magmatic systems have been observed in the zircon crystals in many volcanic systems (e.g., Bachmann et al., 2007a; Reid et al., 1997). Here, we note that recent geochronology and diffusion modeling studies suggest short rejuvenation timescales before an eruption (months to years, e.g., Druitt et al., 2012). These studies provide an important link between the remobilization of magma and state of the magma chamber at the time of eruption, which does not necessarily contradict the argument of long-term evolution of the magma body from initiation of dike intrusions to evolution of highly crystalline magma body.

1.5. The volcanic-plutonic connection

A closely related topic is the connection between volcanic and plutonic rocks. Despite extensive field, petrologic, and geophysical studies conducted over the past century, the link between volcanic and plutonic rocks is still debated because direct observations of volcanic and plutonic rocks in the same setting are not available. The presence of large plutons in the field usually necessitates extreme rates of erosion of overlying crustal material, and their volcanic equivalents, if any. On the other hand, when volcanic rocks are present, plutonic rocks must reside at deeper crust, challenging the suggestion of the connection between volcanic products and their associated plutonic residues.

The volcanic and plutonic rocks resemble in many characteristics, however they also differ in some aspects (details of many studies reviewed in Bachmann et al., 2007b). Some studies argue that they are closely related because they are spatially and petrologically very similar. In addition, seismic imaging models have identified partially molten regions in the crust of many volcanic regions (e.g., Lees, 2007; Lutter et al., 1995). In contrast, others argue that volcanic products are not necessarily the erupted portions of the solidified plutons because they include different compositional ranges, can have different minerals, and resemble different stages of magma evolution.

In this context, my future work will entail addressing the questions concerning the connection between volcanic and plutonic rocks by studying a unique magmatic system, the Ivrea-Verbona Zone in north Italy. In this system, it is suggested that the volcanic and plutonic rocks found in the region belong to one single magmatic system (Quick et al., 2009). This region has a very complex geology because Alpine tectonics juxtaposed the volcanic and plutonic rocks in the same region, which can belong to one eruptive system or multiple magmatic systems. In chapter 5, I give the background information and my proposed future work in this region in order to give insights to volcanic-plutonic connection arguments by high-precision U-Pb geochronology and thermal modeling to constrain the time and length scales of magma bodies during the evolution of this system.

CHAPTER 2

THE ROLE OF EXTENSION ON MAGMA GENERATION IN RIFT SYSTEMS

Tectonic extension and magmatism often act in concert to modify the thermal, mechanical, and chemical structure of the crust. Quantifying the effects of extension and magma flux on melting relationships in the crust is fundamental to determining the rate of crustal melting versus fractionation, magma residence time, and the growth of continental crust in rift environments. Here, together with Josef Dufek, we develop a numerical model that accounts for extension and thermal-petrographic processes in diverse extensional settings in order to understand the coupled control of tectonic extension and magma emplacement on crustal thermal evolution. In this chapter, I introduce the thermal model and show the influence of extensional tectonic rates on the melt volume and evolution in the crust. In the next chapter I show the evolution of melt fraction in the crust and formation and longevity of magma bodies.

Our thermal calculations show that magma flux exerts the primary control on melt generation. Tectonic extension amplifies the volume of melt residing in the crustal column. Diking into an extending crust produces hybrid magmas composed of 1) residual melt remaining after partial crystallization of basalt (mantle-derived melt) and 2) melt from partial melting of the crust (crustal melt). We find that in an extending crust, mantle-derived melts are more prevalent than crustal melts across a range of magma fluxes, tectonic extension rates, and magmatic water contents. In most of the conditions, crustal temperatures do not reach their solidus temperatures to initiate partial melting of these igneous lithologies. Energy balance calculations show that the total enthalpy transported by dikes is primarily used for increasing the sensible heat of the cold surrounding crust with little energy contributing to latent heat of melting the crust (maximum crustal melting efficiency is 6%). Our results demonstrate the importance of tectonics in augmenting melt production, composition, and crustal evolution in active magmatic systems. This work is published as a part of the following paper: Karakas, O., Dufek, J., 2015. Melt evolution and residence in extending crust: Thermal modeling of the crust and crustal magmas. Earth and Planetary Science Letters 425, 131-144. DOI: http://dx.doi.org/10.1016/j.epsl.2015.06.001

2.1. Introduction

The combination of extensional tectonics and magmatic intrusion has long been recognized to alter the thermal and structural properties of the crust in rifting environments (e.g., Brown and Solar, 1998; Callot et al., 2001; Ebinger and Casey, 2001; McKenzie and Bickle, 1988; Mohr, 1982; Sengör and Burke, 1978). These two processes are strongly coupled because: 1) both crustal thinning and magmatic intrusions perturb the geothermal gradient, 2) tectonic extension favors vertical propagation of magma following the path perpendicular to the least principal stress direction (e.g., Anderson, 1951), and 3) extensional processes in the crust can control the growth and emplacement of magmatic bodies (e.g., Corti et al., 2003; Gudmundsson, 2006; Jellinek and DePaolo, 2003). However, the interplay of long-term crustal extension and magma intrusions and their exact control on crustal growth, compositional evolution, and thermal evolution remains poorly constrained (e.g., Dufek and Bergantz, 2005; Fitton et al., 1991; Karlstrom et al., 2010; Thompson and Connolly, 1995).

Much of the energy driving these crustal processes derives from mantle melting. While there is a first-order understanding of the relationship between mantle upwelling and melt generation in the mantle, the amount of melt that enters the crust depends on complex non-linear dynamic processes during mantle melt generation, segregation, and transport (e.g., Liang and Parmentier, 2010). These processes are influenced by mantle heterogeneities and several other parameters such as rheology, rift duration, rifting velocity, mantle potential temperature, mechanical boundary layer thickness, decompression rate, presence of volatiles, strain rates, porosity, compaction length, separation velocity, rupture, and dike opening (e.g., Bialas et al., 2010; Brown and Solar, 1998; Buck, 2004; Foucher et al., 1982; McKenzie, 1985; McKenzie and Bickle, 1988; Pedersen and Ro, 1992; Ruppel, 1995; White et al., 1987; Ziegler and Cloetingh, 2004). The complex processes in the mantle lead to significant differences in the timing and volume of magmatism in different rifts and segments, ranging from minor magmatic contribution to intense volcanic activity (e.g., Ruppel, 1995). An open question is how this variability in tectonic rates and mass and energy flux affect the thermal and compositional evolution of crustal magma.

While in many settings both tectonics and magmatic intrusions clearly influence the thermal state of the crust, these processes are often treated in isolation. Geophysical and geodynamic models typically focus on deformation and thermal changes associated with intrusion events and extensional tectonics (e.g., Baer et al., 2008; Corti et al., 2003). Petrologic and thermodynamic studies often focus on the detailed thermal history of magmatic regions by constructing models that consider magmatic intrusion, differentiation, and crustal melting using either a single intrusion (e.g., Bergantz, 1989;

Huppert and Sparks, 1988) or multiple intrusion events (e.g., Annen et al., 2006; Annen and Sparks, 2002; Dufek and Bergantz, 2005; Pedersen et al., 1998; Petford and Gallagher, 2001; Wells, 1980). However, the thermal state of the crust and crustal magmas have not been examined by models that include the interplay of varying tectonic extension rates and detailed thermodynamic and petrologic processes.

To investigate the long-term thermal evolution of the crust that is subjected to tectonic extension and dike injections derived from the mantle, we present a thermo-mechanical numerical model that solves for coupled kinematic and thermodynamic processes. This model is focused on crust-magma interaction, and we do not replicate detailed mantle processes including generation, segregation, and transport of the melt but rather we focus on the heat transfer processes in the crustal domain as a result of variable extension rates and magma input. We systematically examine a parameter space for magma flux and tectonic extension to quantify the length- and time-scales of magma-crust interaction. We also use two different magmatic water contents to examine crustal rifts both above relatively wet and dry mantle. The model accounts for crustal displacement due to intrusions and for extensional tectonics through a specified kinematic condition. In this way, our model differs from prior thermal-petrologic models. We examine the crustal growth and thermal evolution of crustal magmatic systems and give estimates for the origin, location, fraction, temporal evolution, and amount of melt that can be generated in the crustal section. Our model is applicable to rift environments with a pre-existing continental crust.

2.2. Thermo-mechanical model

A two-dimensional thermal model has been developed to simulate tectonic extension of the crustal column and repetitive magma emplacement in the crust to evaluate the crustal heat transfer and thermal evolution of magmas. This model was modified from the work of Dufek and Bergantz (2005) to account for extensional tectonics. In the model, heat transfer is dictated by two processes: 1) basaltic injections that are emplaced in the crust and transport mass and enthalpy from the mantle and 2) tectonic extension of the crust that accounts for crustal thinning and advects heat away from the axis of extension by displacing the previously heated material. Embedded in the model are parameterized thermodynamic relationships determined with the rhyolite-MELTS thermodynamic software (Gualda et al., 2012) to monitor the geochemical evolution of the system and to accurately partition the latent and sensible heat.

Basaltic injections are modeled as multiple dike and sill intrusions emplaced at different levels in the crust. We assume that each intrusion is emplaced in a stochastic manner; that is, the lengths and timing of intrusions into the crust follow a uniform distribution and thus conform to a specified average flux of magma (see supplemental material). Dikes can extend at all levels in the crust and have widths of 50 m, which is comparable with several field observations (e.g., Williams et al., 1995). The sills are relatively smaller in size (100 m thick and 500 m wide) and are emplaced at the tip of dikes.

We treat the intrusion process as instantaneous as dike emplacement is relatively rapid (e.g., Petford et al., 1993; Rubin, 1992) compared to the much longer crustal thermal evolution considered in this study. The dikes and sills intrude the crust by displacing (effectively advecting) crustal material to accommodate their volume within the crust and cool conductively between successive intrusions. Conduction of heat between the intrusions and the surrounding crust can result in melting of the crustal material and cooling and crystallization of the intrusions. We refer to partially molten crust as the 'crustal melt' and the residual melt after partial crystallization of dikes as the 'residual mantle-derived melt'. At each time step, we investigate the volume and distribution of residual and crustal melts separately.

Tectonic extension in the model is specified as a kinematic condition and satisfies conservation of mass. Feedback between thermal evolution, rheology, and strain rate is not considered in the present investigation nor do we consider the feedback between the crustal stress field and diking (e.g., Callot et al., 2002; England, 1983; Lynch and Morgan, 1990). However, by treating the kinematic condition independently we can examine a wide range of extension conditions and examine the sensitivity of the thermal and melting conditions relative to intrusion scenarios that lack deformation. The kinematic condition advects heat in the crust away from the axis of extension continuously and is motivated by geodetic estimates from several rifting environments (e.g., Papazachos et al., 1992), discussed in section 2.2.3. The extension of the crust in this two-dimensional domain is accommodated by thinning of the crust in a near-axis deformation zone (having a half-width of 10 km, Fig. 2), and generates mantle upwelling to replace the displaced crustal material. Due to upwelling, crustal thickness in the model changes continuously over time, which increases the crustal temperatures as the crust thins.

The simplified model geometry is shown in Fig. 2. Although we included the uppermost mantle to treat evolving crustal thickness, our work focuses on how the crustal thermal structure interacts with the basaltic injections and tectonics; therefore our thermal calculations focus on the upper 30 kilometers. We use this structure as a base case for model comparison and to be generally applicable to a number of natural examples, where the continental crustal thickness typically varies between 10 to 35 kilometers in extensional settings (e.g., Platt, 2007; Zhu et al., 2006).

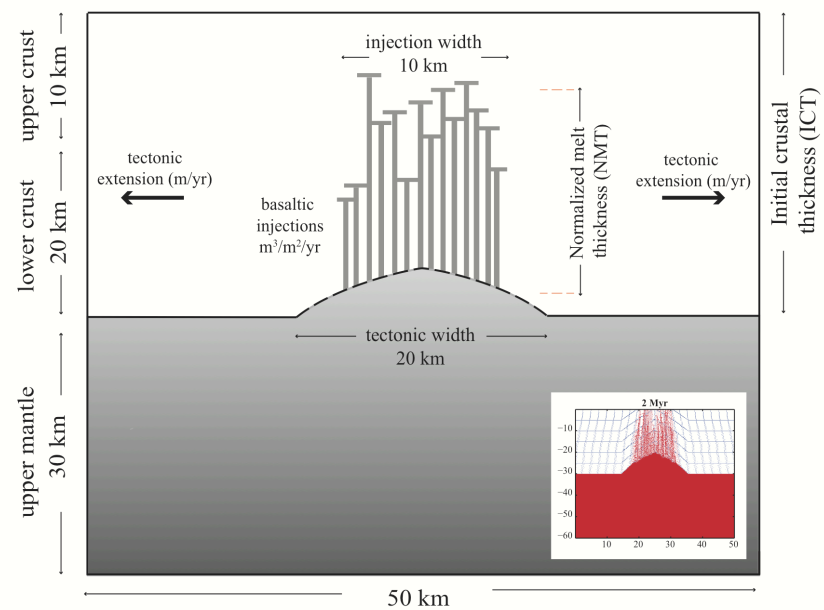

Fig. 2. Conceptual model for thermo-mechanical simulations. The computational domain is an idealized proxy for the crust and uppermost mantle and has three layers: 0-10 km is tonalite, 10-30 km is amphibolite and 30-60 km is peridotite. Diking is localized over the 10 kilometers on the crust-mantle boundary (injection width). Normalizing the two-dimensional area of melt in the domain by the total intrusion width is defined as the normalized melt thickness (NMT). The ratio 'R' represents the ratio of NMT to the initial crustal thickness (ICT). Sills are formed at the tip of the dikes. Emplacement of dikes and sills are accommodated by displacement of the crustal material to conserve mass. Crustal extension is given by a uniform displacement through the crustal column by a defined extension rate. Extension is accommodated by thinning of the crust near-axis (constrained to 10 km half-width) by conservation of mass and induces mantle upwelling. Extension of the crust and mantle upwelling promotes advection of heat in the crust. An example deformation of a regular grid due to extension is shown in the inset. Drawing is not to scale.

We assume tonalitic composition for the initial uppermost 10 km of the model as a proxy for a more silicic upper crust (e.g., Wolf and Wyllie, 1994). The remaining 20 km of the crust in the model is treated as amphibolite (e.g., Helz, 1982; Wolf and Wyllie, 1994) as a proxy for a relatively fertile end-member, similar to observations (e.g., Rudnick and Fountain, 1995) and experimental work (e.g., Beard and Lofgren, 1991; Rapp et al., 1991; Sen and Dunn, 1994; Wolf and Wyllie, 1994).

2.2.1. Initial steady-state geotherm

We calculate the initial steady-state geothermal profile by solving the heat conduction equation with radiogenic heating as a source term, given by

$$k\frac{\partial^2 T}{\partial x_2^2} + \rho H_0 e^{-x_2/l} = 0 \quad . \qquad (1)$$

We assume the boundary conditions

$$T_{surface} = 0°C \quad ; \qquad q_m = q_s + \rho H_0 L \quad . \qquad (2)$$

We assume a representative radiogenic heat production of ~8.0x10^{-10} W/kg near the surface using averaged concentrations from studies on various extensional volcanic regions (e.g., Bailey et al., 2009; Martynov et al., 2010; Price et al., 2010; Turner et al., 1997). We assume that the heat production decays exponentially in the crust down to the characteristic length scale (l) of 16 kilometers (e.g., 1-20 km in Sierra Nevada, Brady et al., 2006; 8-20 km in Dharwar Craton, Kumar and Reddy, 2004). The surface temperature is fixed at 0°C. We use constant mantle heat flux that corresponds to initial surface heat flux of 70 mW/m^2 as a proxy for a variety of tectonic settings (e.g., Currie et al., 2004; Saltus and Lachenbruch, 1991; Shapiro and Ritzwoller, 2004).

2.2.2. Time-dependent thermal modeling and parameterization

The tectonic extension and injection of magma at its liquidus perturb the steady-state thermal profile of the crust. We use a two-dimensional, transient thermal model that accounts for conduction and advection by solving the conservation of thermal energy equation

$$\rho_{mix} c_p \frac{\partial T}{\partial t} + \rho_{mix} c_p v_i \frac{\partial T}{\partial x_i} + \rho_{mix} L \frac{\partial f}{\partial t} = k \frac{\partial^2 T}{\partial x_i^2}, \qquad \text{i=1, 2} \tag{3}$$

where, the velocity (v) of solid material is given by the kinematic deformation condition.

$$\rho_{mix} = f_c \rho_c^{melt} + (1 - f_c)\rho_c^{solid} + f_b \rho_b^{melt} + (1 - f_b)\rho_b^{solid}, \tag{4}$$

$$\frac{\partial f}{\partial t} = \frac{\partial f}{\partial T}\frac{\partial T}{\partial t}. \tag{5}$$

Conservation of mass:

$$\frac{\partial v_i}{\partial x_i} = 0. \tag{6}$$

We note that we simplify the transient equation (3) by neglecting the heat contribution from radiogenic element decay. Although radiogenic heating has an important effect on determining the initial steady-state geothermal profile (1), the energy released by radiogenic decay is significantly lower compared to the energy released by dike intrusions in transient conditions ($E_T^{radiogenic}/E_T^{basalt}$= ~0.01%). This comparison can be achieved by solving simple heat budget equations given below.

The energy budget from crystallization of a dike:

$$E_T^{sensible} = \rho V \int_{T_{geotherm}}^{T_{liquidus}} c_p dT, \tag{7}$$

$$E_T^{latent} = \rho V L, \tag{8}$$

$$E_T^{basalt} = E_T^{sensible} + E_T^{latent}. \tag{9}$$

Energy budget from radiogenic heating:

$$E_T^{radiogenic} = \int_{t_1}^{t_{ref}} \rho V H_0 dt \tag{10}$$

We discretize equation 3 using the finite volume approach described in Patankar (1980). In transient diffusion-advection calculations, we assume a low Biot number for the intrusions (also known as the thermos bottle effect) where the heat transfer between dike injections and the surrounding crust in most magmatic systems is limited by the thermal resistance of the host rock (Bi<<1), and the effect of convection on the thermal evolution of the total magmatic system is comparatively less important (Carrigan, 1988).

We use a non-linear relationship between the melt fraction and temperature (Fig. 3) using parameterized solutions of rhyolite-MELTS software and experiments. For intruding dikes, we use the basaltic andesite composition from Mt. Shasta primitive lava (sample #85-44, Müntener et al., 2001). For amphibolite, we use experimental results from a number of studies (e.g., Rushmer, 1991; Sisson et al., 2005; Wolf and Wyllie, 1994). We use experimental results by Piwinskii and Wyllie (1968) for tonalite.

One of the important components of our model is the application of predictor-corrector algorithm following Voller and Swaminathan (1991) to calculate the numerical convergence for non-linear melt fraction versus temperature relationships gathered from rhyolite-MELTS solutions. This algorithm successfully partitions the total enthalpy change in the system into latent heat and sensible heat during phase changes at each timestep (Petcovic and Dufek, 2005; Voller and Swaminathan, 1991).

Melting of the crust and the state of the intrusions are limited by the thermodynamic properties of the materials and the volume and heat transported by the injections. Following the study of Dufek and Bergantz (2005), we calculate the efficiency of crustal melting as the ratio between the volume of crustal melt based on numerical calculations to the volume of crustal melt based strictly on enthalpy balance arguments (assuming no heat is lost heating the crustal parcels that do not melt). This approach is useful for model comparison where assumptions of lithology and melting properties vary. This is formulated by

$$E\% = 100 \times V_{crust}^{\mathrm{mod.}} / V_{crust}^{eff.} \quad , \qquad (2)$$

$$V_{crust}^{eff.} = \rho_m V_m \left(C_p^m \Delta T_m + L_m \right) / \rho_c \left(C_p^c \Delta T_c + L_c f \right) \quad , \qquad (3)$$

where, $V_{crust}^{\mathrm{mod.}}$ is the volume of crustal melt that is generated when the enthalpy released from basaltic dikes is diffused to the crustal section, and $V_{crust}^{eff.}$ is the volume of crustal melt when the enthalpy released from basaltic material is used only on the crustal material that melts. Subscripts m and c refer to mantle-derived and crustal materials, respectively.

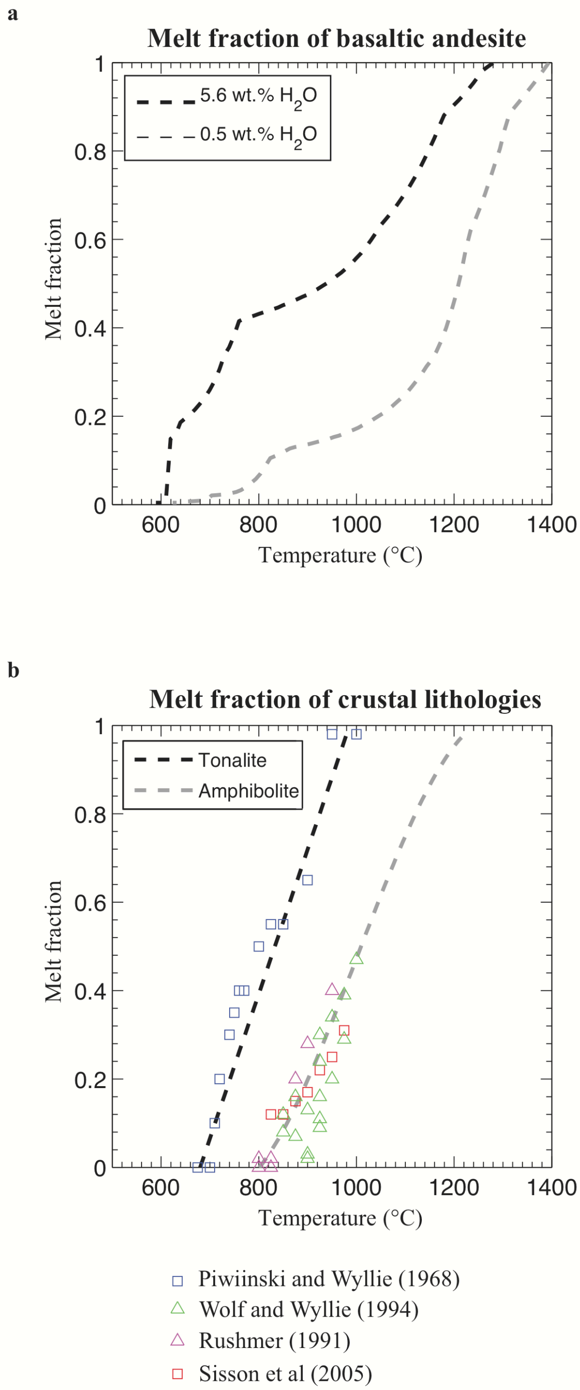

Fig. 3. (a) Equilibrium crystallization of basaltic andesite based on Mt. Shasta primitive lava composition (sample #85-44, Muntener et al., 2001) at 9 kbar. Melt fraction as a function of temperature and water content (5.6 wt.% and 0.5 wt.%) is calculated with rhyolite-MELTS thermodynamic software (Gualda et al., 2012) and (b) Melt fraction as a function of temperature for the crustal lithologies. Parameterized melt fractions of tonalite is based on melting experiments of Piwiinski and Wyllie (1968). Amphibolite parameterization is based on the experiments of Wolf and Wyllie (1994), Rushmer (1991), and Sisson et al. (2005).

2.2.3. Parameter space

We varied extensional rates, magma input, and water content of the intruded magma with the same initial crustal conditions and examine the resulting thermal profile and melting relations in the crusts of different rift environments. Although different initial assumptions will result in variable melting characteristics, constant initial conditions allow for comparison of model sensitivity to melt flux and extension rates. We varied the extension rates between 2, 5, 7, 10, and 15 mm/yr. The extension values of 2 mm/yr and 15 mm/yr are comparable to β values of ~1.5 and ~4 in McKenzie and Bickle (1988), respectively. This range is also comparable to estimated rates in different extensional settings (~1 to ~13 mm/yr, e.g., Bilham et al., 1999; Brothers et al., 2009; Dewey and Lamb, 1992; Morgan et al., 2008; Papazachos et al., 1992; Stamps et al., 2008). The simulations are conducted for up to 2 million years to explore the response of the crust to tectonic extension and dike intrusions over long time periods.

We varied the mean period of time between successive intrusion events from 15 to 100 kyr for each separate set of simulation. We also simulated a set of simulation with no magma flux. Our choice of flux values corresponds to a range of 0 to 10^{-2} m^3/m^2 per year and brackets the magma flux estimates suggested in seismic, gravity, and thermal studies (10^{-4} to 10^{-3} m^3/m^2 per year, e.g., Courtillot and Renne, 2003; Crisp, 1984; Dimalanta et al., 2002; Grunder, 1995). These observations probably underestimate the rate of magmatic input (e.g., Jagoutz and Schmidt, 2013; Jicha et al., 2006) because thermal estimates usually assume efficient enthalpy transfer (e.g., Dufek and Bergantz,

2005) and geophysical calculations neglect some mechanisms, such as sediment subduction, tectonic erosion, and delamination/foundering (e.g., Ducea, 2002; Jagoutz and Schmidt, 2013; Kay and Kay, 1991; Plank and Langmuir, 1998). The flux values of 0.001 and 0.01 $m^3/m^2/yr$ correspond to melt thicknesses of 1 km and 10 km per million years, which is also comparable to melt generation thickness estimates in McKenzie and Bickle (1988), within β values of ~1.5 to 4.

The effect of initial magmatic water content on the crystallization path of the intruded melt is depicted in Fig. 3. In the thermodynamic model, amphibole first appears around 0.40 melt fraction compared to 0.47 melt fraction in the melting experiments of Müntener et al. (2001) at 12 kbar with ~5 wt% H_2O. Due to limited amphibole solid-solution data, the amphibole thermodynamic model only includes pargasite and potentially underpredicts amphibole stability in the hydrous end-member. However, the difference appears to be in an acceptable range (for calculating melt volumes) between rhyolite-MELTS calculations and Müntener et al. (2001) experiments. In our model, we use 0.5 wt.% H_2O (referred to as dry injections) and 5.6 wt.% H_2O (referred to as wet injections, comparable to sample #85-44 B686, Müntener et al., 2001) for the dikes to bracket the range observed in different rift settings (0.5 wt.% to ~6 wt.% H_2O, e.g., Dunbar et al., 1989; Moore and Carmichael, 1998; Roggensack, 2001; Stolper and Newman, 1994; Walker et al., 2003).

2.3. Results

We consider both the long-term crustal thermal evolution that is a result of cumulative intrusions and extension and short-term interactions associated with individual intrusions (Fig. 4). We quantify the volume of crustal and mantle-derived melts, and the efficiency of crustal melting as a function of magma flux, extension rate, and magmatic water content.

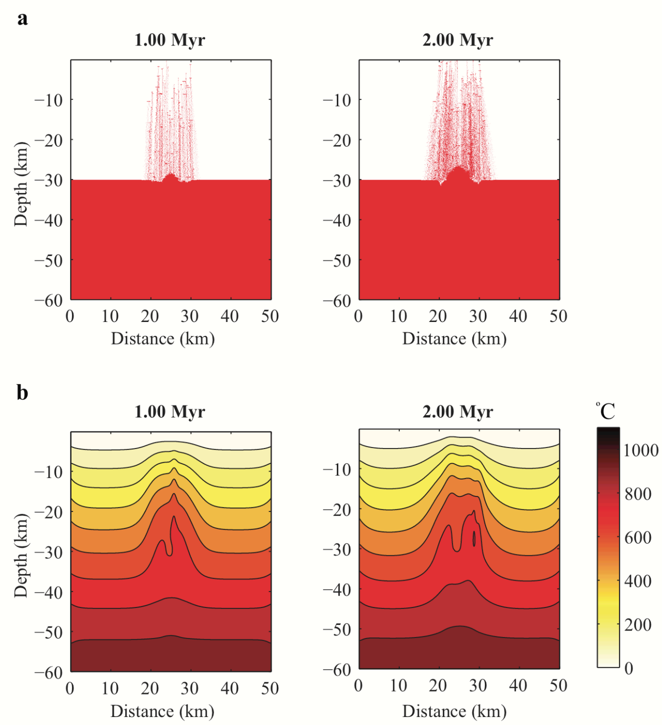

Fig. 4. An example simulation that represents diking, tectonic extension and resulting crustal thermal profile at one point in time. (a) Stochastic dike intrusions from mantle into the crust and (b) temperature perturbation due to intrusion events. The simulation represents an environment with 0.006 $m^3/m^2/yr$ basalt flux and 0.002 m/yr tectonic extension. Water content of the intruded magma is 5.6 wt.%.

2.3.1. Melt thickness in the crust over time

To investigate the effect of magma flux and tectonics on crustal magmas, we examine: 1) a fixed tectonic extension rate with varied magma flux and water content, 2) a fixed magma flux with varied extension and water content, and 3) varied tectonic extension, magma flux, and water contents (Figs. 5-7). Similar to earlier thermal models on melt emplacement in the crust (e.g., Annen et al., 2006; Dufek and Bergantz, 2005), we observe that the amount of melt in the crust is strongly controlled by the magma flux. For a given extension rate, the amount of crustal and residual mantle-derived melt increases with time and increasing flux because progressive accumulation of mantle-derived magma transports mass and enthalpy to the crust (Fig. 5). Mantle-derived melt progressively accumulates in the crust over time when the injection frequency is faster than the time required for conducting the heat away from the intrusion (e.g., Dufek and Bergantz, 2005; Petford and Gallagher, 2001). Due to enthalpy transfer by the intruded melt, the temperatures of crustal lithologies can increase above their solidi and partial melting processes initiate. Eventually, partially molten regions in the crust become a mixture of mantle-derived and crustal melts compositionally. In all conditions examined, the mantle-derived melt is significantly greater than the crustal melt although there is considerable variability (Fig. 5). The maximum amount of total melt is generated in 2 million years when the flux is 10^{-2} $m^3/m^2/yr$. In these conditions, the crustal melt to residual mantle-derived melt ratio is about 1:25 in environments with wet injections and about 1:3 in environments with dry injections.

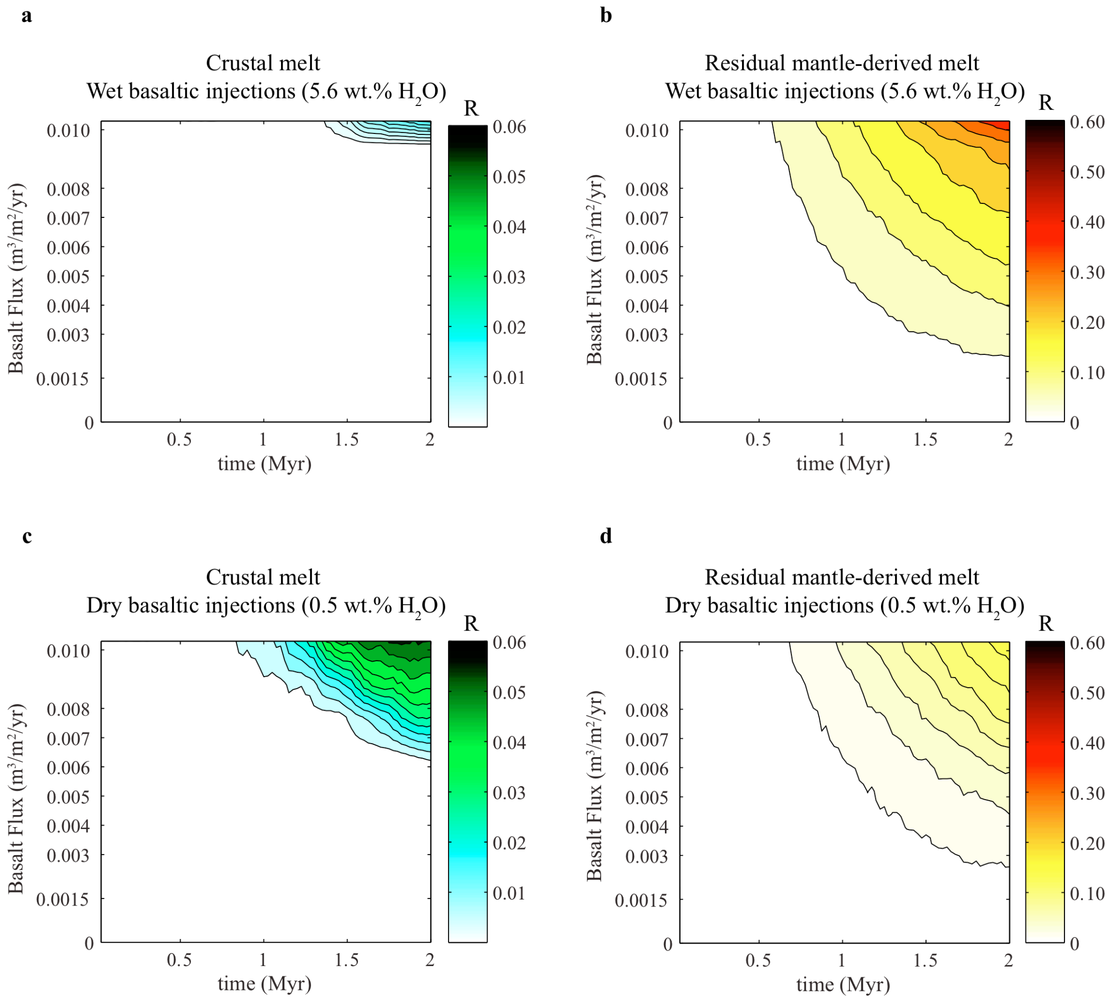

Fig. 5. Evolution of crustal and residual mantle-derived melts as a function of time when the extension is fixed (intermediate, 0.007 m/yr). R is the ratio of normalized melt thickness (NMT, Fig. 2) to the initial crustal thickness (ICT, Fig. 2). A compilation of 16 sets of simulations with basalt fluxes ranging from 0 to 0.010 $m^3/m^2/yr$ are shown. In (a-b) wet basaltic injections and in (c-d) dry basaltic injections are simulated. Note the order of magnitude difference between crustal (a, c) and residual mantle-derived melts (b, d) in the color bars.

We examine the effect of water content in all simulations due to its role in modifying the thermal and compositional evolution of magma (e.g., Green, 1972). As depicted in Fig. 5, in wet injection scenarios, the thickness of residual mantle-derived melt is higher (twice in maximum conditions) and crustal melt is lower (1/4th in maximum conditions) than dry injection scenarios. Such behavior reflects the crystallization behavior of the injected basalt as a function of water content: 1) the liquidus temperature of dry magma is higher than wet magma and thus can induce greater rates of crustal melting and 2) the minerals in the wet magma (e.g., amphibole) are stable in their melt phases at lower temperatures, therefore the melt fraction of wet magma is higher than the dry magma at low temperatures (Fig. 3).

Extension of the crustal column results in mantle upwelling and heat advection by replacing the crustal material, which promotes thicker melt columns (Fig. 6). Extension transports the enthalpy laterally by advecting the heated parcels of the crust, and can increase the amount of melt generated in the crust by up to 5 times when the magma flux is intermediate. Here, we note that the mantle upwelling changes the boundary conditions but not the flux of melt as it is treated independently. In maximum extension conditions (0.015 m/yr extension at 2 million years), the ratio of crustal melt to residual mantle-derived melt thickness is about 1:50 in wet injection scenarios. This ratio is about 1:5 in the dry injection scenarios. The decrease in the amount of crustal melt after ~1.2 million years is attributed to the concentration of the extension and diking at the center of the domain. In the cases of high extension and high flux, the center of the domain is saturated with mantle-derived melt because the crustal material is pushed away by the extensional forces over time. Therefore, further melting of the crust is limited after ~1.2 million years. Similar to previous observations (Fig. 5), the residual mantle-derived and crustal melt amounts are strongly dependent on the water content of the injections. The ratio of crustal melt thicknesses in wet injection to dry injection scenario is 1:4. This ratio is about 2:1 for residual mantle-derived melt thickness.

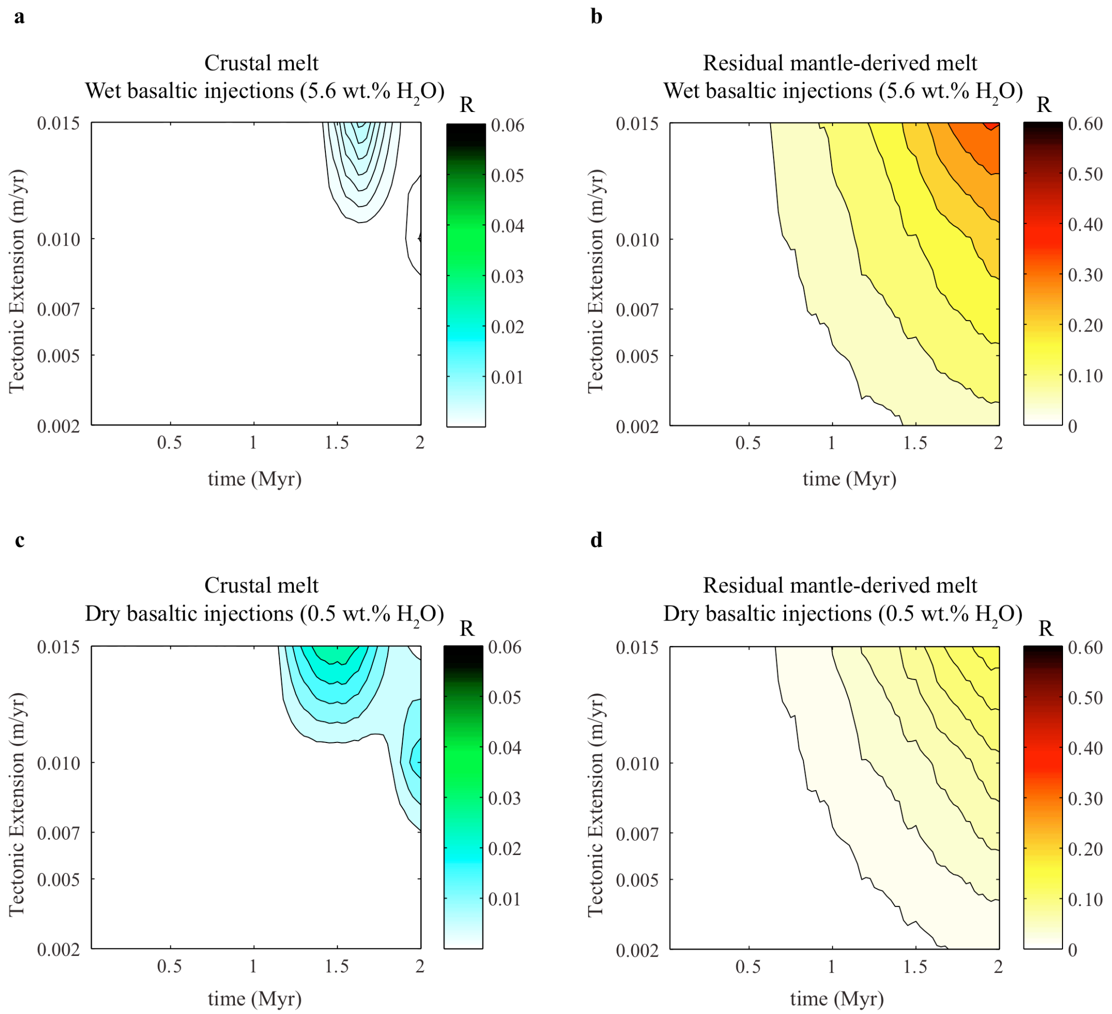

Fig. 6. Evolution of crustal and residual mantle-derived melts as a function of time when the basalt flux is fixed (intermediate, 0.006 $m^3/m^2/yr$). R is the ratio of normalized melt thickness (NMT, Fig. 2) to the initial crustal thickness (ICT, Fig. 2). A compilation of 5 sets of simulations with tectonic extension ranging from 0.002 to 0.015 m/yr is shown. In (a-b) wet basaltic injections and in (c-d) dry basaltic injections are simulated. Note the order of magnitude difference between the crustal (a, c) and residual mantle-derived melts (b ,d) in the color bars.

When both magma flux and tectonic extension are maximized, large accumulations of melt develop in the crust over time (Fig. 7). In the highest flux and extension conditions, the maximum melt thickness with wet intrusions is almost two times larger than the dry conditions. The influence of tectonic extension on melt generation is more prominent when the flux increases (>0.004 $m^3/m^2/yr$ in wet and >0.007 $m^3/m^2/yr$ in dry cases). In addition to the mantle upwelling, high magma flux at the center of the domain heats the crust significantly and extension advects the enthalpy in the crustal column. In comparison with the static models, addition of tectonic extension calculations implies that lower basalt fluxes can generate the same amount of melt volumes in the crust.

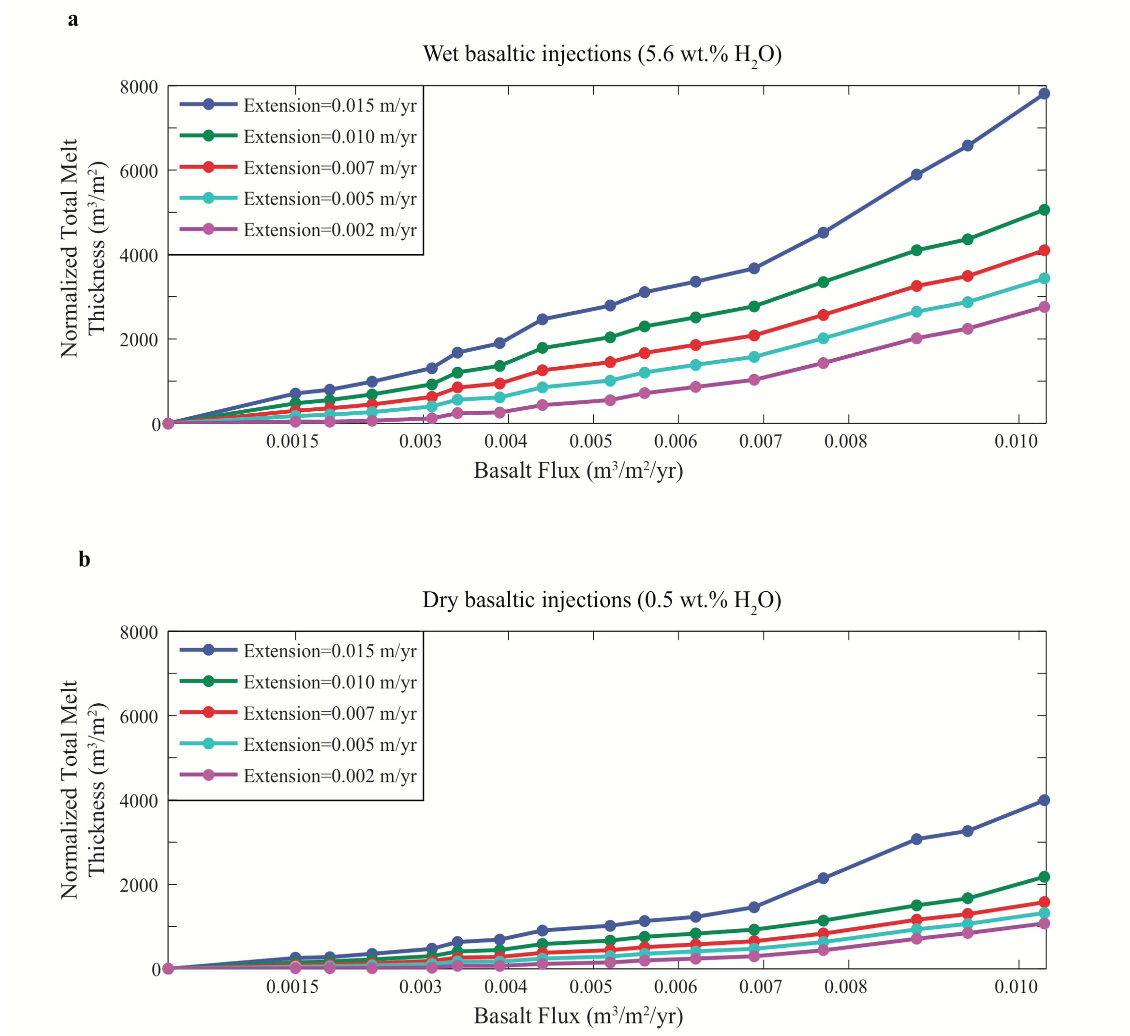

Fig. 7. Normalized thickness of total melt (total of crustal and residual mantle-derived melts) in the crust as a function of basalt flux and tectonic rate. All simulated environments are shown with varying basalt flux (16 flux values, circles) and tectonic extension (5 extension rates, different colored lines). Time is 1 million years after the initiation of tectonic extension and diking events. (a) wet (5.6 wt.% H_2O) and (b) dry (0.5 wt.% H_2O) basaltic injections are simulated.

2.3.2. Efficiency of crustal melting

The crustal melting efficiency calculations show the relationship between the total heat transferred from the mantle by dikes and resulting melting in the crust. In all cases, the efficiency is low and means that almost all of the enthalpy from the intrusions is consumed to increase the sensible heat of the crust (Fig. 8). The maximum efficiency of crustal melting in an environment with wet injections is only ~1% with high flux and ~0.3% with intermediate flux (Fig. 8a, b). In dry injection cases, the maximum efficiency of crustal melting is relatively higher, being ~6% and ~4% when the flux is high and intermediate, respectively (Fig. 8c, d).

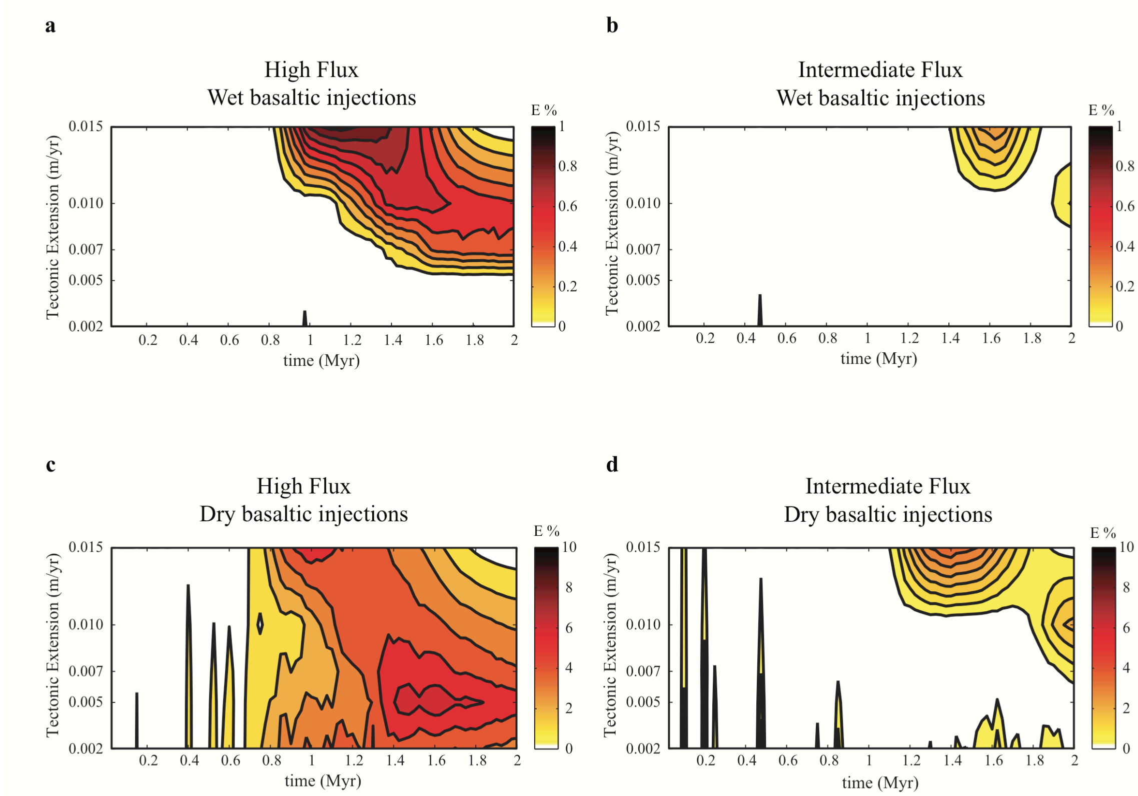

Fig. 8. Crustal melting efficiency as a function of time and tectonic extension. Both wet (5.6 wt.% H_2O) and dry (0.5 wt.% H_2O) basaltic injection scenarios are shown. In (a, c) basalt flux is 0.010 $m^3/m^2/yr$; in (b, d) basalt flux is 0.006 $m^3/m^2/yr$. Note the order of magnitude difference between wet (a, b) and dry injection scenarios (c, d) in the color bars.

Peak crustal melting is observed over a limited time window and is constrained by tectonic extension. This is a result of how we define crustal and mantle-derived materials: we refer to newly crystallized intrusions as mantle-derived material, and the older crust present at the initiation of the simulations as the crustal material. In high flux and extension conditions, the enthalpy from the repeated intrusions that intrude from the center can only melt the previously intruded and solidified mantle-derived material. Therefore, over time, the domain is saturated with mantle-derived material and diluted with the crustal material.

2.4. Discussion of the results

2.4.1. How do extensional processes affect melt location and residence time in the crust?

The advection of crustal material (in response to thinning) enhances melt residence by increasing the thermal gradients compared to previous melting calculations into a static crust (e.g., Annen et al., 2006; Annen and Sparks, 2002; Dufek and Bergantz, 2005; Petford and Gallagher, 2001). Our work shows that the role of extensional processes in augmenting melting is most prominent when also coupled to high magma fluxes (~0.01 $m^3/m^2/yr$, Fig. 7). Under these conditions, tectonic extension amplifies the melt residence in the crust significantly (~3 times thicker melt columns), owing to mantle upwelling and heat advection. The effect of extension is even higher in low fluxes (~0.001 $m^3/m^2/yr$), producing >10 times thicker melt columns when the extension increases from 0.002 m/yr to 0.015 m/yr. However, these extension rates coupled with low melt fluxes cannot create extensive partially molten regions (0.7 km in wet and 0.25

km in dry scenarios) in one million years compared to thick melt columns (>5 km) that can be generated by intermediate to high fluxes.

Therefore, while extensional processes have a significant effect on the thermal evolution of the crust, extension alone is not sufficient to create major crustal magmatic systems. Below a flux value (~0.001 $m^3/m^2/yr$ in wet and ~0.004 $m^3/m^2/yr$ in dry cases), >97% of the emplaced melt solidifies between successive intrusions when extension is low (0.002 m/yr). This is due to the competing effects of: 1) the cooling timescale of the intruded basalt and 2) the period of intrusions that carry enthalpy from the mantle (e.g., Petford and Gallagher, 2001). If the magma flux is high, the heat supply to the magmatic system by dikes will be faster than the heat lost by diffusion. Additionally, the temperature difference between crustal solidus and ambient crustal temperatures decreases with depth, which promotes increasing melting rates in the lower crust (e.g., Dufek and Bergantz, 2005).

Observations in various intraplate and arc settings show that crustal magmatic systems evolve through the contribution of two end-member processes: 1) residual mantle-derived melt from crystallization of intruded magma and 2) crustal melt generated by partial melting of the crust (e.g., Deering et al., 2008; DePaolo, 1981b; DePaolo et al., 1992; Hildreth et al., 1991; Lipman et al., 1978). Our results suggest a combination of these two processes, although hydrous intrusions interacting throughout the crustal column tend to heavily favor residence of mantle-derived melts over crustal melting. This is consistent with recent petrologic studies, particularly those focused on the intrusion of hydrous magmas into the crust (e.g., Bachmann and Bergantz, 2008; Deering et al., 2008; Jagoutz and Schmidt, 2013; Müntener et al., 2001). Trace element and isotopic evidence, where there is sufficient leverage to discern mantle and crustal melts, also indicate a dominant role for fractionation in many regions of relatively thin crust, low basalt flux, and hydrous magmas (e.g., Searchlight Pluton, Gelman et al., 2014; Kohistan, Jagoutz, 2010; Marianas, Peninsular Ranges, Andes, and Aegean Arc, Lee and Bachmann, 2014). However, assimilation of crustal melts occurs in almost all our simulations. While fractionated melts dominate the melt inventory, crustal melt assimilation plays a role in producing compositional diversity (e.g., DePaolo, 1981b), especially in cases where the intruding magma has a high liquidus relative to the solidus of the intruding lithologies (such as our dry intrusion simulations). We note that we only examine the interaction of melt with igneous crust and not with sediments filling the basin developed by extension, which can provide an additional source of material for melting (e.g., McKenzie, 1978).

The maximum efficiency of crustal melting in our simulations is lower than, but comparable to those calculated via convection and over-accretion models (e.g., Huppert and Sparks, 1988; Younker and Vogel, 1976). Crustal melting is more favored in regions where dry melts ascend from the mantle particularly when intruding hydrous lithologies (e.g., Bindeman and Simakin, 2014). It is also significantly controlled by tectonic extension (Fig. 8).

2.4.2. Implications to dry and wet environments

Dry and wet injection scenarios in our model represent two different extensional settings. While highly variable, melt inclusion studies show that back-arc and rifted arcs typically have wet basalts (e.g., Hochstaedter et al., 1990). On the other hand, continental rift magmas, which often have MORB-like melting trends, are typically known as having drier magmas (e.g., Bailey, 1978; Michael, 1995).

We find that wet environments have less crustal contribution compared to dry environments because hydrous dike intrusions are less capable of melting the crust. On the other hand, wet environments have more residual mantle-derived melt compared to dry environments (Fig. 5) because the melt fraction of the dry melt decreases very quickly and stays at lower crystallinity within the same range of temperatures (Fig. 3). This suggests higher crustal melting efficiency in continental rifts compared to rifted arcs and back-arc spreading centers.

However, crustal melting of igneous crust in both wet (arcs) and dry (continental rift) conditions is very low. This is exemplified in petrologic studies in different rift settings. For example, in the Taupo Volcanic Zone, which is a well-studied rifted arc, the petrologic study of Deering et al. (2008) on trace element variations suggested magmatic differentiation of mafic material in the lower-middle crust rather than melting of lower crustal lithologies. Similarly, Bachmann et al. (2007a) suggested mantle-derived magma dominance with very small crustal contribution in the Kos Plateau Tuff in the Aegean arc. In the Main Ethiopian Rift, it is suggested that the erupted evolved magma in the Koka and Nazret magmatic segments is mainly derived from partial fractionation of basalts in shallow crustal reservoirs (e.g., Bilham et al., 1999; Boccaletti et al., 1999).

2.4.3. Caveats and model limitations

Geophysical observations of extension rates are often limited to surface estimates and it is not trivial to calculate the extension at depth because tectonic extension may vary nonlinearly in the crustal column (e.g., Buck, 2004; Villamor and Berryman, 2001).

Nevertheless, our model gives estimates of the melt generated in the crust using the surface measurements as a constraint. Similarly, estimating magma flux (and total mass budgets) for a particular region remains difficult and may vary in time. In our calculations, we focused on general proxy compositions for crustal layering to examine the overall sensitivity of the system to intrusions and extension. Due to these simplifications, caution should be used in making detailed comparisons with specific settings where the lithology may vary.

Additionally, our model does not include rheological feedback in determining dike propagation and emplacement in the crust. Structural discontinuities, heterogeneities, brittle-ductile transition, and magmatic stoping likely influence the melt emplacement depth (e.g., Clemens and Mawer, 1992; Gudmundsson, 2006; John, 1988; Marsh, 1982; Parsons et al., 1992; Petford et al., 1994).

2.5. Conclusions

We developed a thermal model that estimates the time and lengthscales of the melt evolution in the crust in different rift settings given their basalt flux, extension rates, and magmatic water contents. Our simulations indicate that geologically reasonable fluxes (>0.004 $m^3/m^2/yr$) of hydrous magmas (5.6 wt.% H_2O) with intermediate-high extension conditions (>0.005 m/yr) promote extensive mush regions with long residence times (>10^5 years). The evolution of melt in the crust is primarily controlled by the magma flux. The control of tectonic extension is prominent in high flux conditions and increases the amount of melt significantly. The total melt in the crust is a mixture of crustal and mantle-derived material with mantle-derived melt dominating the overall volume. Dry injections result in higher crustal melting efficiency compared to wet basaltic injections, however, even with the optimal conditions, the maximum crustal melting efficiency is very low (~6%).

CHAPTER 3

MELT FRACTION AND RESIDENCE IN EXTENDING CRUST

This chapter focuses on the formation and evolution of mush regions and two-dimensional distribution of melt fraction in the crustal portions of diverse rift settings, using the thermal model and conditions of (Karakas and Dufek, 2015). We particularly examine the melt as it evolves in the upper and lower crust in response to basalt flux and tectonic extension. In the lower crust, an extensive mush region develops for most of the conditions. Upper crustal crystalline mush is produced by continuous emplacement of magma with geologically reasonable flux and extension rates on timescales of 10^6 years. Addition of tectonic effects and non-linear melt fraction relationships demonstrates that the magma flux required to sustain partially molten regions in the upper crust is within the range of estimates of magmatic flux in many rifting regions (~10^{-4} to 10^{-3} km^3/yr) and at least an order of magnitude lower than previous modeling estimates. This work is published as a part of the following reference: Karakas, O., Dufek, J., 2015. Melt evolution and residence in extending crust: Thermal modeling of the crust and crustal magmas. Earth and Planetary Science Letters 425, 131-144. DOI: http://dx.doi.org/10.1016/j.epsl.2015.06.001

3.1. Introduction

It is widely accepted that large volumes of magma can emplace in the crustal portions of rift settings (e.g., McKenzie and Bickle, 1988; White and McKenzie, 1989; White, 1993), however in many systems, the origin, longevity, and location of melt in the crust remain controversial (e.g., Deering et al., 2011; Schmitt and Vazquez, 2006). A key question is how the mass and energy are balanced in the crust in response to magma emplacement and extensional tectonics. Numerical and geochemical models have suggested either partial melting of the crust (e.g., Bindeman and Simakin, 2014; Conrad et al., 1988; Fyfe, 1973) or fractional crystallization of the parental magma (e.g., Baker et al., 1977; Barberi et al., 1975; Jagoutz, 2010; Mahood and Baker, 1986; O'Hara, 1977) as the main process that explains crustal layering and petrologic diversity observed in volcanic settings. It is likely that both processes operate to different degrees (e.g., DePaolo, 1981b), but in many systems quantitative understanding can remain elusive. Understanding the physical parameters that determine crustal melting versus residence of mantle-derived magmas in the crust has a bearing on the mass balance of rifts and the generation of new crustal material (e.g., Condie, 1982; Rudnick and Fountain, 1995; White et al., 2006).

A closely related issue is that of melt residence time in crustal domains. Observational evidence from exposed plutons and erupted volcanics constrains our current understanding of crustal thermal evolution. Long residence times at low melt fractions have been often argued for crustal magmas (e.g., Bachmann et al., 2007a; Hildreth, 2004; Reid et al., 1997). In opposition to this, others have argued that, if the magma bodies do not erupt on relatively short timescales, then they must completely solidify to form plutons (e.g., Glazner et al., 2004; Tappa et al., 2011). The key to understanding the generation and thermal and compositional evolution of crustal magmas is 1) determining the thermal budget of these systems, and 2) assessing the relative amount of crustal melt versus fractionated melt derived from the mantle.

Here, we quantify the volume of crustal and mantle-derived melts, melt fraction, longevity of connected melt pockets, and the efficiency of crustal melting as a function of magma flux, extension rate, and magmatic water content using the assumptions and conditions of (Karakas and Dufek, 2015). For consistency, we show the results of the high and intermediate flux, intermediate tectonic extension in dry and wet injection scenarios.

3.2. Results

3.2.1. Area of the Melt Residing in the Crust

We quantify the melt fraction and the area it covers in the crustal domain when the time is 1×10^6 years. The maximum fraction of melt is 0.55 in simulations with wet injections when the flux is high (Fig. 9a) while a melt fraction of 0.40 covers the significant portion of the melted area (~30 km^2). The maximum melt fraction is 0.35 when the basalt flux is intermediate (Fig. 9b) while the melted area is mainly dominated by 0.2 – 0.3 melt fraction. In the environments with basaltic injections with low water content, the high basalt flux (Fig. 9c) shows a maximum melt fraction of 0.25 while the dominant melt fraction is ~0.1 and covers an area of ~65 km^2. Our results indicate that water content has a primary control on the melt fraction in the crust. The melt fraction produced by wet basaltic injections is higher than dry injection conditions in general. In dry scenarios the mush is highly crystalline (more evolved melt) while wet injections tend to produce mushes with higher melt fractions (less evolved melt).

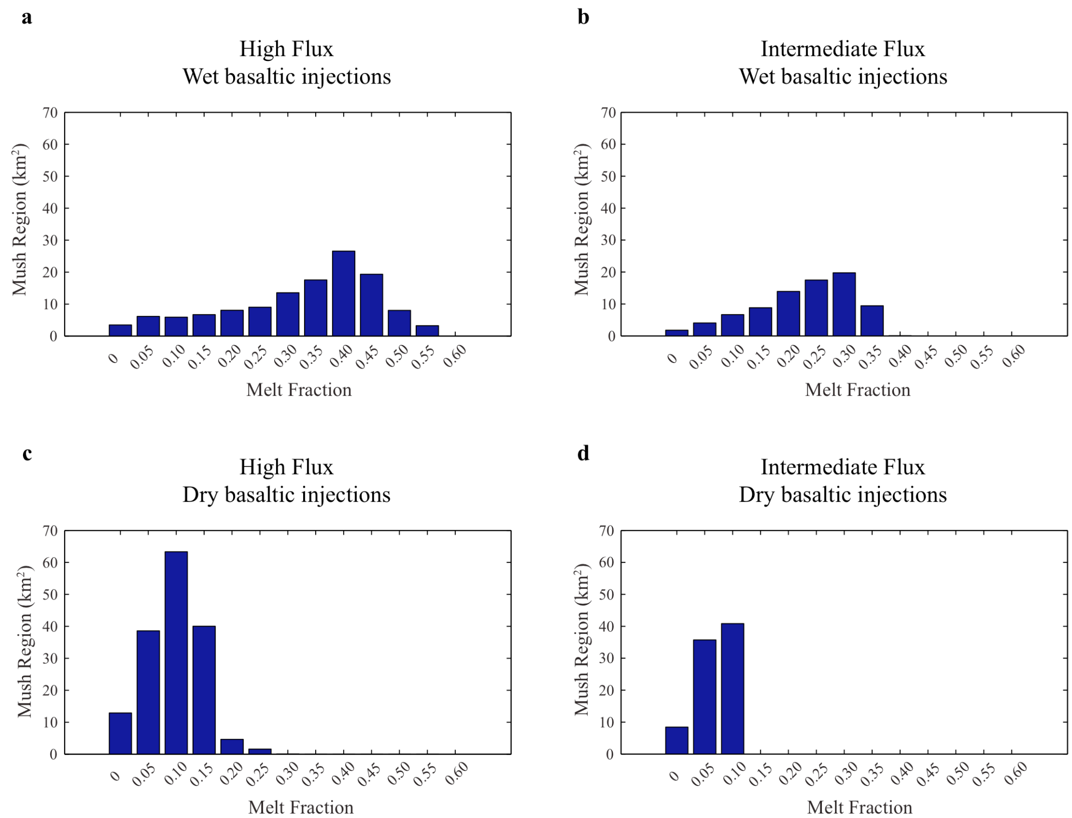

Fig. 9. The area that the melt covers in the crustal domain and corresponding melt fraction after 10^6 years of basaltic injections. Both wet (5.6 wt.% H_2O) and dry basaltic injection (0.5 wt.% H_2O) scenarios are shown. Tectonic extension is 0.007 m/yr for all the simulations. In (a, c) basalt flux is 0.010 $m^3/m^2/yr$; in (b, d) basalt flux is 0.006 $m^3/m^2/yr$. The maximum, mean, and dominant melt fractions are primarily controlled by the water content of the injected dikes. In the cases with wet injections, the mush region shows higher melt fractions. Basalt flux has a secondary control on the melt fractions.

3.2.2. Mush regions in the lower and upper crust

An extensive area of crystal-rich mush is developed in the lower crust with high and intermediate flux at intermediate tectonic extension (Fig. 10). In wet injection scenarios, the melt fraction is higher in general and covers a more extensive area compared to dry injection scenarios. The melt fraction increases towards the center of the mush body along the axis of extension and is maximum at the base of the amphibolitic lower crust. This is also true for the tonalitic upper crust when the conditions permit upper crustal mush generation. In both cases, the partially molten region that straddles the center of the domain buffers cooling through the release of latent heat, and therefore, preserves the heat at the center.

The upper crust starts to develop a persistent melt domain in wet and high flux conditions after approximately one million years (Fig.10a, c), although periodically small bodies form and solidify in the upper crust with shorter incubation periods. Additionally, in dry injection conditions with intermediate flux, an upper crustal crystal-rich mush develops after two million years (Fig. 10d) due to high liquidus temperatures of the dry injections. This suggests that it is possible to create sustained upper crustal melt regions with geologically reasonable basalt fluxes (>0.006 $m^3/m^2/yr$) on million year timescales. The upper crustal mush is larger and has higher melt fraction in wet injection scenarios compared to dry scenarios.

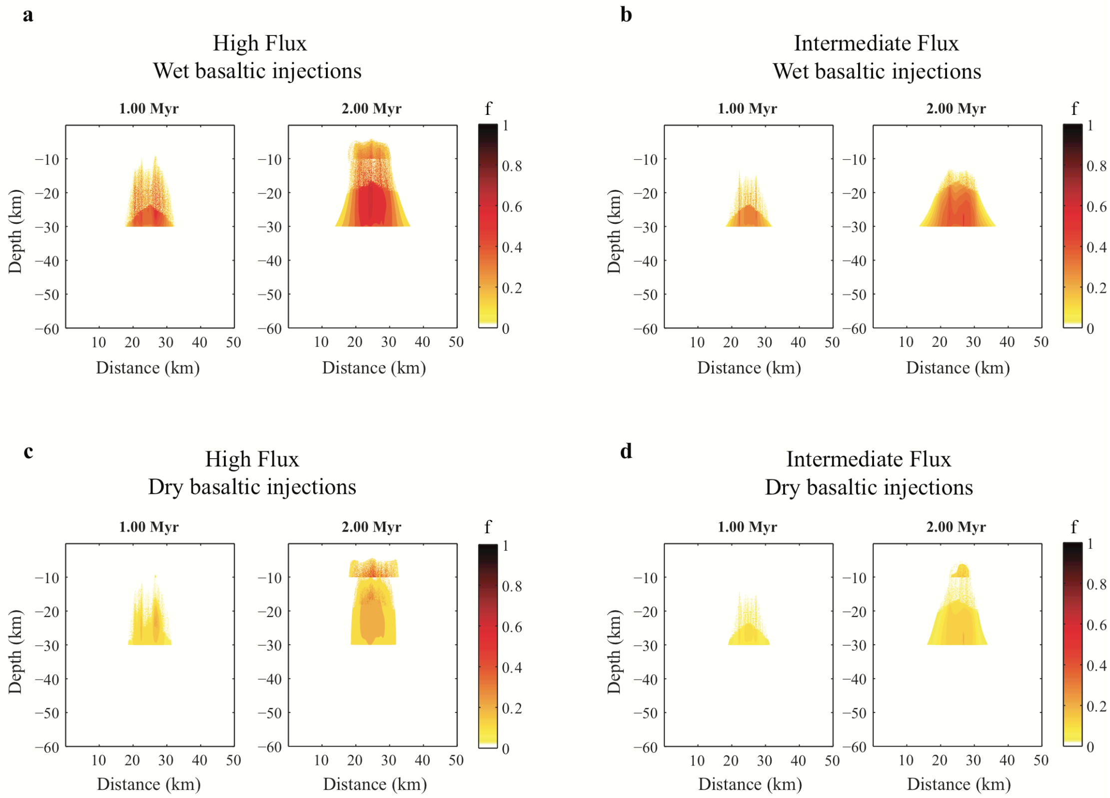

Fig. 10. Distribution of melt fraction (f) in the two-dimensional crustal domain after 1 and 2 million years of tectonic extension and diking events. Both wet (5.6 wt.% H_2O) and dry (0.5 wt.% H_2O) basaltic injection scenarios are shown. In (a, c) basalt flux is 0.010 $m^3/m^2/yr$; in (b, d) basalt flux is 0.006 $m^3/m^2/yr$. Tectonic extension is intermediate (0.007 m/yr) in all simulations.

3.2.3. Melt storage in the crust

Although reasonable flux and extension rates can create extensive areas of melt in the crust, these melt regions often include very low melt fraction and/or can reside in multiple levels in the crust. In order to estimate the evolution, longevity, and continuous size of the melt bodies in the crust, we employ a metric that assumes that neighboring melted sections with melt fractions greater than 0.25 can combine to form individual melt storage systems. Our choice here represents melt exchange for moderate melt fraction in a crystalline (50-75% crystallinity) mush region (e.g., Bachmann and Bergantz, 2004; Mangan and Marsh, 1992; Marsh, 1988).

The water content of the injections exerts an important control on the formation of crustal magma bodies (Fig. 11). A large partially molten region dominates in the crust in wet injection conditions (Fig. 11a, b). This melt is located in the lower crust (Fig. 11a, b) and its growth rate accelerates after 0.5 million years. The temperature of the lower crustal section increases in response to the enthalpy provided by the dike intrusions and the area of melt extend over 250 km^2 (high flux) and 100 km^2 (intermediate flux) in 2 million years (Figs. 11a, b). These estimates are consistent with intrusive volume estimations in the crust of Nicaragua (90 to 180 km^3/km/Ma, Morgan et al., 2008) and Kenya rift zone (250 to 500 km^2, Morley, 1994).

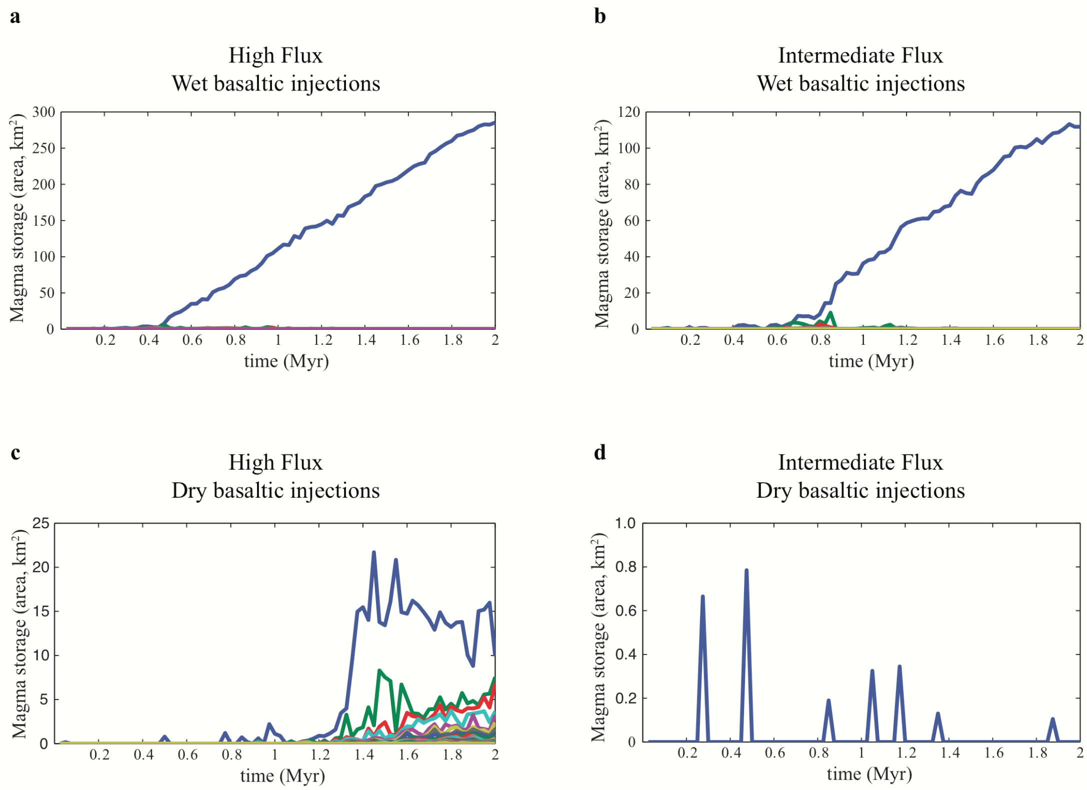

Fig. 11. Longevity of interconnected melt bodies (f>0.25) and their area in the two-dimensional crustal domain. Both wet (5.6 wt.% H_2O) and dry (0.5 wt.% H_2O) basaltic injection scenarios are shown. In (a, c) basalt flux is 0.010 $m^3/m^2/yr$; in (b, d) basalt flux is 0.006 $m^3/m^2/yr$. Tectonic extension is intermediate (0.007 m/yr) in all simulations. Different colors represent individual melt bodies. Note the difference in y-scale in (a-d).

In time, the surrounding small, isolated melt bodies either solidify or join the large partially molten zone. In the simulations with dry intrusions and the highest flux (Fig. 11c), there are a number of individual melt pockets; however, all of them are relatively small in size (<20 km^2). The melt pockets are small (<1 km^2) with dry intrusions and intermediate flux (Fig. 11d).

3.3. Discussion

Our results indicate that it is thermally viable to create extensive partially molten regions in the crust (>10 km thick in two million years, Fig. 10) with geologically reasonable flux and extension rates (>0.004 $m^3/m^2/yr$ and >0.005 m/yr for most cases). In the lower crust, these melts reside at low melt fraction (<0.2 in most of the cases) and persist in part because they are buffered by latent heat at high crystallinity (e.g., Dufek and Bergantz, 2005; Huber et al., 2009; Marsh, 1981). The assumptions of localized tectonic extension and repeated diking events likely contribute to heat preservation and construction of mush regions. There are relatively limited geophysical constraints on the expanse and residence time for lower crustal melt that focus on: 1) petrologic observations on exhumed lower crustal terrains that include for example Ivrea, North Italy (e.g., Sinigoi et al., 1994; Voshage et al., 1990; Wedepohl, 1995); Kohistan, Pakistan (e.g., Burg, 2011; Dhuime et al., 2009; Jagoutz et al., 2007; Jagoutz and Schmidt, 2012); Fraser and Musgrave Ranges, Australia (e.g., Fletcher et al., 1991; White et al., 1999); Sierra Nevada and Peninsular Ranges, California (e.g., DePaolo, 1981a; Pickett and Saleeby, 1993); Fiordland, New Zealand (e.g., Klepeis et al., 2003) and 2) seismic studies exemplified by Main Ethiopian Rift (e.g., Keranen et al., 2004) and Western United States (e.g., McCarthy and Thompson, 1988). However, while useful, these observations provide a limited picture of the temporal history of lower crustal magmas.

While relatively little is known about lower crustal mush regions, observations of eruptive products (e.g., Bachmann and Bergantz, 2008; Hildreth, 1979; Hildreth, 2004) provide valuable information about processes in the mid-upper crustal mush reservoirs.

Although our study does not model magma segregation and extraction from crystalline residue, our results suggest thermal conditions that can allow for development of upper crustal mush systems within reasonable magma flux (>0.006 $m^3/m^2/yr$), extension rate (>0.007 m/yr), and timescales (10^5-10^6 years). High flux (0.01 $m^3/m^2/yr$) and intermediate extension rate (0.007 m/yr) can create large upper crustal mush regions, therefore, increased extension rates will allow for more extensive upper crustal bodies. Additionally, dry injections create an upper crustal mush with intermediate flux due to their high liquidus temperatures. From the initial conditions specified it takes greater than one million years for mid-upper crust to construct mush zones, although certainly crust starting with a higher initial geotherm would necessarily develop mush regions more quickly. The long residence time of many of these systems at low melt fraction is consistent with preferential melt extraction and segregation at these low melt fractions. In the eruptive record, if melt is preferentially extracted at low fraction and some primary melt also erupts it should produce the compositional gaps that are seen in many volcanic series (Dufek and Bachmann, 2010). In this particular case, the compositional gap would be between the intruding basalt and melt in equilibrium with 60-90 % crystals by volume. Based on the experimental studies of similar compositions and conditions, this roughly corresponds to andesitic compositions (e.g., Müntener et al., 2001; Sisson et al., 2005).

The thermal residence time of mid-upper crustal magma bodies has been the topic of much recent work (e.g., Annen, 2009; Gelman et al., 2013) as these systems are important for the assembly of large, caldera forming eruptions. Although some geochemical studies suggest >10^5-10^6 years for longevity of upper crustal melt reservoirs (e.g., Christensen and DePaolo, 1993; Costa, 2008) with potentially short timescales of rejuvenation prior to eruption (e.g., Barboni and Schoene, 2014; Burgisser and Bergantz, 2011; Cooper and Kent, 2014), previous conductive thermal models indicate that systems of the size sufficient to produce caldera forming eruptions persist at those timescales only in high magma flux conditions (10^{-2}-10^{-1} km^3/yr, Annen, 2009). In a recent work, Gelman et al. (2013) suggested that these magma bodies could form and reside in the upper crust with lower fluxes (<5-8x10^{-3} km^3/yr) for longer timescales (1.2 million years with 10^{-2} km^3/yr). These magma emplacement rates are consistent or somewhat higher than estimates from individual large eruptions (10^{-3} to 10^{-2} km^3/yr in Altiplano, de Silva and Gosnold, 2007; 10^{-2} km^3/yr in Taupo Volcanic Zone, Wilson et al., 2006).

Yet, calculations of average magma emplacement rates inferred from long-term volcanic input rates are on the order of 10^{-3}-10^{-4} km^3/yr (Crisp, 1984) and previous studies suggested short residence times of magmas in these regimes (e.g., Tappa et al., 2011). In our model, assuming an injection area of 10 km x 10 km as representative of the areal footprint of large caldera forming eruptions, we estimate 10^{-3} km^3/yr and 4-6x10^{-4} km^3/yr for the highest and intermediate flux values, respectively. For these conditions, we do observe long-lived upper crustal magma reservoirs (>10^5 years), however, for the majority of their lifetimes they are at low melt fraction and might not be eruptible (Marsh, 1981).

3.3.1. Implications to natural settings

Our model indicates two different compositional evolution scenarios in dry and wet magma injection conditions. While in wet environments only one large melt accumulation region evolves through time; a number of melt bodies formed isolated lenses that stagnate at multiple levels in the crust and evolve through time in dry environments. We suggest that these melt bodies will likely evolve compositionally differently because they stall and differentiate at multiple levels in the crust. Therefore, these bodies that come from the same source at approximately the same time are expected to be compositionally distinct, suggesting greater compositional diversity in magmas of environments with dry injections. A similar mechanism was suggested by Bloomer et al. (1989), where they observed variable geochemistry of Kenya rift volcanic rocks that are spatially distributed over a small area (a few tens of kilometers). Bloomer et al. (1989) argued that this variety might show the presence of individual melt pockets at depth or variations in the degrees of partial melting or fractionation.

3.4. Conclusions

In most of the conditions tested, the melt stays at low melt fraction at both lower and upper crustal depths for the majority of its history. We find that under optimal conditions magma can stay molten in the mid to lower crust on million-year timescales. Under the conditions tested in the model, magma flux exerts a dominant control on the volume and longevity of melt, with extensional tectonics and magmatic water content also imposing strong controls on melt generation and longevity in extending crust.

CHAPTER 4

CASE STUDY: THERMAL AND PETROLOGIC CONSTRAINTS ON LOWER CRUSTAL MELT ACCUMULATION IN THE SALTON SEA GEOTHERMAL FIELD

The Salton Sea Geothermal Field is one of the youngest volcanic regions (5.9-0.5 ka) and hottest geothermal systems in the continental United States. Delineating heat and mass transfer in the crust of magmatic geothermal systems is important for geothermal energy exploration and economic geology, however quantification of the heat transfer in these systems coupled to magma evolution remains elusive. In the Salton Sea Geothermal Field, concurrent volcanism, extension, subsidence, and sedimentation over the past 0.5 to 1.0 Ma have created the thermal and compositional structure of the crust in this region. Here, in collaboration with Josef Dufek, Margaret Mangan (USGS), and Heather Wright (UGSG), we investigate the flux of magma required in the lower crust to drive the observed surface heat flux in this system and explain the observed petrologic constraints. To address this coupled intrusive-tectonic-sedimentation problem, we use a two-dimensional finite volume model and investigate the compositional and thermal evolution of the lower crustal melt underlying the Salton Sea Geothermal Field. We find that given a range of estimated basalt fluxes, lower crustal melt evolves from fractional crystallization of the basalt with minor crustal assimilation, in agreement with $\delta^{18}O$ isotope results. We bracket the long residence time melt fraction between 0.2-0.4, which can stay in a mush state on ca. 10^5-year timescales. In order to thermally sustain the partially molten lower crustal reservoir in this young thin system, we argue that the melt flux must be close to the flux values of 0.008 to 0.010 $m^3/m^2/yr$, which is within the range of long-term magma fluxes constrained by several studies.

4.1. Introduction

The mass and the enthalpy balance in the crust of rift settings is essential for understanding their thermal budget and magma evolution, but has been poorly constrained by petrologic, thermal, and geophysical studies (e.g., Mohr, 1982; Sengör and Burke, 1978; Ziegler and Cloetingh, 2004). In many rift settings, it is suggested that the primitive magma emplaces at deep crustal levels as dikes, evolves thermally and compositionally, intrudes in the upper crust and continues to evolve in response to the new temperature and pressure conditions in the shallow crust (e.g., Corti et al., 2003; DePaolo and Daley, 2000; Pearce and Cann, 1973; Schmitt and Vazquez, 2006). Tectonic extension and magma recharge significantly control the thermal and compositional evolution of magma in rift settings, particularly in areas of high extension and high heat flux (Daniels et al., 2014; Deering et al., 2011; Karakas and Dufek, 2015). In several rift environments, a wide range of eruptive styles, magma volumes, compositions, and timescales have been reported (e.g., Costa, 2008; Wilson, 2008). However, quantitative constraints that relate the crustal heat transfer and regional tectonomagmatic processes is lacking.

The Salton Sea Geothermal Field (SSGF) of the western USA is an exceptional environment to study the interaction of tectonic extension and magma emplacement. This area is one of the hottest and largest geothermal systems on Earth with measured energy production of ~1 TWh/yr with a greater potential in the future (Bertani, 2005; Hulen et al., 2002). Despite the number of observations that explained the tectonic evolution and erupted products of this system (Brothers et al., 2009; Lachenbruch et al., 1985; Schmitt and Hulen, 2008), controversy remains on the lower crustal heat source, melt fraction, origin of magma, and the potential heat budget of the system.

A major topic of debate is the origin of bimodal eruptive products composed of basaltic subsurface dikes and rhyolite lavas (Robinson et al., 1976), which include granitic, mafic, and sedimentary xenoliths. A number of mechanisms have been suggested for the formation of these magmas in the Salton Trough: 1) fractional crystallization of parental magma to form the evolved high-silica end-member (Herzig and Jacobs, 1994; Schmitt et al., 2013), 2) melting of the crustal lithologies in response to basalt emplacement (Hulen et al., 2002), 3) partial melting of mantle peridotite (Robinson et al., 1976), and 4) partial melting of previously intruded, hydrothermally altered basalt (Schmitt and Vazquez, 2006). The key to understanding the heat transfer and magma evolution in this system is constraining the energy and mass influx from the mantle in the form of basalt intrusions.

Here, we quantify the thermal and compositional evolution of lower crustal melt accumulation in the SSGF by using a thermodynamic model that simulates tectonic extension, sedimentation, and diking in the crust from initiation of extensional tectonic processes at 1 Ma to present. We simulate a range of different initial scenarios to match the present day configuration of the SSGF magmatism and give quantitative constraints to lower crustal magma evolution. We show that the lower continental crust of the SSGF must be displaced by dike intrusions and tectonic extension over time. In all our cases, the results indicate that the lower crustal magma reservoir is mainly derived from fractional crystallization of primitive magma with minor assimilation of crustal material.

4.2. Geologic Setting

4.2.1. Tectonic evolution of the Salton Trough

The Salton Sea Geothermal Field is one of the three northernmost pull-apart basins (Fig. 12) generated by extension and subsidence due to the San Andreas Fault (SAF) and the Imperial Fault (IF) offset (Elders et al., 1972; Lonsdale, 1989). The present day tectonic configuration of the Salton Sea is suggested to be a result of two-stage tectonic evolution, which started ~500 ka by block rotation between San Jacinto Fault (SJF) and SAF (Brothers et al., 2009). The second stage of evolution developed the SAF-IF step-over that concentrated extension in two locations: the Mesquite Basin and the southeastern shore of the Salton Sea. The extension rate in SSGF in the last 500 ka, calculated by subsidence and sedimentation rates, is 11.5 mm/yr (Brothers et al., 2009). Subsidence (~3 mm/yr, Larsen and Reilinger, 1991) has been approximately matched by sedimentation (2.2-3.8 mm/yr, Schmitt and Hulen, 2008) and kept the surface elevation near sea level (Lachenbruch et al., 1985). The wells in the Salton Trough measure an average surface heat flow of 140 mW/m^2, which is more than twice the adjacent Sierra Nevada (39±12 mW/m^2, Sass et al., 1971). The heat flow in the SSGF locally peaks to > 600 mW/m^2 (Lachenbruch et al., 1985).

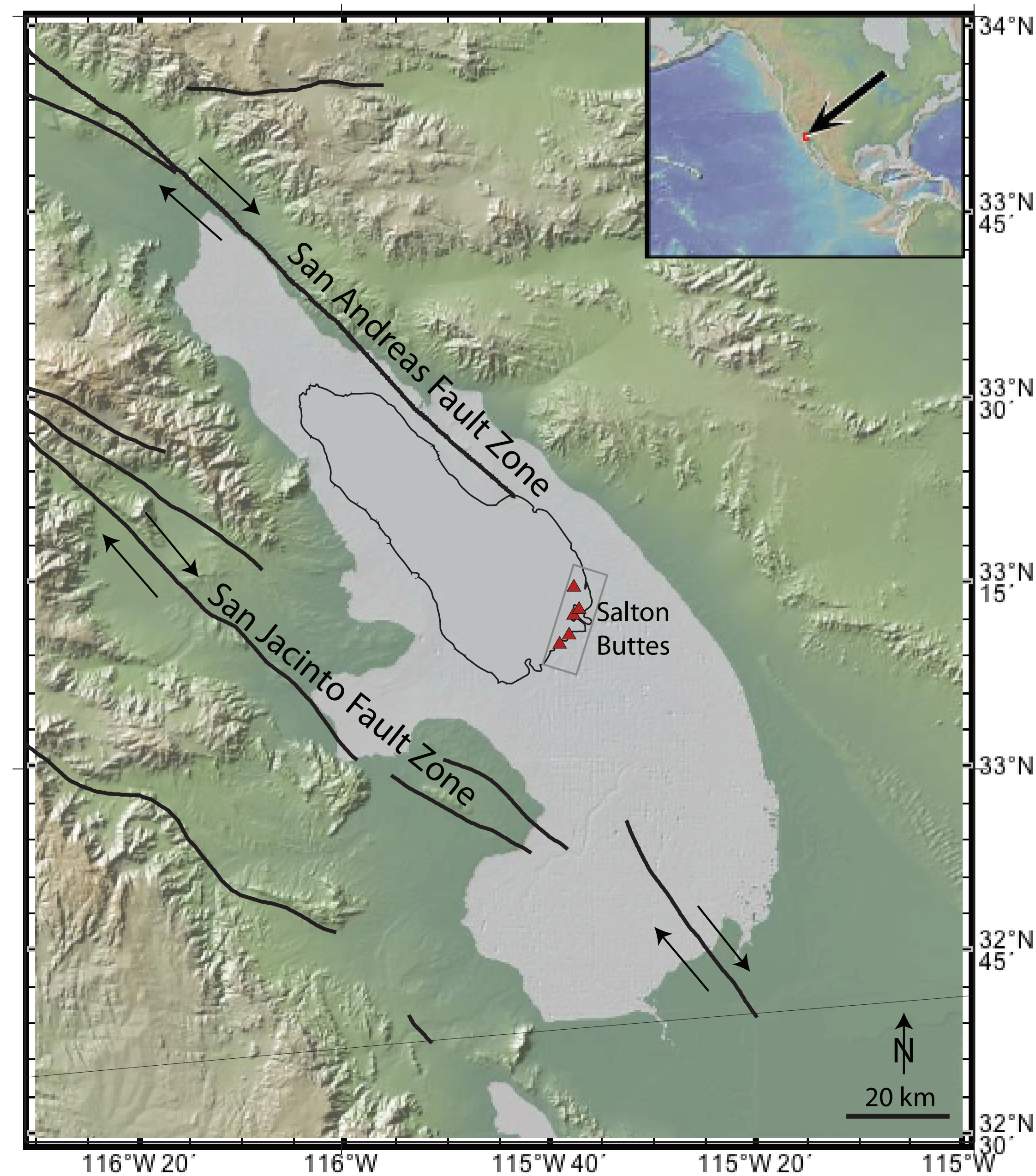

Fig. 12. Map of the Salton Trough (30 m DEM). Major faults in the area and location of the Salton Buttes are shown.

4.2.2. Crustal layering in the Salton Sea region

The compositional crustal layering in the Salton Sea (Fig. 13) area is constrained by seismic experiments (e.g., Fuis et al., 1984), scientific boreholes, and xenoliths present in the erupted products (Schmitt and Vazquez, 2006). The uppermost part of the crust (<5 km) is unconsolidated sediments deposited from Colorado River sediments, mainly sand, silt, clay, sandstone, siltstone, and claystone (Fuis and Kohler, 1984; Herzig and Elders, 1988a). This layer is underlain by metamorphosed sediments (Muffler and White, 1969), which are mainly composed of greenschist facies metasedimentary rocks (Herzig and Jacobs, 1994; Robinson et al., 1976). Above 10 km, seismic wave velocities increase gradually with depth while retaining physical continuity, suggesting hydrothermal alteration and thermal metamorphism of sediments due to rapid burial and heating (Fuis et al., 1984; McDowell, 1987; McKibben and Hardie, 1997). The lower 10-18 km of the crust is inferred to be a gabbroic layer, formed by extension-related magma emplacement (Lachenbruch et al., 1985), which also has been observed in the shallower crust by the geothermal boreholes (Elders and Sass, 1988).

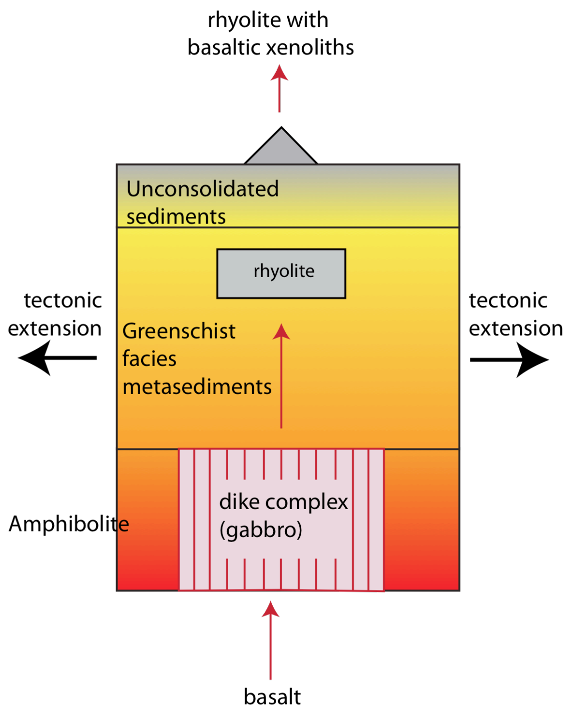

Fig. 13. Conceptual three-layered model for initial Salton Sea crustal layering and magmatism.

4.2.3. Magmatism in the Salton Sea Geothermal Field

Magmatism at the surface is restricted to five rhyolitic domes -the Salton buttes- on the southeastern shore of the Salton Sea (Schmitt and Hulen, 2008). The domes lie over a 7 km-long horizon that is suggested to delineate the extensional processes at depth, and likely share a common feeder dike at depth (Kelley and Soske, 1936; Robinson et al., 1976). Rhyolitic lavas from Salton buttes contain xenoliths that include granophyres and amphibole-bearing basalts (Schmitt and Vazquez, 2006). In addition to xenoliths, data from wells that cut through dikes and sills also show bimodal magmatism: rhyolitic bodies and basaltic dikes, sills, and flows (Robinson et al., 1976; Schmitt and Vazquez, 2006). Schmitt and Vazquez (2006) note multiple populations of zircon crystallization, which they infer to be generated by multiple thermal pulses that caused melting and recycling of preexisting basaltic crust. Using whole-rock Nd-isotopes and zircon oxygen isotopes, Schmitt and Hulen (2008) developed a petrogenetic model where they argue that injection of basaltic magma re-melted the hydrothermally altered MORB-like basaltic crust and resulted in rhyolitic magmatism. They argue that this re-melting occurred episodically over 400 ka and was localized in extent.

A recent discovery of extrusive rhyolites and tuffs at 1.7 km depth in the eastern SSGF shows ancient volcanism in the area and is a stratigraphic marker that shows the age of previous volcanism and sedimentation rates (Hulen and Pulka, 2001). Scientific boreholes cut two nearby extrusive rhyolitic bodies with thickness of 150 and 300 meters. Overlying the rhyolitic bodies are the tuff layers, showing the same compositional and textural characteristics as the underlying rhyolites. The age of this rhyolite bodies were estimated as ~0.73 Ma, by comparing the age of a nearby tuff deposit about 4 km north of the buried rhyolite (Hulen and Pulka, 2001). This nearby deposit is located at 1.7 km depth and suggested to be the distal fallout deposit of Bishop Tuff eruption (Herzig and Elders, 1988a, b) because of its compositional similarity as the Bishop Tuff deposits (dated as ~0.76 Ma, Van den Bogaard and Schirnick, 1995).

4.3. Transient thermal model

A two-dimensional finite volume model is constructed to investigate the thermal evolution of the Salton Sea starting from the initiation of spreading until present. This model is modified from (Karakas and Dufek, 2015) to account for Salton Sea conditions. The model includes extension of the crustal column, sedimentation at the surface, and magma emplacement into the crust (Fig. 14). Tectonic extension and sedimentation follow conservation of mass by active extension of the crustal column and continuous sedimentation on the surface. These kinematic conditions are constrained by seismic interpretations (Brothers et al., 2009); but do not include detailed topology of faults in the region. The tectonic extension in the model is accommodated by thinning of the crust near the center of extension. Concurrently, sedimentation results in thickening of the uppermost sedimentary layer and subsidence of the lower layers. Tectonic extension, sedimentation, and subsidence have significant impact on crustal heat transfer by advecting the heated crust through time.

Magma emplacement in the crust is assumed to be incremental as a series of dikes and sills. The average flux into the crust is imposed through a mean injection frequency, allow the exact timing of individual intrusion is stochastic and described by a uniform distribution. To conserve mass, emplaced dikes are accommodated in the crust by laterally displacing material to either side and sills are accommodated by displacing crustal material downward. Dikes are intruded from the base of the crust up to a maximum of 10 km depth. This range of depths is consistent with seismic observations of a gabbro layer between ~10 to ~18 km depth (Fuis et al., 1984). It is assumed that sedimentation and tectonic extension do not affect the depth of intrusions.

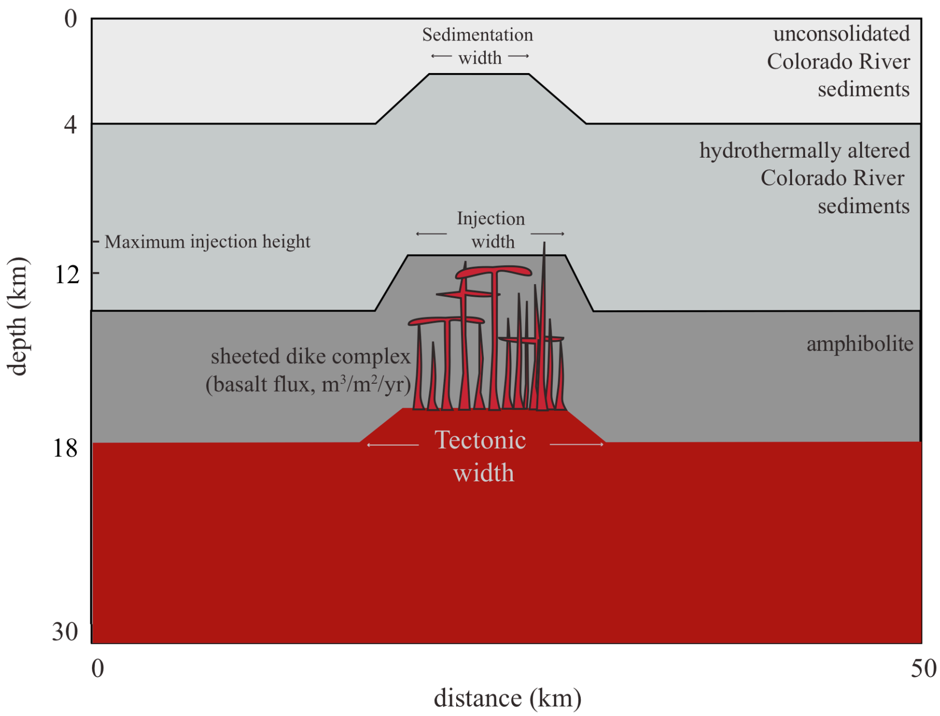

Fig. 14. Conceptual model for Salton Buttes magmatism. The computational domain is an idealized proxy for crustal column and uppermost mantle and consists of three layers: 0-4 km is unconsolidated sediments, 4-18 km is hydrothermally altered metasediments, and 18-30 km is mantle peridotite. Sedimentation is focused over a width at the surface (sedimentation width) and subsides lower crustal layers due to conservation of mass. Sedimentation and subsidence rate are at near-equilibrium, which keeps the surface level at sea level. Diking is localized over the 10 kilometers on the crust-mantle boundary (injection width). Sills are formed at the tip of the dikes. The length of the dikes are randomized while maximum height for dike injections is set at 10 km. Emplacement of dikes and sills are accommodated by displacement of the crustal material to conserve mass. Crustal extension is informed by a uniform displacement through the crustal column by a defined extension rate. Extension is accommodated by thinning of the crust near-axis (tectonic width) by conservation of mass and induces mantle upwelling. Extension of the crust and mantle upwelling promotes advection of heat in the crust. Drawing is not to scale.

The thermodynamic evolution of the crust due to magma emplacement, extensional tectonics, and sedimentation is calculated solving time-dependent thermal diffusion and advection equations. Detailed calculations and assumptions of the thermal model are explained in Karakas and Dufek (2015). Evolving geochemistry and latent and sensible heat of the system are calculated by parameterization of the non-linear melt fraction relationship as a function of temperature using rhyolite-MELTS thermodynamic software (Gualda et al., 2012) for different crustal lithologies and emplaced basalt (Fig. 15). The partitioning of sensible and latent heat in these non-linear relationships is done through an iterative approach (Voller and Swaminathan, 1991).

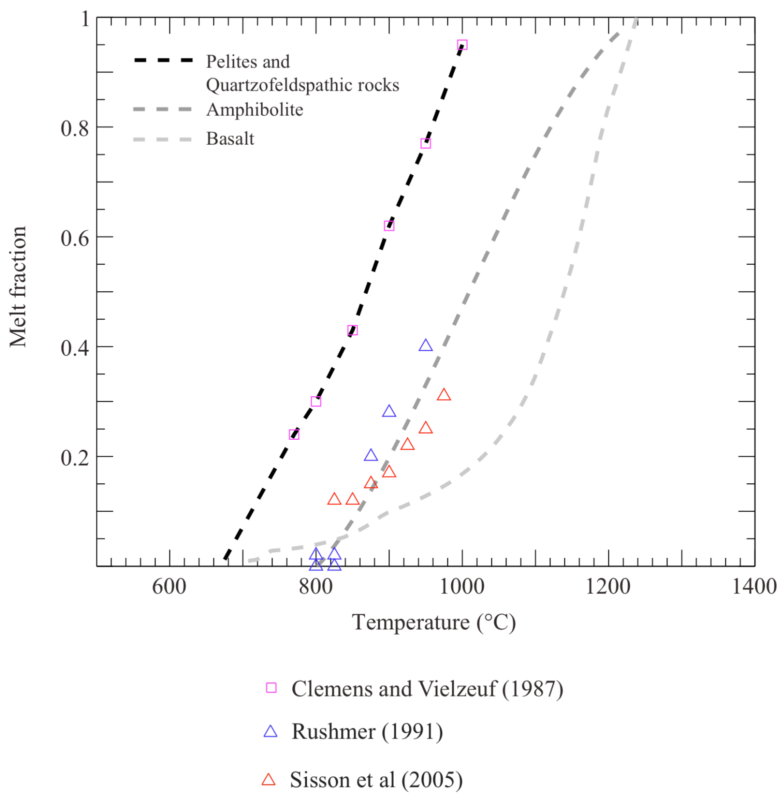

Fig. 15. Melt fraction vs temperature relationship of 1) most primitive mafic composition based on average of 3 bulk chemical analyses by XRF of mafic xenoliths in the Salton Sea Geothermal Field (Herzig and Jacobs 1991) at 4.4 kbar. Melt fraction as a function of temperature and water content (0.5 wt.% H_2O) is calculated with rhyolite-MELTS thermodynamic software (Gualda et al., 2012) and 2) Pelites and Quartzofeldspathic rocks at 5 kbar pressure and 1.0 wt% water content. Parameterized from fluid-absent melting experiments of Clemens and Vielzeuf (1987). The solidus temperature is assumed as 680 C.

Using the crustal layering suggested by Fuis et al. (1984), thermal and mechanical properties of each crustal layer are defined (Fig. 15). For sediments, fluid absent melting of pelites and quartzofeldspathic rocks (5 kbars and 1.0 wt% H_2O) as a function of temperature is parameterized from experimental results of Clemens and Vielzeuf (1987). Rhyolite-MELTS calculations are performed for the melt fraction- temperature relationship of crystallizing basalt (4.4 kbars and 0.5 wt% H_2O) and for the liquidus temperature of the amphibolite composition (2.0 wt% H_2O). Basaltic composition is from the average of three XRF bulk chemical analyses of mafic xenoliths (Herzig and Jacobs, 1991). Due to the rifting mechanism of the SSGF, we assume that the magmatic water content is ~0.5 wt% H_2O, typical of MORB magmas. Here, we note that the basalt xenoliths in the rhyolite magma in SSGF were found to show similar ε_{Nd} ratios as the East Pacific Rise and Alarcon Ridge basalts (Herzig and Jacobs, 1994; Robinson et al., 1976; Schmitt et al., 2013). The amphibolite melt fraction to temperature relationship is parameterized from the experimental results of Rushmer (1991), Sisson et al. (2005), and Wolf and Wyllie (1994).

While seismic experiments in the area represent the present day crustal layering of the Salton Sea, the initial state of the crust at the time of initiation of spreading is not well constrained because the long-term tectonic evolution has occurred as different stages within several million years. Studies have argued different timescales and compositions for the presence and destruction of the initial crystalline basement in the lower crust. Current studies based on basaltic xenoliths in erupted products (Schmitt and Vazquez, 2006), seismic data (Fuis et al., 1984), and scientific boreholes (Elders and Sass, 1988) suggest that the lower crust is composed of basaltic intrusions that eventually became the lower crustal gabbroic layer. Some petrogenetic models argue that an initial crystalline basement of the Salton Sea area was ruptured and intruded by basalts, and formed the present day configuration (Elders, 1979; Schmitt and Vazquez, 2006). The initial crustal basement that is absent in today's crustal configuration is likely the continental crust that was formed during the subduction period by dehydration melting of the mantle wedge. Correspondingly, seismic models that study the Gulf of California reveal a high-velocity layer in the lower crust in the south of the Salton Through that was suggested to be mafic continental arc basement (e.g., Nicolas, 1985).

Based on these observations, we simulate an initial three-layered crust with unconsolidated sediments at the top, metasediments in the mid-crust, and an amphibolite layer in the lower crust. The lower amphibolitic crust is a representation of hydrous mafic lower crust and hence a fertile end-member, therefore represents and upper limit for crustal melt production. These conditions enable study of the formation and evolution of the lowermost crust of the SSGF. Intrusion of dikes into the lower portions of the crust start with the initiation of spreading (1.0 Ma) and accumulate in the lower crust over time to form the gabbroic layer. We choose 1.0 Ma time scale for the magmatic system as the buried rhyolites at approximately 1.7 km depth were suggested to be erupted ca. 0.73 Ma (Hulen and Pulka, 2001). Considering the sedimentation rate of 2.2 to 3.8 mm/yr, we suggest that the evolution of the magmatic system must be close to 1 Myr; however several assumptions regarding the sedimentation and erosion rates, age calculations, thickness measurements, and the relationship between the eruption and initiation of tectonic extension possibly include some uncertainty. While analyzing our results, we also consider the calculations of Brothers et al. (2009) and compare and discuss our findings at 500 ka.

We examine a parameter space based on geophysical and petrologic observations from the present day geometry and volcanism in the SSGF. In particular, we vary: 1) average tectonic extension rate, and 2) basalt flux entering the crust. We vary the average extension rate between 5, 8, and 10 mm/yr. Since the average basalt flux is not constrained for SSGF, we consider a range of plausible values estimated in diverse volcanic settings (10-4 to 10-3 m3/m2/yr, Crisp, 1984). The successful results that match the present day crustal layer thicknesses, surface heat flux, and petrology are used to put constraints on the melt production, heat budget, extensional tectonics, and composition of the lower crustal melt over time.

4.4. Results

To illustrate the geometry of the simulations and potential outcomes, best-fit models show composition, temperature, melt fraction, and surface heat flux through time for a single scenario (Fig. 16). All results are summarized in Tables 1 and 2. The selection of best-fit models requires that the results of the final timestep match the observations of crustal thicknesses, surface heat flux, crustal geotherm, petrology, and volume of the erupted products (Tables 1 and 2). In this way, this selection helps constrain the lower crustal heat source of the Salton Buttes volcanic region and gives information about the initial conditions, long-term magma evolution, and basalt flux.

Intrusions from the mantle into the crust generate a lower crustal mush region, mainly composed of mantle-derived melt with minor assimilation of crustal melt. The intruded melt solidifies quickly after the basalt intrusions in early time steps (~200 kyr), however as heat slowly builds up in the crust with repeated injections, partially molten regions start to develop in the lower crust in time. In low flux conditions (<0.0085 $m^3/m^2/yr$), the accumulated melt is entirely composed of closed system fractionation of basalt with <150 m thickness. The heat supplied by the intruded volume of basalt certainly heats the surrounding crust and increases the sensible heat, but our results show that the energy supplied by the intrusions is not enough to reach the latent heat of the amphibolitic crustal lithologies therefore crustal melting is not observed. Locally and temporally, we observe melting of the crustal material just after the injection, however in the long-term evolution of the crustal thermal profile, crustal material is stable in its solid phase. When the flux is intermediate to high (0.0085 to 0.010 $m^3/m^2/yr$) and extension is high (0.010 m/yr), the thickness of mantle-derived melt (from basalt fractionation) increases up to ~500 meters. Crustal material starts to melt by the heat provided from basaltic injections, however the maximum thickness of the melted crustal material is < 100 meters. In these conditions, the total melt thickness is restricted to a few hundred meters over 10^5 year timescales (Table 1).

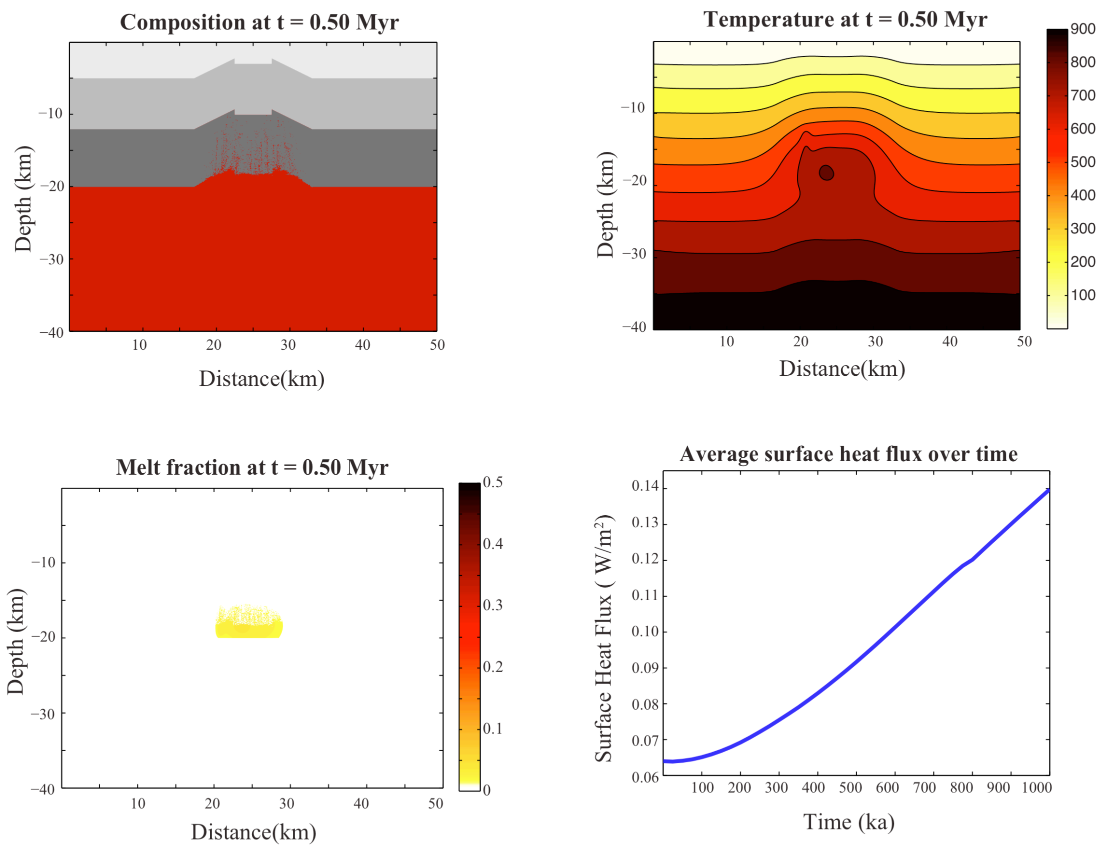

Fig. 16. Snapshots of composition, temperature, melt fraction after 500 ka and evolution of surface heat flux over time that correspond to two-layered crustal simulations.

The crustal material starts to melt after 0.5 Ma when basalt flux is > 0.0085 $m^3/m^2/yr$ (Fig. 17), however the amount of crustal melt is very low compared to mantle-derived melt (only a few tens of meters in thickness, Fig. 17 and Table 1). The low rates of crustal melt production indicate that the enthalpy transferred from dike emplacement mainly affects the sensible heat of the crustal material, and rarely does the temperature of the preexisting crust rise above its solidus. In this case, the lithology assumed is amphibolite and a more refractory lithology would produce even less melt. This observation is consistent with the observations of $^{87}Sr/^{86}Sr$ and ε_{Nd} isotope ratios of Salton Sea erupted products (Schmitt et al., 2013) and previous thermal models in diverse volcanic settings with thin crust (Dufek and Bergantz, 2005; Karakas and Dufek, 2015).

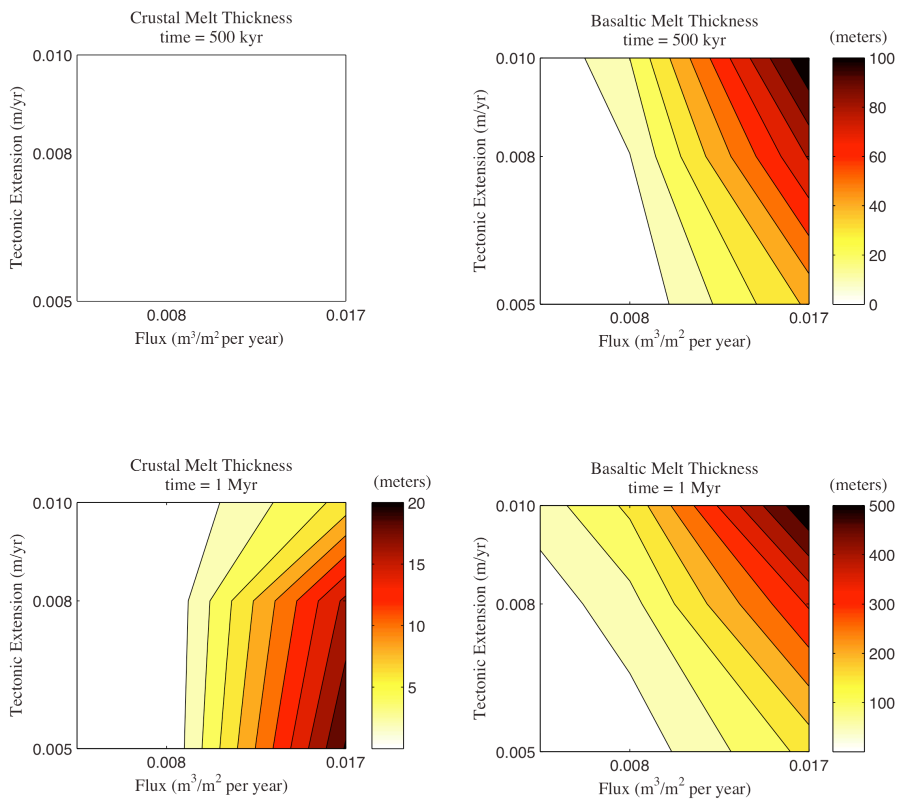

Fig. 17. Evolution of crustal- and mantle-derived melts over time that correspond to three-layered crustal simulations.

The amount of mantle-derived magma increases in response to high extension rates and high basalt flux. This is because magma flux brings significant enthalpy and volume into the crust over time, which is advected within the lower crust by tectonic extension.

Therefore, basalt emplaced around the axis of extension intrudes into warmer lower crust composed of previously intruded basaltic material. This results in partial re-melting of the previously intruded basaltic dikes as well as buffered heat transfer between new intrusions and the surrounding, cold crust. Partial re-melting of the previously intruded basalt was suggested as a viable mechanism by Schmitt and Vazquez (2006) for the rhyolitic magma formation. In our conditions, we do observe re-melting of the previous basaltic dikes, however, it has a smaller contribution compared to the residual melt remained after basalt crystallization.

The amount of crustal melt is relatively insignificant in all simulations (<20%). Crustal melting increases as a function of initial crustal thickness, mantle heat flux, and basalt flux. In the low flux conditions, we do not observe melting of the crust regardless of the tectonic extension rate because the amount of crustal melting is mainly controlled by the heat supplied by the melt coming from the mantle. In high flux conditions, the amount of crustal melt in different extensional rates is < 30 meters. Therefore, we suggest that the main contribution to the magma evolution in the Salton Sea is from fractional crystallization of basalt. These results are consistent with $^{87}Sr/^{86}Sr$ and ε_{Nd} isotope ratios that suggested limited assimilation by the basement (Schmitt and Vazquez, 2006; Schmitt et al., 2013). In addition, based on the low $\delta^{18}O$ values in the rhyolite zircons, Schmitt and Vazquez (2006) ruled out generation of rhyolite from crustal melting and fractionation of unaltered MORB basalt. Instead, they suggested that the evolved melt must be derived from altered basalt, which must have undergone hydrothermal alteration and exchanged isotopes with the circulating water.

Table 1. Model results for varying basalt flux and tectonic extension rates

Time (years)	Intrusion frequency	Average basalt flux over time (m3/m2/yr)	Tectonic extesion (m/yr)	Normalized basalt melt volume (m)	Normalized crustal melt volume (m)
10^6	100	0.00425	-0.01	70	0
10^6	100	0.00425	-0.008	20	0
10^6	100	0.00425	-0.005	1	0
10^6	50	0.0085	-0.01	150	0
10^6	50	0.0085	-0.008	80	0
10^6	50	0.0085	-0.005	15	0
10^6	25	0.017	-0.01	550	5
10^6	25	0.017	-0.008	350	10
10^6	25	0.017	-0.005	150	30

Melt fraction is between 0.2 - 0.4 for most simulations (>0.085 $m^3/m^2/yr$ and >0.05 m/yr in 100 kyr timescales) and once the magma body is produced; it stays partially molten during all its lifetime given the incremental magma assembly with the specified flux of > 0.0085 $m^3/m^2/yr$. However, the magma body is highly crystalline during its residence in the crust. The calculated melt factions (0.2-0.4) in our model correspond to roughly andesitic to dacitic compositions in the experiments (Müntener et al., 2001; Sisson et al., 2005) because the silicic content of the basaltic parent after fractional crystallization corresponds to ~60-75% in this melt fraction range (Sisson et al., 2005). Here, we note that Sisson et al. (2005) melting experiments were carried under 700 MPa therefore represents mid crustal conditions; whereas Müntener et al. (2001) experiments were carried under 1.2 GPa, representing deep crustal conditions in thick regions (~40 km). Therefore, silica contents of the melt under these varied pressure regions are different because of the stability of different mineral phases. In low pressure conditions melting experiments showed generation of rhyolite in low melt fractions (<0.3, Sisson et al., 2005) whereas in high pressure conditions magma composition trends towards more mafic compositions in similar melt fractions (Müntener et al., 2001). Therefore, generation of eruptive rhyolites at depth is not plausible in general due to wrong pressure regions. We note that, some rhyolite can be produced at deeper crust in rift settings, however the dominant amount of melt is not felsic if considered in aggregate.

Table 2. Simulations with varied initial mantle heat flux and crustal thickness

Time (years)	Intrusion frequency	Average basalt flux over time ($m^3/m^2/yr$)	Tectonic extension (m/yr)	Crustal thickness (km)	Surface heat flux (mW/m^2)
10^6	50	0.0085	-0.005	20	70
10^6	50	0.0085	-0.005	20	80
10^6	50	0.0085	-0.005	20	90
10^6	50	0.0085	-0.005	22	70
10^6	50	0.0085	-0.005	22	80
10^6	50	0.0085	-0.005	22	90
10^6	50	0.0085	-0.005	24	70
10^6	50	0.0085	-0.005	24	80
10^6	50	0.0085	-0.005	24	90

4.5. Discussion

We find that basalt flux and tectonic extension are strongly coupled in distributing heat in the crust, and can result in a partially molten region in the lower crust of the Salton Sea. Our models indicate a combination of rapid thinning and high basalt flux (0.008-0.010 $m^3/m^2/yr$) from the mantle in order to match the crustal signatures evident today. The basalt flux values <0.008 $m^3/m^2/yr$ combined with low tectonic extension ~0.005 m/yr showed almost no partial melt in the lower crust in the timescales and conditions that we consider (1 Myr). Low basalt fluxes (<0.008 $m^3/m^2/yr$) combined with high tectonic extensions (>0.005 m/yr) create partially molten regions with only basalt fractionation without any crustal component. For mantle of equal fertility, increasing extension leads to more melt production in the upper mantle and can result in higher volume flux entering the crust (McKenzie and Bickle, 1988).

Field investigations on the eruptive volcanic volumes in several volcanic settings show that the crustal magma reservoirs can contain magma volumes up to 10 times larger than the erupted volumes (White et al., 2006) although there is likely a high degree of variability in different volcanic centers. In our 2D simulations, assuming that the footprint of the surface expression of one dome is 10 km^2 at the Moho, lower crustal plutonic volume for each dome gives 4 to 6 km^3 volume. Roughly, using 1:10 ratio for the volcanic-plutonic volumes gives 0.4 – 0.6 km^3 of erupted volume for one individual dome and 2 – 3 km^3 for total eruptive volume for five domes in the Salton Sea area, comparable to the estimated total volume of <5 km^3 (Robinson et al., 1976).

The melt fraction in the best-fit regime exists for prolonged periods of time at 0.2-0.4 melt fraction. This melt fraction range suggests generation of dominantly andesitic to dacitic melt, and is in the range of preferential melt extraction where melt is extracted more efficiently during high melt fraction compaction compared to both higher and lower melt fractions (Dufek and Bachmann, 2010). In the case of Salton Buttes, we suggest that the partial melt produced in the lower crustal magma reservoir forms the dacitic melt source that intruded in the shallow crust, which eventually formed the geothermal system and through crystal fractionation evolved to rhyolite that erupted at the surface.

The simulated intrusions scenarios that most closely match present conditions are most consistent with more evolved melts forming primarily from the fractional crystallization of basaltic magma with minor crustal contribution. Similarly, the Sr-Nd ratios on rhyolites and xenoliths of basalt and granophyric granite suggests that Salton

Butte volcanic products are mainly generated from fractionation of basalt with <10% crustal assimilation (Herzig and Jacobs, 1994). Schmitt and Vazquez (2006) study on basaltic xenoliths also suggests only minor crustal assimilation for the SSGF erupted rhyolites based on their low $^{87}Sr/^{86}Sr$ with elevated ε_{Nd} ratios.

An important observation of Schmitt et al. (2013) is that the most evolved and the most primitive compositions of the Cerro Prieto Basin, which is the adjacent extensional basin south of the Salton Sea, almost overlap in composition with the products of the Salton Buttes. However, their main difference is bimodal character of the SSGF volcanics with a dominant rhyolitic composition, while the Cerro Prieto rocks have intermediate compositions. This could be due to the longevity of the systems and different basalt influx and extension conditions.

The thermodynamic model outlined here favors an initial three-layered crust for the SSGF or at the very least an initial mafic lower crust, which is likely absent today due to diking and extension events. This is also supported by studies that observed subduction-related continental crust in the south of SSGF (Nicolas, 1985; Schmitt et al., 2013).

During the formation of amagmatic rift basins, only the extensional processes can raise the geotherm significantly because of the heat-flow from the mantle crust boundary (McKenzie, 1978). In the Salton Sea geothermal field, thin crust and high rates of tectonic extension suggest higher temperatures in the lower crust compared to other rift settings with lower extensional rates (e.g., 4 mm/yr extension in Ethiopian Rift, Bilham et al., 1999). Therefore, high mantle heat flow in the Salton Sea makes the crust more prone to preserve partially molten regions because of the high initial geotherm. This is due to very high rates of localized extension (thinner crust in time) and resulting localized high basalt flux. However, we note that the base of the crust of Salton Sea is relatively thin relative to many continental arc settings; where significant crustal assimilation is prohibited and the magma is primarily evolved from the mantle-derived basaltic parent. Similarly, the thermal model of Dufek and Bergantz (2005) suggests that crustal melting processes are less prominent than fractionation of basalt given conditions of thin crust (<40 km) over long timescales (>few million years).

In our model, we restrict the tectonic extension and diking over a specified width on the mantle-crust boundary. Lachenbruch et al. (1985) suggest that, the extension should be distributed over a wide area (~150 km) in the Salton Trough in order to accommodate substantial magmatic addition with almost no crustal melting signatures, and to explain the observed heat flux with the extension and sedimentation rates. However, absence of any syn-rift magmatism outside the ~15 km zone around SSGF, age and stratigraphic depth of the rhyolite bodies (Schmitt and Vazquez, 2006) and the tectonic configuration of the Salton Trough by seismic interpretations (Brothers et al., 2009) suggested that the tectonic extension and magmatism must be localized in narrow zones. Our thermal model shows that localized continuous extension and repetitive magmatism over a million-year timescale can accommodate large volumes of magma to the crust without producing large crustal melting signatures. The crustal melting rate is limited due to thin crust, compositional layering (crystalline lower crust), and initial conditions. In these conditions, substantial melting of the crust requires excessive energy input, elevated initial geotherm, and initial non-crystalline lower crust.

The present work is necessarily a simplification of the geometry of SSGF extensional system and composition of Salton Buttes volcanic products, and uses a parameter space for extension and magma flux to constrain the lower crustal melt volume. We assume that the extension, magma flux, and sedimentation rates are fixed throughout the simulations. These values may have varied over time and within the crustal profile during rift evolution. However, their rate of change through time and space are complex non-linear functions of several parameters such as rheology, strain rate, presence of volatiles, pressure, and porosity (e.g., Buck, 2004; McKenzie, 1985; Ruppel, 1995), many of which are poorly constrained. In the present model, we use values that have been constrained in the SSGF by various petrologic, field, and geophysical studies. We use a range of parameter space constrained in other rift settings when the specific values for the SSGF are not currently specified (e.g., basalt flux, tectonic extension, initial lower crustal lithology, initial crustal thickness, mantle heat flow). This approach allows us to provide upper and lower quantitative constraints to the volume (0.5-1 km thick mush), melt fraction (0.2-0.4), and evolution of the lower crustal melt (dacitic melt formed in ~0.5 to 1 Myr mainly by fractionation of basalt) of the SSGF.

4.6. Conclusions

Given initial conditions that result in surface heat fluxes and volcanic products that agree with present day observations, our thermal equilibrium calculations suggest a 0.5 - 1 km thick, partially molten lower crustal mush zone with minor crustal assimilation. The melt derived from fractional crystallization of basaltic melt is at least an order of magnitude greater than the crustal melt in most of the conditions. The melt fraction in this lower crustal mush region is between 0.2-0.4 within the range of model assumptions and timescales. We suggest that the pre-existing lower continental crust composed of amphibolitic layer is ruptured with extensional tectonics, followed by intrusion of basalt with high flux in the crust to form a new gabbroic crust over 0.5 – 1 Ma.

CHAPTER 5

TIMESCALES INVOLVED IN THE CONSTRUCTION OF A MAGMATIC CRUSTAL COLUMN, THE IVREA-VERBANO ZONE AND SERIE DEI LAGHI OF SOUTHERN ALPS

Understanding the processes that lead to large-scale caldera-forming eruptions is of fundamental importance to science and society. The size and style of these eruptions are determined by complex nonlinear magmatic processes during the emplacement and residence of voluminous magma in the Earth's crust. Building on my current research, I aim to quantify the time and length scales involved in the thermal and compositional evolution of the Ivrea-Verbano Zone and Serie dei Laghi magmatic system of the Alps (north Italy) in my future research. This study will entail conducting a geological field campaign, performing geochronological analysis on field samples, and constructing a thermo-petrographic numerical model. This research will utilize advanced high-precision U/Pb dating techniques on field samples in order to reduce the error on published age constraints. In particular, I aim to test the hypothesis that this magmatic system belongs to one single event, which makes the region a unique natural laboratory to study magma evolution from its generation at depth to eruption at the surface. In order to give quantitative constraints, I will use a novel numerical model that solves for conservation of mass and energy in the crustal magmatic systems in rift environments. The numerical model will investigate the thermal and chemical evolution of magma and will be constrained by previous geochemical characterizations of many different units of the

Ivrea-Verbano Zone and the Seire dei Laghi magmatic system and the results of geochronological analysis.

5.1. Introduction

Large-scale caldera forming eruptions can produce cataclysmic explosions that represent hazard to humans and the environment. These eruptions often produce voluminous eruptive products (1000-5000 km^3, e.g., Bachmann and Bergantz, 2008a) withdrawn from extensive magma reservoirs located at different depths in the crust (de Silva and Gosnold, 2007; White, 1993; White et al., 2006). It is estimated that the crustal magma reservoirs can contain magma volumes up to 10 times larger than the erupted volumes (White et al., 2006). The crustal magma bodies can grow and evolve over millions of years by progressive emplacement of primitive magma transported from the mantle into the crust. This observation opens important questions about the mass and energy balance and consequent 'room problem' in the crust (O'Hara, 1998; Tuttle and Bowen, 1958): What are the conditions that permit extensive volumes of magma to be emplaced and reside in the crust over millions of years? How does the magma evolve thermally and chemically? How long do partially molten regions exist in the crust before they erupt at the surface or cool below their solidi to form plutonic rocks? In order to address these questions, I will conduct a field campaign, perform geochronological analysis on field samples, and construct a numerical model to investigate the complete picture of magma evolution and residence in the crust.

The Ivrea-Verbano Zone (IVZ) and Serie dei Laghi (SdL) volcanic system in the Alps of northwestern Italy provides a unique opportunity to investigate a record of a complete magmatic system. In this region, lower, middle, and upper crustal intrusive units and eruptive units of a single major magmatic event can be observed in-situ. My main goal is to achieve tight and accurate age constraints for the magmatic processes in this system. To accomplish this, I will combine numerical thermal and chemical modeling with field expedition and geochronological analysis in collaboration with ETH, UNIGE, and UNIL research teams. Our approach will include sample collection in the field followed by geochronological analysis on zircon crystals. This will constrain ages of the magmatic products. Finally, we will construct a numerical model, which will give quantitative constraints to the long-term thermal and compositional evolution and longevity of the system. We will compare and constrain the numerical model with the geochronological analysis and previous petrologic studies, following the pioneering work of Barboza and Bergantz (2000). The concurrent treatment of these parameters is expected to provide a better understanding of the complex dynamics inherent to active volcanic systems.

5.2. Background and Motivation

5.2.1. Magma emplacement in the crust

The journey of the magma from its generation at depth to eruption at the Earth's surface is a fundamental topic in volcanology; however, the time and lengthscales during magma residence in the crust remain unclear. The emplacement of magma in the crust is often strongly coupled to far-field tectonic stresses. In rift environments like the IVZ and SdL of southern Alps, extension of the crust due to large-scale tectonics leads to melt generation in the mantle. The buoyant melt rises into the crust, where it can reside and differentiate over long timescales. The thermal and chemical evolution of the melt forms various compositions at different levels in the crust. Over time, magma progressively emplaces from the mantle into the lower crust and within the crust, and hence, leads to complex patterns of thermal and chemical interactions due to transport of enthalpy and volume of parental melt. Finally, large of volumes of magma can erupt depending on the thermal, compositional, mechanical, and rheological conditions in mid-upper crustal magma bodies. The observed diversity in the eruption styles, volumes, and compositions at different volcanic centers, therefore, depend on the magmatic processes that occur in the upper 10-15 km of the crust (e.g., Bachmann and Bergantz, 2008b).

5.2.2. Sesia Magmatic System: "The unprecedented volcanic field"

In this research, we will use plutonic and volcanic record to constrain the processes that formed the magmatic system in the northern Alps. Three main units make up this system, namely: (1) deep crustal Ivrea-Verbano Zone, (2) mid-upper crustal Serie dei Laghi, and (3) erupted volcanic products (Fig. 18). The IVZ represents the deep crustal plutons of high temperature and high-pressure rocks (~25 km) and is one of the best examples of magmatic underplating that is exposed on the Earth's surface due to millions of years of tectonic processes and erosion. SdL represents the middle to upper crustal amphibolite-facies metamorphic rocks and granites (e.g., Sinigoi et al, 2011). The silica-rich erupted volcanic rocks (rhyolites) are situated in the southern part of the region and must represent the most evolved magma in the system. Quick et al (2009) have recognized caldera walls in the south of Sesia Valley and interpret it as collapse of ~13 km diameter caldera following a large-scale eruption. These three units (IVZ, SdL, and erupted products) have been investigated as separate units for decades.

In this system, the geochronological study (U-Pb dating of zircon) of Quick et al. (2009) revealed the spatial and temporal kinship of plutonic and volcanic rocks. This interpretation led Quick et al. (2009) to argue that the magmatic system must represent a single crustal unit of one magmatic event, referred to as the “Sesia magmatic system”. While in many systems the volcanic and plutonic rocks of a single eruptive record cannot be observed in the field; the complex Alpine tectonics in the Sesia Valley region juxtaposed different magmatic units that are argued to represent a continuum of magmatic and volcanic processes of one single system. Sinigoi et al (2011) summarized the major magmatic events from progressive evolution of magma in the crust to the large-scale caldera-forming eruption in the region as follows: 1) partial melting of mid-lower crust generated large volumes of crust hybridized with mafic melts, 2) the melt intruded in the upper crust, 3) crystallized to granitic plutons and erupted dacite and rhyolite, including a caldera-forming eruption (Fig. 18). While extensive field, geochemical, geochronological, and geodynamical research has been done in the region (e.g., Barboza and Bergantz, 2000; Rutter et al, 1999; Voshage et al., 1990; Sinigoi et al., 2011), quantitative constraints of thermal and compositional evolution of the system remain unclear. In particular, the state, sizes, and shapes of magma reservoirs need to be better determined. In this research, I plan to investigate the longevity and the thermal and chemical evolution of the Sesia magmatic system in order to address questions posed in the introduction.

<u>Timescales and longevity of the magmatic system</u>

The key to understanding the assembly of large, caldera-forming eruptions is constraining the residence time of crustal magma bodies, which can be achieved by recent advances on geochronological techniques. For example, zircon dating can provide important information about duration of crystallization and associated compositional state of a reservoir at the time of zircon crystallization (Bachmann et al., 2007a; Schmitt and Vazquez, 2006; Wotzlaw et al., 2013). Although the recent geochronological study (U-Pb dating of zircon using SIMS) of Quick et al. (2009) revealed important information about the plutonic and volcanic rocks in the Sesia magmatic system; the published data have wide error bars (between ±2 to ±11 million years). The time gap in the error bars can be improved, using state-of-the-art CA-TIMS-TEA methods (e.g., Mattinson, 2005; Schoene et al., 2010) in order to test Quick et al. (2009)'s suggestion that the area represents one single magmatic unit. This is the main aim of this research plan.

Thermal and compositional evolution of the magma

The thermal and physical conditions in the crustal magmatic systems significantly influence the magma evolution and eruption conditions. For example, in many explosive systems including the Sesia magmatic system, the primary magma that is emplaced from the mantle is mafic in composition; however, the erupted magma is usually more silicic. A key question is what are the crustal conditions that result in diverse silicic compositions in the crust from a common mantle-derived mafic source. Different mechanisms have been suggested for the formation of evolved magmas; however, relative importance of these processes still remains unclear. Over the last century, two main hypotheses have emerged about the origin of magmatism and the formation of evolved magmas. First, do evolved magmas primarily derive from the fractional crystallization of a basaltic parent (with some assimilation of pre-existing crustal lithologies), or from partial melting of the crust (Annen et al., 2006; Berlo et al., 2004;

Conrad et al., 1988; Dufek and Bergantz, 2005; Jagoutz, 2010; Jagoutz et al., 2009; Lee and Bachmann, 2014; Schmitt and Vazquez, 2006)? Second, are plutonic and volcanic rocks two end-members of the same system, or do they form separately under different mechanisms (Bachmann et al., 2007b; Gelman et al., 2014; Glazner et al., 2004)**?**

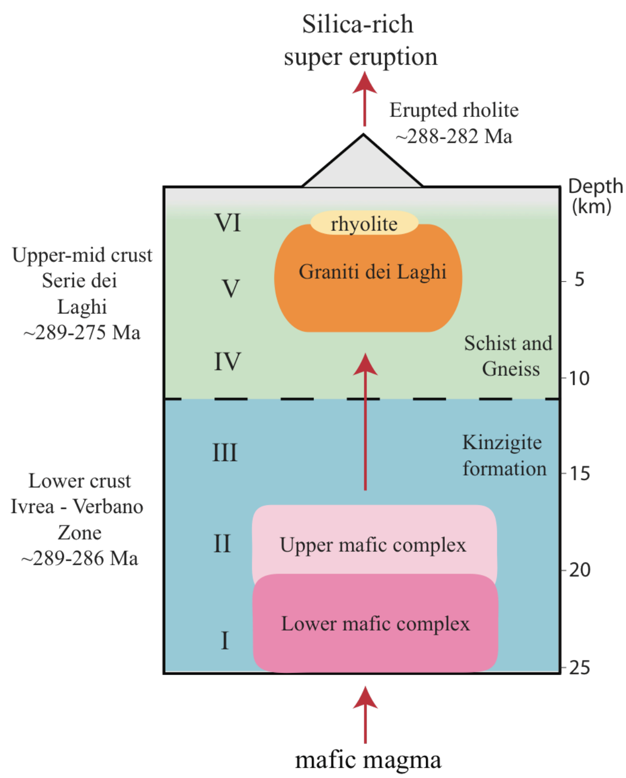

Fig. 18. Conceptual model proposed for evolution of the Sesia magmatic system, after Quick et al. (2009), Barboza and Bergantz (2000), and Sinigoi et al. (2011).

In the Ivrea-Verbano Zone, Barboza and Bergantz (1996) developed a convective thermal model to investigate melt generation and extraction by simulating mafic sill injection and resulting dehydration melting of crustal rocks. Sinigoi et al. (2011) constructed a simplified 1-D conductive heat flow model that simulates progressive melt intrusion in the crust of the Sesia magmatic system. This approach led Sinigoi et al. (2011) to calculate the thermal balance between the crust and the intruded material; however, lack of geochemical modeling led them to suggest the magma evolution qualitatively. The aim of my future research is to construct detailed thermodynamic and compositional modeling of magma evolution by incremental magma assembly and tectonic extension in the system in order to understand (1) the link between mafic intrusions at depth and large-scale silicic volcanism at the surface and (2) the state of the reservoirs that lead to this chemical differentiation.

5.3. Anticipated research

I aim to constrain the evolution and residence of the magma in the Sesia system using geochronological analysis and tie this information with detailed numerical modeling together with previously characterized samples from geochemical analyses. Our approach is as follows. In the fieldwork, a team of geologists will sample plutonic and volcanic products from critical areas in the area. Careful observations and field data will provide critical context for dating. Geochronological analyses will be conducted on the collected samples. The numerical model will be constructed in order to give quantitative constraints to thermal and compositional evolution of magma. This will ultimately be linked to the eruptive record gathered from previous geochemical analyses and zircon dating from this study. Accuracy of the thermal model is very important and can give information about the initial conditions and evolution of the magmatic system, which will guide to address the questions presented in the introduction.

Task 1: Conducting fieldwork. The fieldwork will be focused on sample collection from critical points around the volcanic system. Sampling should cover as many units as possible in order to prevent biased sampling. A first field campaign is planned for Fall 2015, but a second is possible in 2016, if necessary. Moreover, previously sampled key locations, preserved in rock collections in ETHZ, can also be used. We will collect samples starting from the deepest crustal units and will sample progressively upwards to middle and upper crustal plutonic rocks and finally to the volcanic rocks at the surface. The sampling locations are marked in Fig. 18 that will include the Mafic Complex in the southwest of the area (lowermost unit, points I and II) and traveling to Kinzigite Formation (roof of the Mafic Complex, top of the lower crust, location III), then to mid-upper crustal granitic bodies (points V and IV) and finally to volcanics and caldera wall exposure (location VI). There are two reasons for these sampling locations: 1) testing the previously published data with a higher resolution geochronological analysis in order to reduce previously published errors and 2) extensive sampling of additional units in order to provide a more comprehensive dataset for the purposes of this research plan.

Task 2: High precision geochronological analysis. The dating analysis will be consisted of two parts: 1) conducting zircon geochronology on the collected field samples (and previously acquired, and already characterized samples) with high-precision U/Pb using CA-TIMS and 2) processing and interpretation of the raw data. The facilities needed for isotope analysis are included in the Institute of Geochemistry and Petrology laboratories in ETHZ. Since the compositional evolution (and hence the zircon saturation point) of the system is dependent on different parameters such as temperature, pressure, and water content, it is very important to track the compositional evolution of the system accurately, where use of numerical models can be crucial.

Task 3: Modeling the thermal and compositional evolution of the magmatic system. The numerical model will be based on the research that I conducted with Josef Dufek at the Georgia Institute of Technology (Karakas and Dufek, 2015). This two-dimensional finite-volume model solves for transient thermal diffusion-advection (Patankar, 1980) in extensional tectonic systems. The model considers the progressive magma emplacement and tectonic extension in the crust and calculates: (1) the thermal evolution of the magma body and the surrounding crust, (2) volume of crustal and mantle-derived melts due to evolving temperature, and (3) fraction, geometry, and depth of the magma residing in the crust. For the purposes of the proposed project, the numerical model will be modified to get the most accurate results for the specific conditions for the Sesia magmatic system.

The numerical model will be the first to test the region by examining incremental assembly and monitoring the longevity of the system. There are a number of points that will make the model different than the current thermal models. First, we will account for the extensional tectonics in the area. This is an important component in the heat transfer processes because extension promotes heat advection in the system. Second, we will account for different magmatic water contents, which were shown to have an important affect on compositional evolution of the system by controlling the crystallization behavior of the magma. Third, we will monitor the major and minor elements, volume, and fraction of melt as the system evolves. For the purposes of this project, the output of the model and petrologic analyses should be consistent.

5.4. Expected outcome of the future research

This work will investigate the thermal and geochemical evolution of the Ivrea-Verbona Zone and Serie dei Laghi of southern Alps by conducting 1) field campaign, 2) geochronological analysis, and 3) thermal modeling. This approach is expected to provide a better understanding to the volcanic-plutonic connection. I also expect this research to address important topics in volcanology including the timescales and generation of evolved magmas, and the thermal and compositional conditions that lead to large-scale caldera-forming eruptions. An improved understanding of the underlying physical aspects of crustal magmatic systems is key to hazard assessment, geothermal energy exploration, and ore deposits.

REFERENCES

Allegre, C., Minster, J., 1978. Quantitative models of trace element behavior in magmatic processes. Earth and Planetary Science Letters 38, 1-25.

Anderson, E.M., 1951. The Dynamics of Faulting and Dyke Formation with Application to Britain. Oliver and Boyd, Edinburgh.

Annen, C., 2009. From plutons to magma chambers: Thermal constraints on the accumulation of eruptible silicic magma in the upper crust. Earth and Planetary Science Letters 284, 409-416.

Annen, C., Blundy, J.D., Sparks, R.S.J., 2006. The genesis of intermediate and silicic magmas in deep crustal hot zones. Journal of Petrology 47, 505-539.

Annen, C., Sparks, R.S.J., 2002. Effects of repetitive emplacement of basaltic intrusions on thermal evolution and melt generation in the crust. Earth and Planetary Science Letters 203, 937-955.

Bachmann, O., Bergantz, G.W., 2004. On the origin of crystal-poor rhyolites: extracted from batholithic crystal mushes. Journal of Petrology 45, 1565-1582.

Bachmann, O., Bergantz, G.W., 2008. Rhyolites and their Source Mushes across Tectonic Settings. Journal of Petrology 49, 2277-2285.

Bachmann, O., Charlier, B., Lowenstern, J., 2007a. Zircon crystallization and recycling in the magma chamber of the rhyolitic Kos Plateau Tuff (Aegean arc). Geology 35, 73-76.

Bachmann, O., Dungan, M.A., Lipman, P.W., 2002. The Fish Canyon magma body, San Juan volcanic field, Colorado: rejuvenation and eruption of an upper-crustal batholith. Journal of Petrology 43, 1469-1503.

Bachmann, O., Miller, C., De Silva, S., 2007b. The volcanic–plutonic connection as a stage for understanding crustal magmatism. Journal of Volcanology and Geothermal Research 167, 1-23.

Bacon, C.R., Druitt, T.H., 1988. Compositional evolution of the zoned calcalkaline magma chamber of Mount Mazama, Crater Lake, Oregon. Contributions to Mineralogy and Petrology 98, 224-256.

Bacon, C.R., Lowenstern, J.B., 2005. Late Pleistocene granodiorite source for recycled zircon and phenocrysts in rhyodacite lava at Crater Lake, Oregon. Earth and Planetary Science Letters 233, 277-293.

Baer, G., Hamiel, Y., Shamir, G., Nof, R., 2008. Evolution of a magma-driven earthquake swarm and triggering of the nearby Oldoinyo Lengai eruption, as resolved by InSAR, ground observations and elastic modeling, East African Rift, 2007. Earth and Planetary Science Letters 272, 339-352.

Bailey, D., 1978. Continental rifting and mantle degassing, Petrology and geochemistry of continental rifts. Springer, pp. 1-13.

Bailey, J.C., Jensen, E.S., Hansen, A., Kann, A.D.J., Kann, K., 2009. Formation of heterogeneous magmatic series beneath North Santorini, South Aegean island arc. Lithos 110, 20-36.

Baker, B.H., Goles, G.G., Leeman, W.P., Lindstrom, M.M., 1977. Geochemistry and petrogenesis of a basalt-benmoreite-trachyte suite from the southern part of the Gregory Rift, Kenya. Contributions to Mineralogy and Petrology 64, 303-332.

Barberi, F., Ferrara, G., Santacroce, R., Treuil, M., Varet, J., 1975. A transitional basalt-pantellerite sequence of fractional crystallization, the Boina Centre (Afar Rift, Ethiopia). Journal of Petrology 16, 22-56.

Barboni, M., Schoene, B., 2014. Short eruption window revealed by absolute crystal growth rates in a granitic magma. Nature Geoscience.

Barboza, S.A., Bergantz, G.W., 2000. Metamorphism and anatexis in the mafic complex contact aureole, Ivrea Zone, Northern Italy. Journal of Petrology 41, 1307-1327.

Beard, J.S., Lofgren, G.E., 1991. Dehydration melting and water-saturated melting of basaltic and andesitic greenstones and amphibolites at 1, 3, and 6. 9 kb. Journal of Petrology 32, 365-401.

Bergantz, G.W., 1989. Underplating and partial melting-Implications for melt generation and extraction Science 245, 1093-1095.

Berlo, K., Turner, S., Blundy, J., Hawkesworth, C., 2004. The extent of U-series disequilibria produced during partial melting of the lower crust with implications for the formation of the Mount St. Helens dacites. Contributions to Mineralogy and Petrology 148, 122-130.

Bertani, R., 2005. World geothermal power generation in the period 2001–2005. Geothermics 34, 651-690.

Bialas, R.W., Buck, W.R., Qin, R., 2010. How much magma is required to rift a continent? Earth and Planetary Science Letters 292, 68-78.

Bilham, R., Bendick, R., Larson, K., Mohr, P., Braun, J., Tesfaye, S., Asfaw, L., 1999. Secular and tidal strain across the Main Ethiopian Rift. Geophysical Research Letters 26, 2789-2792.

Bindeman, I., Simakin, A., 2014. Rhyolites—Hard to produce, but easy to recycle and sequester: Integrating microgeochemical observations and numerical models. Geosphere 10, 930-957.

Bloomer, S.H., Curtis, P.C., Karson, J.A., 1989. Geochemical variation of Quaternary basaltic volcanics in the Turkana Rift, northern Kenya. Journal of African Earth Sciences (and the Middle East) 8, 511-532.

Boccaletti, M., Mazzuoli, R., Bonini, M., Trua, T., Abebe, B., 1999. Plio-Quaternary volcanotectonic activity in the northern sector of the Main Ethiopian Rift: relationships with oblique rifting. Journal of African Earth Sciences 29, 679-698.

Bowen, N.L., 1928. The evolution of igneous rocks. Dover publications, New York.

Brady, R.J., Ducea, M.N., Kidder, S.B., Saleeby, J.B., 2006. The distribution of radiogenic heat production as a function of depth in the Sierra Nevada Batholith, California. Lithos 86, 229-244.

Brothers, D.S., Driscoll, N.W., Kent, G.M., Harding, A.J., Babcock, J.M., Baskin, R.L., 2009. Tectonic evolution of the Salton Sea inferred from seismic reflection data. Nature Geoscience 2, 581-584.

Brown, M., Solar, G.S., 1998. Shear-zone systems and melts: feedback relations and self-organization in orogenic belts. Journal of Structural Geology 20, 211-227.

Buck, W.R., 2004. Consequences of asthenospheric variability on continental rifting. Rheology and deformation of the lithosphere at continental margins 62, 1-30.

Burg, J.P., 2011. The Asia–Kohistan–India collision: review and discussion, Arc-continent collision. Springer, pp. 279-309.

Burgisser, A., Bergantz, G.W., 2011. A rapid mechanism to remobilize and homogenize highly crystalline magma bodies. Nature 471, 212-215.

Callot, J.P., Geoffroy, L., Brun, J.P., 2002. Development of volcanic passive margins: Three-dimensional laboratory models. Tectonics 21.

Callot, J.P., Grigne, C., Geoffroy, L., Brun, J.P., 2001. Development of volcanic passive margins: Two-dimensional laboratory models. Tectonics 20, 148-159.

Carey, S., Sigurdsson, H., Gardner, J., Criswell, W., 1990. Variations in column height and magma discharge during the May 18, 1980 eruption of Mount St. Helens. Journal of Volcanology and Geothermal Research 43, 99-112.

Carrigan, C.R., 1988. Biot-number and thermos bottle effect- Implications for magma-chamber convection Geology 16, 771-774.

Chayes, F., 1963. Relative abundance of intermediate members of the oceanic basalt-trachyte association. Journal of Geophysical Research 68, 1519-1534.

Chouet, B.A., 1996. Long-period volcano seismicity: its source and use in eruption forecasting.

Christensen, J.N., DePaolo, D.J., 1993. Time scales of large volume silicic magma systems: Sr isotopic systematics of phenocrysts and glass from the Bishop Tuff, Long Valley, California. Contributions to Mineralogy and Petrology 113, 100-114.

Clemens, J., Mawer, C., 1992. Granitic magma transport by fracture propagation. Tectonophysics 204, 339-360.

Clemens, J.D., Vielzeuf, D., 1987. Constraints on melting and magma production in the crust Earth and Planetary Science Letters 86, 287-306.

Condie, K., 1982. Plate tectonics and crustal evolution. Plate tectonics and crustal evolution.. KC Condie. Pergamon Press, Oxford-New York-Frankfurt-Paris-Sydney-Toronto-Tokyo. 9+ 310 pp.(1982). ISBN 0-08-028075-7. 1.

Conrad, W.K., Nicholls, I., Wall, V., 1988. Water-saturated and-undersaturated melting of metaluminous and peraluminous crustal compositions at 10 kb: evidence for the origin of silicic magmas in the Taupo Volcanic Zone, New Zealand, and other occurrences. Journal of Petrology 29, 765-803.

Cooper, K.M., Kent, A.J., 2014. Rapid remobilization of magmatic crystals kept in cold storage. Nature.

Corti, G., Bonini, M., Conticelli, S., Innocenti, F., Manetti, P., Sokoutis, D., 2003. Analogue modelling of continental extension: a review focused on the relations between the patterns of deformation and the presence of magma. Earth-Science Reviews 63, 169-247.

Costa, F., 2008. Residence times of silicic magmas associated with calderas. Developments in volcanology 10, 1-55.

Courtillot, V.E., Renne, P.R., 2003. On the ages of flood basalt events. Comptes Rendus Geoscience 335, 113-140.

Crisp, J.A., 1984. Rates of magma emplacement and volcanic output. Journal of Volcanology and Geothermal Research 20, 177-211.

Currie, C.A., Wang, K., Hyndman, R.D., He, J.H., 2004. The thermal effects of steady-state slab-driven mantle flow above a subducting plate: the Cascadia subduction zone and backarc. Earth and Planetary Science Letters 223, 35-48.

Daly, R.A., 1914. Igneous rocks and their origin. McGraw-Hill book company, inc.

Daniels, K., Bastow, I., Keir, D., Sparks, R., Menand, T., 2014. Thermal models of dyke intrusion during development of continent–ocean transition. Earth and Planetary Science Letters 385, 145-153.

de Silva, S.L., Gosnold, W.D., 2007. Episodic construction of batholiths: Insights from the spatiotemporal development of an ignimbrite flare-up. Journal of Volcanology and Geothermal Research 167, 320-335.

Deering, C., Bachmann, O., Dufek, J., Gravley, D., 2011. Rift-related transition from andesite to rhyolite volcanism in the Taupo Volcanic Zone (New Zealand) controlled by crystal–melt dynamics in mush zones with variable mineral assemblages. Journal of Petrology 52, 2243-2263.

Deering, C., Cole, J., Vogel, T., 2008. A rhyolite compositional continuum governed by lower crustal source conditions in the Taupo Volcanic Zone, New Zealand. Journal of Petrology 49, 2245-2276.

DePaolo, D.J., 1981a. A neodymium and strontium isotopic study of the Mesozoic calc-alkaline granitic batholiths of the Sierra Nevada and Peninsular Ranges, California. Journal of Geophysical Research: Solid Earth (1978–2012) 86, 10470-10488.

DePaolo, D.J., 1981b. Trace-element and isotopic effects of combined wallrock assimilation and fractional crystallization Earth and Planetary Science Letters 53, 189-202.

DePaolo, D.J., Daley, E.E., 2000. Neodymium isotopes in basalts of the southwest basin and range and lithospheric thinning during continental extension. Chemical Geology 169, 157-185.

DePaolo, D.J., Perry, F.V., Baldridge, W.S., 1992. Crustal versus mantle sources of granitic magmas-A 2-parameter model based on Nd isotopic studies. Transactions of the Royal Society of Edinburgh-Earth Sciences 83, 439-446.

Dewey, J., Lamb, S., 1992. Active tectonics of the Andes. Tectonophysics 205, 79-95.

Dhuime, B., Bosch, D., Garrido, C.J., Bodinier, J.-L., Bruguier, O., Hussain, S.S., Dawood, H., 2009. Geochemical architecture of the lower-to middle-crustal section of a paleo-island arc (Kohistan Complex, Jijal–Kamila area, northern Pakistan): implications for the evolution of an oceanic subduction zone. Journal of Petrology 50, 531-569.

Dimalanta, C., Taira, A., Yumul, G.P., Tokuyama, H., Mochizuki, K., 2002. New rates of western Pacific island arc magmatism from seismic and gravity data. Earth and Planetary Science Letters 202, 105-115.

Druitt, T., Costa, F., Deloule, E., Dungan, M., Scaillet, B., 2012. Decadal to monthly timescales of magma transfer and reservoir growth at a caldera volcano. Nature 482, 77-80.

Ducea, M.N., 2002. Constraints on the bulk composition and root foundering rates of continental arcs: A California arc perspective. Journal of Geophysical Research-Solid Earth 107.

Dufek, J., Bachmann, O., 2010. Quantum magmatism: Magmatic compositional gaps generated by melt-crystal dynamics. Geology 38, 687-690.

Dufek, J., Bergantz, G.W., 2005. Lower crustal magma genesis and preservation: A stochastic framework for the evaluation of basalt-crust interaction. Journal of Petrology 46, 2167-2195.

Dunbar, N.W., Hervig, R.L., Kyle, P.R., 1989. Determination of pre-eruptive H2O, F and Cl contents of silicic magmas using melt inclusions: examples from Taupo volcanic center, New Zealand. Bulletin of Volcanology 51, 177-184.

Ebinger, C.J., Casey, M., 2001. Continental breakup in magmatic provinces: An Ethiopian example. Geology 29, 527-530.

Elders, W., 1979. The geological background of the geothermal fields of the Salton Trough, Geology and Geothermics of the Salton Trough. Campus Museum Contribution, University of California Riverside 5, pp. 1-19.

Elders, W.A., Rex, R.W., Meidav, T., Robinson, P.T., Biehler, S., 1972. Crustal Spreading in Southern California. Science 178, 15-24.

England, P., 1983. Constraints on extension of continental lithosphere. Journal of Geophysical Research: Solid Earth (1978–2012) 88, 1145-1152.

Fitton, J.G., James, D., Leeman, W.P., 1991. Basic magmatism associated with late Cenozoic extension in the western United States - Compositional variations in space and time Journal of Geophysical Research-Solid Earth and Planets 96, 13693-13711.

Fletcher, I.R., Myers, J.S., Ahmat, A.L., 1991. Isotopic evidence on the age and origin of the Fraser Complex, Western Australia: a sample of Mid-Proterozoic lower crust. Chemical Geology: Isotope Geoscience section 87, 197-216.

Foucher, J.-P., Le Pichon, X., Sibuet, J.-C., Roberts, D., Chenet, P.-Y., Bally, A., Oxburgh, E., Kent, P., Dewey, J., Bott, M., 1982. The Ocean--Continent Transition in the Uniform Lithospheric Stretching Model: Role of Partial Melting in the Mantle [and Discussion]. Philosophical Transactions of the Royal Society of London. Series A, Mathematical and Physical Sciences 305, 27-43.

Fuis, G., Mooney, W., Healy, J., McMechan, G., Lutter, W., 1984. A seismic refraction survey of the Imperial Valley region, California. Journal of Geophysical Research: Solid Earth (1978–2012) 89, 1165-1189.

Fuis, G.S., Kohler, W.M., 1984. Crustal structure and tectonics of the Imperial Valley region, California.

Fyfe, W., 1973. The granulite facies, partial melting and the Archaean crust. Philosophical Transactions for the Royal Society of London. Series A, Mathematical and Physical Sciences, 457-461.

Gelman, S.E., Deering, C.D., Bachmann, O., Huber, C., Gutiérrez, F.J., 2014. Identifying the crystal graveyards remaining after large silicic eruptions. Earth and Planetary Science Letters 403, 299-306.

Gelman, S.E., Gutiérrez, F.J., Bachmann, O., 2013. On the longevity of large upper crustal silicic magma reservoirs. Geology 41, 759-762.

Gill, J.B., 1981. Orogenic andesites and plate tectonics. Springer-Verlag Berlin.

Glazner, A.F., Bartley, J.M., Coleman, D.S., Gray, W., Taylor, R.Z., 2004. Are plutons assembled over millions of years by amalgamation from small magma chambers? GSA today 14, 4-12.

Green, T.H., 1972. Crystallization of calc-alkaline andesite under controlled high-pressure hydrous conditions. Contributions to Mineralogy and Petrology 34, 150-166.

Grove, T.L., Parman, S.W., Bowring, S.A., Price, R.C., Baker, M.B., 2002. The role of an H2O-rich fluid component in the generation of primitive basaltic andesites and andesites from the Mt. Shasta region, N California. Contributions to Mineralogy and Petrology 142, 375-396.

Grunder, A.L., 1995. Material and thermal roles of basalt in crustal magmatism - Case study from eastern Nevada Geology 23, 952-956.

Gualda, G.A., Ghiorso, M.S., Lemons, R.V., Carley, T.L., 2012. Rhyolite-MELTS: a modified calibration of MELTS optimized for silica-rich, fluid-bearing magmatic systems. Journal of Petrology 53, 875-890.

Gudmundsson, A., 2006. How local stresses control magma-chamber ruptures, dyke injections, and eruptions in composite volcanoes. Earth-Science Reviews 79, 1-31.

Harker, A., 1894. Carrock Fell: a Study in the Variation of Igneous Rock-Masses—Part I. The Gabbro. Quarterly Journal of the Geological Society 50, 311-337.

Harker, A., 1909. The Natural History of Igneous Rocks. MacMillan, New York.

Harlow, D.H., Power, J.A., Laguerta, E.P., Ambubuyog, G., White, R.A., Hoblitt, R.P., 1996. Precursory seismicity and forecasting of the June 15, 1991, eruption of Mount Pinatubo. Fire and mud: Eruptions and lahars of Mount Pinatubo, Philippines, 223-247.

Harrison, A., White, R., 2004. Crustal structure of the Taupo Volcanic Zone, New Zealand: stretching and igneous intrusion. Geophysical Research Letters 31.

Helz, R.T., 1982. , Experimental studies of amphibole stability; Phase relations and compositions of amphiboles produced in studies of the melting behavior of rocks. Reviews in Mineralogy and Geochemistry 9, 279-353.

Herzig, C., Jacobs, D., 1991. Late Cenozoic basaltic magmatism in the Salton Trough; Implications for tectonic development. The diversity of mineral and energy resources of southern California: Society of Economic Geologists Guidebook Series 12, 104-116.

Herzig, C.T., Elders, W.A., 1988a. NATURE AND SIGNIFICANCE OF IGNEOUS ROCKS CORED IN THE STATE 2–14 RESEARCH BOREHOLE: SALTON SEA SCIENTIFIC DRILLING PROJECT, CALIFORNIA. Journal of Geophysical Research: Solid Earth (1978–2012) 93, 13069-13080.

Herzig, C.T., Elders, W.A., 1988b. Probable occurrence of the Bishop Tuff in the Salton Sea scientific drilling project borehole. Salton Sea Geothermal System, California: Transactions, Geothermal Resources Council 12, 115-120.

Herzig, C.T., Jacobs, D.C., 1994. Cenozoic volcanism and two-stage extension in the Salton trough, southern California and northern Baja California. Geology 22, 991-994.

Hildreth, W., 1979. The Bishop Tuff: evidence for the origin of compositional zonation in silicic magma chambers. Geological Society of America Special Papers 180, 43-76.

Hildreth, W., 1981. Gradients in silicic magma chambers - Implications for lithospheric magmatism Journal of Geophysical Research 86, 153-192.

Hildreth, W., 2004. Volcanological perspectives on Long Valley, Mammoth Mountain, and Mono Craters: several contiguous but discrete systems. Journal of Volcanology and Geothermal Research 136, 169-198.

Hildreth, W., Halliday, A.N., Christiansen, R.L., 1991. Isotopic and chemical evidence concerning the genesis and contamination of basaltic and rhyolitic magma beneath the Yellowstone plateau volcanic field Journal of Petrology 32, 63-138.

Hildreth, W., Moorbath, S., 1988. Crustal contributions to arc magmatism in the Andes of central Chile Contributions to Mineralogy and Petrology 98, 455-489.

Hochstaedter, A.G., Gill, J.B., Kusakabe, M., Newman, S., Pringle, M., Taylor, B., Fryer, P., 1990. Volcanism in the Sumisu Rift .1. Major element, volatile, and stable isotope geochemistry Earth and Planetary Science Letters 100, 179-194.

Huang, H.-H., Lin, F.-C., Schmandt, B., Farrell, J., Smith, R.B., Tsai, V.C., 2015. The Yellowstone magmatic system from the mantle plume to the upper crust. Science, aaa5648.

Huber, C., Bachmann, O., Manga, M., 2009. Homogenization processes in silicic magma chambers by stirring and mushification (latent heat buffering). Earth and Planetary Science Letters 283, 38-47.

Hulen, J., Pulka, F., 2001. Newly-discovered, ancient extrusive rhyolite in the Salton Sea geothermal field, Imperial Valley, California, Proceedings, Twenty-Sixth Workshop on Geothermal Reservoir Engineering SGP-TR-168, Stanford University, Stanford, pp. 1-16.

Hulen, J.B., Kaspereit, D., Norton, D.L., Osborn, W., Pulka, F.S., Bloomquist, R., 2002. Refined conceptual modeling and a new resource estimate for the Salton Sea geothermal field, Imperial Valley, California. TRANSACTIONS-GEOTHERMAL RESOURCES COUNCIL, 29-36.

Huppert, H.E., Sparks, R.S.J., 1988. The generation of granitic magmas by intrusion of basalt into continental crust Journal of Petrology 29, 599-624.

Jagoutz, O., Müntener, O., Ulmer, P., Pettke, T., Burg, J.-P., Dawood, H., Hussain, S., 2007. Petrology and mineral chemistry of lower crustal intrusions: the Chilas Complex, Kohistan (NW Pakistan). Journal of Petrology 48, 1895-1953.

Jagoutz, O., Schmidt, M., 2012. The formation and bulk composition of modern juvenile continental crust: The Kohistan arc. Chemical Geology 298, 79-96.

Jagoutz, O., Schmidt, M.W., 2013. The composition of the foundered complement to the continental crust and a re-evaluation of fluxes in arcs. Earth and Planetary Science Letters 371, 177-190.

Jagoutz, O.E., 2010. Construction of the granitoid crust of an island arc. Part II: a quantitative petrogenetic model. Contributions to Mineralogy and Petrology 160, 359-381.

Jagoutz, O.E., Burg, J.-P., Hussain, S., Dawood, H., Pettke, T., Iizuka, T., Maruyama, S., 2009. Construction of the granitoid crust of an island arc part I: geochronological and geochemical constraints from the plutonic Kohistan (NW Pakistan). Contributions to Mineralogy and Petrology 158, 739-755.

Jellinek, A.M., DePaolo, D.J., 2003. A model for the origin of large silicic magma chambers: precursors of caldera-forming eruptions. Bulletin of Volcanology 65, 363-381.

Jicha, B.R., Scholl, D.W., Singer, B.S., Yogodzinski, G.M., Kay, S.M., 2006. Revised age of Aleutian Island Arc formation implies high rate of magma production. Geology 34, 661-664.

John, B.E., 1988. Structural reconstruction and zonation of a tilted mid-crustal magma chamber: The felsic Chemehuevi Mountains plutonic suite. Geology 16, 613-617.

Jull, M., Kelemen, P., 2001. On the conditions for lower crustal convective instability. Journal of Geophysical Research: Solid Earth (1978–2012) 106, 6423-6446.

Karakas, O., Dufek, J., 2015. Melt evolution and residence in extending crust: Thermal modeling of the crust and crustal magmas. Earth and Planetary Science Letters 425, 131-144.

Karakas, O., Dufek, J., Mangan, M.T., Wright, H.M., Thermal and petrologic constraints on lower crustal melt accumulation in the Salton Sea Geothermal Field. (in prep).

Karlstrom, L., Dufek, J., Manga, M., 2010. Magma chamber stability in arc and continental crust. Journal of Volcanology and Geothermal Research 190, 249-270.

Kay, R.W., Kay, S.M., 1991. Creation and destruction of lower continental crust Geologische Rundschau 80, 259-278.

Kay, R.W., Kay, S.M., 1993. Delamination and delamination magmatism. Tectonophysics 219, 177-189.

Kelley, V.C., Soske, J., 1936. Origin of the Salton volcanic domes, Salton Sea, California. The Journal of Geology, 496-509.

Kendall, J.-M., Stuart, G., Ebinger, C., Bastow, I., Keir, D., 2005. Magma-assisted rifting in Ethiopia. Nature 433, 146-148.

Keranen, K., Klemperer, S., Gloaguen, R., Group, E.W., 2004. Three-dimensional seismic imaging of a protoridge axis in the Main Ethiopian rift. Geology 32, 949-952.

Klepeis, K.A., Clarke, G.L., Rushmer, T., 2003. Magma transport and coupling between deformation and magmatism in the continental lithosphere. GSA TODAY 13, 4-11.

Kumar, P.S., Reddy, G.K., 2004. Radioelements and heat production of an exposed Archaean crustal cross-section, Dharwar craton, South India. Earth and Planetary Science Letters 224, 309-324.

Kushiro, I., 2001. Partial melting experiments on peridotite and origin of mid-ocean ridge basalt. Annual Review of Earth and Planetary Sciences 29, 71-107.

Lachenbruch, A.H., Sass, J., Galanis, S., 1985. Heat flow in southernmost California and the origin of the Salton Trough. Journal of Geophysical Research: Solid Earth (1978–2012) 90, 6709-6736.

Larsen, S., Reilinger, R., 1991. Age constraints for the present fault configuration in the Imperial Valley, California: Evidence for northwestward propagation of the Gulf of California rift system. Journal of Geophysical Research: Solid Earth (1978–2012) 96, 10339-10346.

Lee, C.-T.A., Bachmann, O., 2014. How important is the role of crystal fractionation in making intermediate magmas? Insights from Zr and P systematics. Earth and Planetary Science Letters 393, 266-274.

Lees, J.M., 2007. Seismic tomography of magmatic systems. Journal of Volcanology and Geothermal Research 167, 37-56.

Lees, J.M., Crosson, R.S., 1990. Tomographic imaging of local earthquake delay times for three-dimensional velocity variation in western Washington. Journal of Geophysical Research: Solid Earth (1978–2012) 95, 4763-4776.

Liang, Y., Parmentier, E.M., 2010. A two-porosity double lithology model for partial melting, melt transport and melt–rock reaction in the mantle: Mass conservation equations and trace element transport. Journal of Petrology, egp086.

Lipman, P.W., Doe, B.R., Hedge, C.E., Steven, T.A., 1978. Petrologic evolution of San-Juan volcanic field, southwestern Colorado - Pb and Sr isotope evidence Geological Society of America Bulletin 89, 59-82.

Lonsdale, P., 1989. Geology and tectonic history of the Gulf of California. The eastern Pacific Ocean and Hawaii: Boulder, Colorado, Geological Society of America, Geology of North America, v. N, 499-521.

Lutter, W.J., Roberts, P.M., Thurber, C.H., Steck, L., Fehler, M.C., Stafford, D.G., Baldridge, W.S., Zeichert, T.A., 1995. Teleseismic P-wave image of crust and upper mantle structure beneath the Valles Caldera, New Mexico: Initial Results from the 1993 JTEX Passive Array. Geophysical research letters 22, 505-508.

Lynch, H.D., Morgan, P., 1990. Finite-element models of continental extension. Tectonophysics 174, 115-135.

Mahood, G.A., 1981. Chemical evolution of a Pleistocene rhyolitic center: Sierra la Primavera, Jalisco, Mexico. Contributions to Mineralogy and Petrology 77, 129-149.

Mahood, G.A., Baker, D.R., 1986. Experimental constraints on depths of fractionation of mildly alkalic basalts and associated felsic rocks: Pantelleria, Strait of Sicily. Contributions to Mineralogy and Petrology 93, 251-264.

Mangan, M.T., Marsh, B.D., 1992. Solidification front fractionation in phenocryst-free sheet-like magma bodies. The Journal of Geology, 605-620.

Marsh, B., 1981. On the crystallinity, probability of occurrence, and rheology of lava and magma. Contributions to Mineralogy and Petrology 78, 85-98.

Marsh, B.D., 1982. On the mechanics of igneous diapirism, stoping, and zone melting. American Journal of Science 282, 808-855.

Marsh, B.D., 1988. Crystal capture, sorting, and retention in convecting magma. Geological Society of America Bulletin 100, 1720-1737.

Martynov, Y.A., Khanchuk, A.I., Kimura, J.I., Rybin, A.V., Martynov, A.Y., 2010. Geochemistry and Petrogenesis of Volcanic Rocks in the Kuril Island Arc. Petrology 18, 489-513.

McCarthy, J., Thompson, G.A., 1988. Seismic imaging of extended crust with emphasis on the western United States. Geological Society of America Bulletin 100, 1361-1374.

McDowell, S., 1987. Geothermal alteration of sediments in the Salton Sea scientific drill hole: Petrophysical properties and mass changes during alteration: Final report. Michigan Technological Univ., Houghton (USA). Dept. of Geology and Geological Engineering.

McKenzie, D., 1978. Some remarks on the development of sedimentary basins. Earth and planetary science letters 40, 25-32.

McKenzie, D., 1985. The extraction of magma from the crust and mantle. Earth and Planetary Science Letters 74, 81-91.

McKenzie, D., Bickle, M., 1988. The volume and composition of melt generated by extension of the lithosphere. Journal of petrology 29, 625-679.

McKibben, M., Hardie, L., 1997. Ore-forming brines in active continental rifts. Geochemistry of hydrothermal ore deposits 3rd edition. John Wiley and Sons, New York.

Menand, T., Annen, C., de Saint Blanquat, M., 2015. Rates of magma transfer in the crust: Insights into magma reservoir recharge and pluton growth. Geology 43, 199-202.

Michael, P., 1995. Regionally distinctive sources of depleted MORB: Evidence from trace elements and H< sub> 2</sub> O. Earth and Planetary Science Letters 131, 301-320.

Mohr, P., 1982. Musings on continental rifts. Continental and oceanic rifts, 293-309.

Moore, G., Carmichael, I., 1998. The hydrous phase equilibria (to 3 kbar) of an andesite and basaltic andesite from western Mexico: constraints on water content and conditions of phenocryst growth. Contributions to Mineralogy and Petrology 130, 304-319.

Morgan, J.P., Ranero, C.R., Vannucchi, P., 2008. Intra-arc extension in Central America: links between plate motions, tectonics, volcanism, and geochemistry. Earth and Planetary Science Letters 272, 365-371.

Morley, C., 1994. Interaction of deep and shallow processes in the evolution of the Kenya rift. Tectonophysics 236, 81-91.

Muffler, L.P., White, D.E., 1969. Active metamorphism of Upper Cenozoic sediments in the Salton Sea geothermal field and the Salton Trough, southeastern California. Geological Society of America Bulletin 80, 157-182.

Müntener, O., Kelemen, P.B., Grove, T.L., 2001. The role of H2O during crystallization of primitive arc magmas under uppermost mantle conditions and genesis of igneous pyroxenites: an experimental study. Contributions to Mineralogy and Petrology 141, 643-658.

Newman, A.V., Stiros, S., Feng, L., Psimoulis, P., Moschas, F., Saltogianni, V., Jiang, Y., Papazachos, C., Panagiotopoulos, D., Karagianni, E., 2012. Recent geodetic unrest at Santorini Caldera, Greece. Geophysical Research Letters 39.

Nicolas, A., 1985. Novel type of crust produced during continental rifting. Nature 315, 112-115.

O'Hara, M., 1977. Geochemical evolution during fractional crystallisation of a periodically refilled magma chamber. Nature 266, 503-507.

O'Hara, M., 1998. Volcanic plumbing and the space problem—thermal and geochemical consequences of large-scale assimilation in ocean island development. Journal of Petrology 39, 1077-1089.

Papale, P., Dobran, F., 1994. Magma flow along the volcanic conduit during the Plinian and pyroclastic flow phases of the May 18, 1980, Mount St. Helens eruption. Journal of Geophysical Research: Solid Earth (1978–2012) 99, 4355-4373.

Papazachos, C., Kiratzi, A., Papazachos, B., 1992. Rates of active crustal deformation in the Aegean and the surrounding area. Journal of geodynamics 16, 147-179.

Parsons, T., Sleep, N.H., Thompson, G.A., 1992. Host rock rheology controls on the emplacement of tabular intrusions: Implications for underplating of extending crust. Tectonics 11, 1348-1356.

Patankar, S., 1980. Numerical heat transfer and fluid flow. CRC Press.

Pearce, J.A., Cann, J., 1973. Tectonic setting of basic volcanic rocks determined using trace element analyses. Earth and planetary science letters 19, 290-300.

Pedersen, T., Heeremans, M., van der Beek, P., 1998. Models of crustal anatexis in volcanic rifts: applications to southern Finland and the Oslo Graben, southeast Norway. Geophysical Journal International 132, 239-255.

Pedersen, T., Ro, H.E., 1992. Finite duration extension and decompression melting. Earth and planetary science letters 113, 15-22.

Petcovic, H.L., Dufek, J.D., 2005. Modeling magma flow and cooling in dikes: Implications for emplacement of Columbia River flood basalts. Journal of Geophysical Research-Solid Earth 110.

Petford, N., Gallagher, K., 2001. Partial melting of mafic (amphibolitic) lower crust by periodic influx of basaltic magma. Earth and Planetary Science Letters 193, 483-499.

Petford, N., Kerr, R.C., Lister, J.R., 1993. Dike transport of granitoid magmas Geology 21, 845-848.

Petford, N., Lister, J.R., Kerr, R.C., 1994. The ascent of felsic magmas in dykes. Lithos 32, 161-168.

Pickett, D.A., Saleeby, J.B., 1993. Thermobarometric constraints on the depth of exposure and conditions of plutonism and metamorphism at deep levels of the Sierra Nevada Batholith, Tehachapi Mountains, California. Journal of Geophysical Research: Solid Earth (1978–2012) 98, 609-629.

Piwinskii, A., Wyllie, P., 1968. Experimental studies of igneous rock series: a zoned pluton in the Wallowa batholith, Oregon. The Journal of Geology, 205-234.

Plank, T., Langmuir, C.H., 1998. The chemical composition of subducting sediment and its consequences for the crust and mantle. Chemical Geology 145, 325-394.

Platt, J.P., 2007. From orogenic hinterlands to Mediterranean-style back-arc basins: a comparative analysis. Journal of the Geological Society 164, 297-311.

Price, R.C., Turner, S., Cook, C., Hobden, B., Smith, I.E.M., Gamble, J.A., Handley, H., Maas, R., Mobis, A., 2010. Crustal and mantle influences and U-Th-Ra disequilibrium in andesitic lavas of Ngauruhoe volcano, New Zealand. Chemical Geology 277, 355-373.

Quick, J., Sinigoi, S., Peressini, G., Demarchi, G., Wooden, J., Sbisà, A., 2009. Magmatic plumbing of a large Permian caldera exposed to a depth of 25 km. Geology 37, 603-606.

Rapp, R.P., Watson, E.B., Miller, C.F., 1991. Partial melting of amphibolite/eclogite and the origin of Archean trondhjemites and tonalites. Precambrian Research 51, 1-25.

Reid, M.R., Coath, C.D., Harrison, T.M., McKeegan, K.D., 1997. Prolonged residence times for the youngest rhyolites associated with Long Valley Caldera: 230 Th—238 U ion microprobe dating of young zircons. Earth and Planetary Science Letters 150, 27-39.

Robinson, P.T., Elders, W.A., Muffler, L., 1976. Quaternary volcanism in the Salton Sea geothermal field, Imperial Valley, California. Geological Society of America Bulletin 87, 347-360.

Roggensack, K., 2001. Sizing up crystals and their melt inclusions: a new approach to crystallization studies. Earth and Planetary Science Letters 187, 221-237.

Rubin, A.M., 1992. Dike-induced faulting and graben subsidence in volcanic rift zones. Journal of Geophysical Research: Solid Earth (1978–2012) 97, 1839-1858.

Rudnick, R.L., Fountain, D.M., 1995. Nature and composition of the continental crust: a lower crustal perspective. Reviews of Geophysics 33, 267-309.

Ruppel, C., 1995. Extensional processes in continental lithosphere. Journal of Geophysical Research: Solid Earth (1978–2012) 100, 24187-24215.

Rushmer, T., 1991. Partial melting of two amphibolites: contrasting experimental results under fluid-absent conditions. Contributions to Mineralogy and Petrology 107, 41-59.

Saltus, R.W., Lachenbruch, A.H., 1991. Thermal evolution of the Sierra Nevada: Tectonic implications of new heat flow data. Tectonics 10, 325-344.

Sass, J.H., Lachenbruch, A.H., Munroe, R.J., Greene, G.W., Moses, T.H., 1971. Heat flow in the western United States. Journal of Geophysical Research 76, 6376-6413.

Schmitt, A., Vazquez, J., 2006. Alteration and remelting of nascent oceanic crust during continental rupture: evidence from zircon geochemistry of rhyolites and xenoliths from the Salton Trough, California. Earth and Planetary Science Letters 252, 260-274.

Schmitt, A.K., Hulen, J.B., 2008. Buried rhyolites within the active, high-temperature Salton Sea geothermal system. Journal of Volcanology and Geothermal Research 178, 708-718.

Schmitt, A.K., Martín, A., Weber, B., Stockli, D.F., Zou, H., Shen, C.-C., 2013. Oceanic magmatism in sedimentary basins of the northern Gulf of California rift. Geological Society of America Bulletin 125, 1833-1850.

Sen, C., Dunn, T., 1994. Dehydration melting of a basaltic composition amphibolite at 1.5 and 2.0 GPa - Implications for the origin of adakites Contributions to Mineralogy and Petrology 117, 394-409.

Sengör, A., Burke, K., 1978. Relative timing of rifting and volcanism on Earth and its tectonic implications. Geophysical Research Letters 5, 419-421.

Shapiro, N.M., Ritzwoller, M.H., 2004. Inferring surface heat flux distributions guided by a global seismic model: particular application to Antarctica. Earth and Planetary Science Letters 223, 213-224.

Shimizu, K., Nakamura, E., Maruyama, S., 2005. The geochemistry of ultramafic to mafic volcanics from the Belingwe Greenstone Belt, Zimbabwe: magmatism in an Archean continental large igneous province. Journal of Petrology 46, 2367-2394.

Sinigoi, S., Quick, J.E., Clemens-Knott, D., Mayer, A., Demarchi, G., Mazzucchelli, M., Negrini, L., Rivalenti, G., 1994. Chemical evolution of a large mafic intrusion in the lower crust, Ivrea-Verbano Zone, northern Italy. Journal of Geophysical Research: Solid Earth (1978–2012) 99, 21575-21590.

Sisson, T., Ratajeski, K., Hankins, W., Glazner, A., 2005. Voluminous granitic magmas from common basaltic sources. Contributions to Mineralogy and Petrology 148, 635-661.

Stamps, D.S., Calais, E., Saria, E., Hartnady, C., Nocquet, J.-M., Ebinger, C.J., Fernandes, R.M., 2008. A kinematic model for the east African rift. Geophysical Research Letters 35.

Stolper, E., Newman, S., 1994. The role of water in the petrogenesis of Mariana trough magmas. Earth and Planetary Science Letters 121, 293-325.

Tappa, M.J., Coleman, D.S., Mills, R.D., Samperton, K.M., 2011. The plutonic record of a silicic ignimbrite from the Latir volcanic field, New Mexico. Geochemistry, Geophysics, Geosystems 12.

Taylor, H.P., 1980. The effects of assimilation of country rocks by magmas on O-18 O-16 and Sr-87 Sr-86 systematics in igneous rocks. Earth and Planetary Science Letters 47, 243-254.

Taylor, S.R., McLennan, S.M., 1985. The continental crust: its composition and evolution.

Thompson, A.B., Connolly, J.A.D., 1995. Melting of the continental crust - Some thermal and petrological constraints on anatexis in continental collision zones and other tectonic settings Journal of Geophysical Research-Solid Earth 100, 15565-15579.

Turner, S., Hawkesworth, C., Rogers, N., Bartlett, J., Worthington, T., Hergt, J., Pearce, J., Smith, I., 1997. U-238-Th-230 disequilibria, magma petrogenesis, and flux rates beneath the depleted Tonga-Kermadec island arc. Geochimica Et Cosmochimica Acta 61, 4855-4884.

Tuttle, O.F., Bowen, N.L., 1958. Origin of granite in the light of experimental studies in the system NaAlSi3O8–KAlSi3O8–SiO2–H2O. Geological Society of America Memoirs 74, 1-146.

Ulmer, P., 2001. Partial melting in the mantle wedge—the role of H 2 O in the genesis of mantle-derived ‘arc-related’magmas. Physics of the Earth and Planetary Interiors 127, 215-232.

Van den Bogaard, P., Schirnick, C., 1995. 40Ar/39Ar laser probe ages of Bishop Tuff quartz phenocrysts substantiate long-lived silicic magma chamber at Long Valley, United States. Geology 23, 759-762.

Villamor, P., Berryman, K., 2001. A late Quaternary extension rate in the Taupo Volcanic Zone, New Zealand, derived from fault slip data. New Zealand Journal of Geology and Geophysics 44, 243-269.

Voller, V., Swaminathan, C., 1991. General source-based method for solidification phase change. Numerical Heat Transfer, 19B 175-189.

Voshage, H., Hofmann, A., Mazzucchelli, M., Rivalenti, G., Sinigoi, S., Raczek, I., Demarchi, G., 1990. Isotopic evidence from the Ivrea Zone for a hybrid lower crust formed by magmatic underplating. Nature 347, 731-736.

Walker, J.A., Roggensack, K., Patino, L.C., Cameron, B.I., Matias, O., 2003. The water and trace element contents of melt inclusions across an active subduction zone. Contributions to Mineralogy and Petrology 146, 62-77.

Wedepohl, K.H., 1995. The composition of the continental crust. Geochimica et cosmochimica Acta 59, 1217-1232.

Wells, P.R.A., 1980. Thermal models for the magmatic accretion and subsequent metamorphism of continental crust Earth and Planetary Science Letters 46, 253-265.

White, R., Clarke, G., Nelson, D., 1999. SHRIMP U-Pb zircon dating of Grenville-age events in the western part of the Musgrave Block, central Australia. Journal of Metamorphic Geology 17, 465-482.

White, R., McKenzie, D., 1989. Magmatism at rift zones: the generation of volcanic continental margins and flood basalts. Journal of Geophysical Research: Solid Earth (1978–2012) 94, 7685-7729.

White, R.S., 1993. Melt production rates in mantle plumes. Philosophical Transactions of the Royal Society of London. Series A: Physical and Engineering Sciences 342, 137-153.

White, R.S., Spence, G.D., Fowler, S.R., McKenzie, D.P., Westbrook, G.K., 1987. Magmatism at rifted continental margins. Nature 330, 439-444.

White, S.M., Crisp, J.A., Spera, F.J., 2006. Long-term volumetric eruption rates and magma budgets. Geochemistry, Geophysics, Geosystems 7.

Williams, M., Hanmer, S., Kopf, C., Darrach, M., 1995. Syntectonic generation and segregation of tonalitic melts from amphibolite dikes in the lower crust, Striding-Athabasca mylonite zone, northern Saskatchewan. Journal of Geophysical Research: Solid Earth (1978–2012) 100, 15717-15734.

Wilson, C., 2001. The 26.5 ka Oruanui eruption, New Zealand: an introduction and overview. Journal of Volcanology and Geothermal Research 112, 133-174.

Wilson, C., Blake, S., Charlier, B., Sutton, A., 2006. The 26· 5 ka Oruanui eruption, Taupo volcano, New Zealand: development, characteristics and evacuation of a large rhyolitic magma body. Journal of Petrology 47, 35-69.

Wilson, C.J., 2008. Supereruptions and supervolcanoes: processes and products. Elements 4, 29-34.

Wolf, M.B., Wyllie, P.J., 1994. Dehydration-melting of amphibolite at 10 kbar - The effects of temperature and time Contributions to Mineralogy and Petrology 115, 369-383.

Wotzlaw, J.-F., Schaltegger, U., Frick, D.A., Dungan, M.A., Gerdes, A., Günther, D., 2013. Tracking the evolution of large-volume silicic magma reservoirs from assembly to supereruption. Geology 41, 867-870.

Younker, L.W., Vogel, T.A., 1976. Plutonism and plate dynamics: The origin of Circum-Pacific batholiths Canadian Mineralogist 14, 238-244.

Zhu, L., Mitchell, B.J., Akyol, N., Cemen, I., Kekovali, K., 2006. Crustal thickness variations in the Aegean region and implications for the extension of continental crust. Journal of Geophysical Research: Solid Earth (1978–2012) 111.

Ziegler, P.A., Cloetingh, S., 2004. Dynamic processes controlling evolution of rifted basins. Earth-Science Reviews 64, 1-50.